



HAL
open science

A synthesis of SNAPO-CO₂ ocean total alkalinity and total dissolved inorganic carbon measurements from 1993 to 2022

Nicolas Metzl, Jonathan Fin, Claire Lo Monaco, Guillaume Bourdin, Samir Alliouane, Jacqueline Boutin, Claude Mignon, Yann Bozec, David Antoine, Pascal Conan, et al.

► **To cite this version:**

Nicolas Metzl, Jonathan Fin, Claire Lo Monaco, Guillaume Bourdin, Samir Alliouane, et al.. A synthesis of SNAPO-CO₂ ocean total alkalinity and total dissolved inorganic carbon measurements from 1993 to 2022. Earth System Science Data, In press, 10.5194/essd-2023-308 . hal-04292340v2

HAL Id: hal-04292340

<https://hal.science/hal-04292340v2>

Submitted on 17 Nov 2023

HAL is a multi-disciplinary open access archive for the deposit and dissemination of scientific research documents, whether they are published or not. The documents may come from teaching and research institutions in France or abroad, or from public or private research centers.

L'archive ouverte pluridisciplinaire **HAL**, est destinée au dépôt et à la diffusion de documents scientifiques de niveau recherche, publiés ou non, émanant des établissements d'enseignement et de recherche français ou étrangers, des laboratoires publics ou privés.



HAL
open science

A synthesis of ocean total alkalinity and dissolved inorganic carbon measurements from 1993 to 2022: the SNAPO-CO2-v1 dataset

Nicolas Metzl, Jonathan Fin, Claire Lo Monaco, Claude Mignon, Samir Alliouane, David Antoine, Guillaume Bourdin, Jacqueline Boutin, Yann Bozec, Pascal Conan, et al.

► To cite this version:

Nicolas Metzl, Jonathan Fin, Claire Lo Monaco, Claude Mignon, Samir Alliouane, et al.. A synthesis of ocean total alkalinity and dissolved inorganic carbon measurements from 1993 to 2022: the SNAPO-CO2-v1 dataset. Earth System Science Data, In press, 10.5194/essd-2023-308 . hal-04292340

HAL Id: hal-04292340

<https://hal.science/hal-04292340>

Submitted on 17 Nov 2023

HAL is a multi-disciplinary open access archive for the deposit and dissemination of scientific research documents, whether they are published or not. The documents may come from teaching and research institutions in France or abroad, or from public or private research centers.

L'archive ouverte pluridisciplinaire **HAL**, est destinée au dépôt et à la diffusion de documents scientifiques de niveau recherche, publiés ou non, émanant des établissements d'enseignement et de recherche français ou étrangers, des laboratoires publics ou privés.

1 A synthesis of SNAPO-CO₂ ocean total alkalinity and total dissolved inorganic carbon measurements from 1993 to 2022

3 Nicolas Metzl¹, Jonathan Fin^{1,2}, Claire Lo Monaco¹, Claude Mignon¹, Samir Alliouane³,
4 David Antoine^{3,4}, Guillaume Bourdin⁵, Jacqueline Boutin¹, Yann Bozec⁶, Pascal Conan^{7,8},
5 Laurent Coppola^{3,8}, Frédéric Diaz^{*}, Eric Douville⁹, Xavier Durrieu de Madron¹⁰, Jean-Pierre
6 Gattuso^{3,11}, Frédéric Gazeau³, Melek Golbol^{8,12}, Bruno Lansard⁹, Dominique Lefèvre¹³,
7 Nathalie Lefèvre¹, Fabien Lombard^{3,14}, Ferial Louanchi¹⁵, Liliane Merlivat¹, Léa Olivier^{1,16},
8 Anne Petrenko¹³, Sébastien Petton¹⁷, Mireille Pujo-Pay⁷, Christophe Rabouille⁹, Gilles
9 Reverdin¹, Céline Ridame¹, Aline Tribollet¹, Vincenzo Vellucci^{8,12}, Thibaut Wagener¹³, Cathy
10 Wimart-Rousseau^{13,18}

11

12 ¹ Laboratoire LOCEAN/IPSL, Sorbonne Université-CNRS-IRD-MNHN, Paris, 75005, France

13 ² OSU Ecce Terra, Sorbonne Université-CNRS, Paris, 75005, France

14 ³ Sorbonne Université, CNRS, Laboratoire d'Océanographie de Villefranche, LOV, F-06230 Villefranche-sur-
15 Mer, France

16 ⁴ Remote Sensing and Satellite Research Group, School of Earth and Planetary Sciences, Curtin University,
17 Perth WA 6845, Australia

18 ⁵ School of Marine Sciences, University of Maine, Orono, USA

19 ⁶ Station Biologique de Roscoff, UMR 7144 – EDYCO-CHIMAR, Roscoff, France

20 ⁷ Sorbonne Université, CNRS, Laboratoire d'Océanographie Microbienne, LOMIC, F-66650 Banyuls-sur-Mer,
21 France

22 ⁸ Sorbonne Université, CNRS, OSU Station Marines, STAMAR, Paris, F-75006, France

23 ⁹ Laboratoire des Sciences du Climat et de l'Environnement, LSCE/IPSL, UMR 8212 CEA- CNRS-UVSQ,
24 Université Paris-Saclay, 91191 Gif-sur-Yvette, France

25 ¹⁰ CEFREM, CNRS-Université de Perpignan Via Domitia, 52 Avenue Paul Alduy, 66860 Perpignan, France

26 ¹¹ Institute for Sustainable Development and International Relations, Sciences Po, 27 rue Saint Guillaume, F-
27 75007 Paris, France

28 ¹² Sorbonne Université, CNRS, Institut de la Mer de Villefranche, IMEV, Villefranche-sur-Mer, F-06230, France

29 ¹³ Aix Marseille Univ, Université de Toulon, CNRS, IRD, MIO, Marseille, France

30 ¹⁴ Research Federation for the study of Global Ocean Systems Ecology and Evolution, FR2022/Tara GOSEE,
31 75000, Paris, France.

32 ¹⁵ CVRM: Laboratoire de Conservation et de Valorisation des Ressources Marines, Ecole Nationale Supérieure
33 des Sciences de la Mer et de l'Aménagement du Littoral (ENSSMAL), Station de recherche de Sidi Fredj,
34 Algeria

35 ¹⁶ Alfred Wegener Institute, Helmholtz Centre for Polar and Marine Research, Bremerhaven, Germany

36 ¹⁷ Ifremer, Univ Brest, CNRS, IRD, LEMAR, F-29840 Argenton, France

37 ¹⁸ GEOMAR Helmholtz Centre for Ocean Research Kiel, 24105 Kiel, Germany

38 * Passed away 14/3/2021

39 *Correspondence to:* Nicolas Metzl (nicolas.metzl@locean.ipsl.fr)

40 **Abstract.** Total alkalinity (A_T) and dissolved inorganic carbon (C_T) in the oceans are important properties
41 to

42 understand the ocean carbon cycle and its link with global change (ocean carbon sinks and sources, ocean
43 acidification) and ultimately find carbon based solutions or mitigation procedures (marine carbon removal). We
44 present a database of more than 44 400 A_T and C_T observations along with basic ancillary data (time and
45 space

46 location, depth, temperature and salinity) in various ocean regions obtained since 1993 mainly in the frame of
47 French projects. This includes both surface and water columns data acquired in open oceans, coastal zones and in
48 the Mediterranean Sea and either from time-series or punctual cruises. Most A_T and C_T data in this
49 synthesis

50 were measured from discrete samples using the same closed-cell potentiometric titration calibrated with Certified

48 Reference Material, with an overall accuracy of $\pm 4 \mu\text{mol kg}^{-1}$ for both A_T and C_T . The data are provided in two
49 separate datasets for the global ocean, and for the Mediterranean Sea (<https://doi.org/10.17882/95414>, Metzl et
50 al., 2023) that offers a direct use for regional or global purposes, e.g. A_T /Salinity relationships, long-term C_T
51 estimates, constraint and validation of diagnostics C_T and A_T reconstructed fields or ocean carbon and coupled
52 climate/carbon models simulations, as well as data derived from Biogeochemical-Argo (BGC-Argo) floats.
53 When associated with other properties, these data can also be used to calculate pH, fugacity of CO_2 ($f\text{CO}_2$) and
54 other carbon system properties to derive ocean acidification rates or air-sea CO_2 fluxes.

55

56 **1 Introduction**

57

58 Since 1750, humans activities have added 700 (± 75) PgC anthropogenic carbon dioxide to the
59 atmosphere by burning fossil fuels, producing cement and changing land use (Friedlingstein et al., 2022) driving
60 up the atmospheric carbon dioxide (CO_2) level and leading to unequivocal global change. The ocean plays a
61 major role in reducing the impact of climate change by absorbing more than 90% of the excess heat in the
62 climate system (Cheng et al., 2020; von Schuckmann et al, 2020, 2023; IPCC, 2022) and about 25% of human
63 released CO_2 (Friedlingstein et al., 2022). However, the oceanic CO_2 uptake changes the chemistry of seawater
64 reducing its buffering capacity (Revelle and Suess, 1957; Jiang et al, 2023a) and leading to a process known as
65 ocean acidification with potential impacts on marine organisms (Fabry et al., 2008; Doney et al., 2009, 2020;
66 Gattuso et al., 2015). With atmospheric CO_2 concentrations, surface ocean temperature and ocean heat content,
67 sea-level, sea-ice and glaciers, the ocean acidification (decrease of pH) is now recognized by the World
68 Meteorological Organization as one of the 7 key properties for global climate indicators (WMO, 2018). In the
69 frame of the 2030 Agenda, the United Nations established a set of Sustainable Development Goals (SDG; United
70 Nations, 2020), including a goal dedicated to the ocean (SDG 14, "Life below water") which calls to "conserve
71 and sustainably use the oceans, seas and marine resources for sustainable development". Ocean acidification is
72 specifically referred in the SDG indicator 14.3.1 coordinated at the Intergovernmental Oceanographic
73 Commission (IOC) of UNESCO. Observing the carbonate system in the oceans and marginal seas and
74 understanding how this system changes over time is thus highly relevant not only to quantify the global ocean
75 carbon budget, the anthropogenic CO_2 inventories or ocean acidification rates, but also to understand and
76 simulate the processes that govern the complex CO_2 cycle in the ocean and to better predict the future evolution
77 of climate and global changes (Eyring et al., 2016; Kwiatkowski et al., 2020; Jiang et al., 2023a).

78 The number and quality of ocean $f\text{CO}_2$, A_T , C_T and pH measurements have increased substantially over
79 the past few decades. Quality-controlled observations are now regularly assembled in global data syntheses such
80 as SOCAT (Surface Ocean CO_2 Atlas, Pfeil et al., 2013; Bakker et al., 2014, 2016) and GLODAP (Global Ocean
81 Data Analysis Project, Key et al., 2004; Olsen et al., 2016, 2019, 2020; Lauvset et al., 2021, 2022). These
82 datasets allow evaluation of properties trends in the global ocean, including the change of the ocean CO_2 sink
83 (e.g. Wanninkhof et al., 2013; Friedlingstein et al., 2022; Watson et al., 2020), anthropogenic CO_2 inventories
84 (e.g. Sabine et al., 2004; Khatiwala et al., 2013; Gruber et al., 2019) and ocean acidification (Lauvset et al.,
85 2015, 2020; Jiang et al., 2019; Feely et al, 2023; Ma et al, 2023). Thanks to publicly available consistent and
86 quality controlled databases new methods were recently developed (Carter et al, 2016; Sauzède et al., 2017;
87 Bittig et al., 2018) to reproduce A_T and C_T distributions from other properties like temperature, salinity and
88 oxygen more often observed in the water column especially from autonomous floats (Claustre et al., 2020;
89 Mignot et al., 2023). These methods (named CANYON-B and CONTENT, Bittig et al., 2018) are now also used

90 to help decisions on GLODAP data quality control or to fill in observational gaps (Olsen et al., 2019, 2020;
91 Tanhua et al., 2019, 2021). The GLODAP data products were also successfully used to construct new global
92 ocean A_T and C_T climatological monthly fields in surface and water column using neural network method (e.g.
93 Broullón et al., 2019, 2020).

94 Following pioneer works that produced various global-ocean climatologies of the sea-surface carbonate
95 system (Millero et al., 1998; Lee et al., 2000, 2006; Takahashi et al., 2002, 2009, 2014; Sasse et al., 2013; Jiang
96 et al., 2019), the coupling of fCO_2 data (from SOCAT) and A_T data (from GLODAP) now enables reconstruction
97 of the full carbonate system in the surface ocean at monthly scale to investigate temporal trends at decadal scale
98 (e.g. Gregor and Gruber, 2021; Keppler et al., 2023).

99 International projects such as SOCAT and GLODAP offer important way to synthesize ocean carbon
100 data. In these projects, each observation is quality controlled offering to users high quality observations for
101 regional or global analysis, either for processes analysis or to constraint or validate of ocean and coupled
102 climate/carbon models (CMIP6, e.g. Lerner et al., 2021). SOCAT is a publicly available synthesis product
103 initiated in 2007 (Metzl et al., 2007) for quality-controlled, surface ocean fCO_2 (fugacity of carbon dioxide)
104 observations made by the international marine carbon research community (Bakker et al., 2016). The first
105 SOCAT version was released in 2011 (Pfeil et al., 2013; Sabine et al., 2013), followed by 6 SOCAT versions
106 (Bakker et al., 2014, 2016). The last version in 2023 includes more than 40 million fCO_2 data with accuracy
107 better than $5 \mu\text{atm}$ (Bakker et al., 2023). One important product from SOCAT is the use of data to estimate
108 global air-sea CO_2 fluxes based on reconstructed pCO_2 fields (e.g. Surface Ocean pCO_2 Mapping
109 Intercomparison, SOCOM, Rödenbeck et al., 2015). Since 2015, these results are included each year for the
110 global carbon budget (Le Quere et al., 2015; Friedlingstein et al., 2022).

111 On the other hand, following WOCE/JGOFS era in the 90s when almost all observations were started to
112 be synthesized in a specific recommended format (Joyce and Corry, 1994), GLODAP focusses on water-column
113 carbon observations (and other properties). Following the original GLODAP data product (Key et al., 2004), the
114 project accumulated many new quality controlled observations. One important achievement from GLODAP is
115 the use of data to estimate the anthropogenic CO_2 inventory or its change over decades (Sabine et al., 2004;
116 Gruber et al., 2019). Both products, SOCAT and GLODAP, are relevant tools to detect oceanic acidification
117 rates (Lauvset et al., 2015; Jiang et al., 2019; Feely et al, 2023; Ma et al, 2023).

118 Although these projects include many international ocean observations there are ocean CO_2 related
119 observations all around the world (published or not published), such as total alkalinity and dissolved inorganic
120 carbon, that are not included in SOCAT or GLODAP. This is because SOCAT accepts and controls only fCO_2
121 data, whereas GLODAP includes and controls water-columns data mainly from WOCE/GO-SHIP/CLIVAR
122 cruises. It should be noticed that many ocean carbon observations in various formats can be also found in
123 dedicated database such as NCEI/OCADS (former CDIAC-Ocean, Jiang et al., 2023b,
124 <https://www.ncei.noaa.gov/products/ocean-carbon-acidification-data-system>), PANGAEA
125 (<https://www.pangaea.de/>) or Seanoë (<https://www.seanoë.org/>). In this context it is recommended to progress in
126 data synthesis of the ocean carbon observations that would offer new high quality products for the community
127 (e.g. for GOA-ON, www.goa-on.org, IOC/SDG 14.1.3, <https://oa.iode.org/>, Tilbrook et al., 2019).

128 In this work, we present a synthesis of more than 44 400 A_T and C_T observations obtained over the
129 1993-2022 period during various cruises or at time-series stations mainly supported by French projects. This
130 dataset merges observations measured with the same instruments thus being analytically coherent. Most of the
131 data have accuracy better than $\pm 4 \mu\text{mol kg}^{-1}$, i.e. between the climate ($\pm 2 \mu\text{mol kg}^{-1}$) and weather ($\pm 10 \mu\text{mol kg}^{-1}$)

132 ¹) goals (Newton et al, 2015; Bockmon and Dickson, 2015). Hereafter this dataset will be cited as SNAPO-CO2-
133 V1. We describe the data assemblage and associated quality control and discuss some potential uses of this
134 dataset.

135

136 **2 Data collections**

137

138 The time series projects and research cruises from which data were collated are listed in Table 1 with
139 references in the Supplementary file (Table S1) and the sampling locations displayed in Figure 1. Sampling was
140 performed either from CTD-Rosette casts (Niskin bottles) or from the ship's seawater supply (intake at about 5m
141 depth depending the ship and swell). Samples collected in 500 mL borosilicate glass bottles were poisoned with
142 100 to 300 μL of HgCl_2 depending on the cruises, closed with greased stoppers (Apiezon®) and held tight using
143 elastic band following the SOP protocol (Dickson et al., 2007). Some samples were also collected in 500 mL
144 bottles closed with screw caps. After completion of each cruise, discrete samples were returned back to the
145 LOCEAN laboratory (Paris, France) and stored in a dark room at 4 °C before analysis generally within 2-3
146 months after sampling (sometimes within a week). Some samples were also measured for specific processes
147 studies on benthic corals (e.g. Maier et al., 2012; McCulloch et al., 2012) or for mesocosm and culture
148 experiments but the data are not included in this synthesis as they do not represent natural ocean state (e.g.
149 addition of Sahara dust during the DUNE project, Ridame et al., 2014).

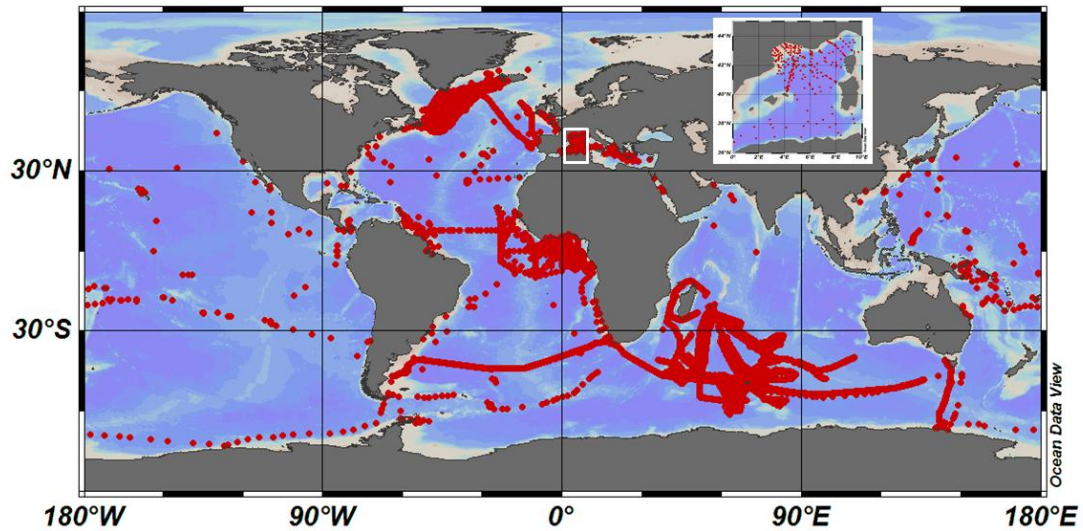
150 As opposed to $p\text{CO}_2$, surface A_T or C_T observations are generally obtained from discrete sampling
151 (measured onboard or onshore). Few cruises offer sea-surface semi-continuous A_T or C_T observations (e.g. Metzl
152 et al., 2006) but new instrumental developments (Seelmann et al., 2020) now enable A_T measurements on Ship of
153 Opportunity Program lines (SOOP). In addition to discrete samples analyzed for various projects conducted
154 mainly in the North Atlantic, Tropical Atlantic, Tropical Pacific, Mediterranean sea and coastal regions (Table
155 1), we complemented this synthesis with A_T and C_T surface observations obtained in the Indian and Southern
156 oceans during the OISO cruises in 1998-2018 (Metzl et al., 2006; Leseurre et al., 2022; data also available at
157 NCEI/OCADS: www.nodc.noaa.gov/ocads/oceans/VOS_Program/OISO.html) and the recent CLIM-EPARSESES
158 cruise conducted in the Mozambique Channel in April 2019 (Lo Monaco et al., 2020, 2021). For OISO cruises
159 the water-column observations are part of the CARINA (CARbon IN the Atlantic) and GLODAP synthesis
160 products (Lo Monaco et al., 2010; Olsen et al., 2016, 2019, 2020) and not included here. Excepted when
161 specified, all data in this synthesis were obtained using the same technique used either in laboratory or at sea (for
162 OISO 1998-2018 and CLIM-EPARSESES 2019 cruises).

163

164 **Table 1:** List of cruises in the SNAPO-CO2-v1 dataset. This is organized by region: Global Ocean and coastal
 165 zones, and Mediterranean Sea (MedSea). See Tables S1, S2, S4 and S4 in the Supplementary Material for a list
 166 of laboratories, of CRMs used, for references and for DOI of cruises. Nb = the number of data for each cruise or
 167 time-series. * indicates the measurements at sea (surface underway)

168	169	170	171	172	173	174	175	176	177	178	179	180	181	182	183	184	185	186	187	188	189	190	191	192	193	194	195	196	197	198	199	200	201	202	203	204	205	206	207	208	209	210	211	212	213	214
Cruise/Project	Start	End	Region	Sampling	Nb																																									
AWIPEV	2015	2021	Arctic	Surface and sub-surface	195																																									
SURATLANT+RREX	1993	2017	North Atlantic	Surface	2832																																									
OVIDE	2006	2018	North Atlantic	Surface, Water Column	397																																									
STRASSE	2012		North Atlantic	Water Column	205																																									
EUREC4A-OA	2020		North Atlantic	Surface, Water Column	135																																									
PROTEUS	2010		North Atlantic	Water Column	27																																									
CHANNEL	2012	2015	English Channel	Surface	696																																									
SOMLIT-Brest	2008	2019	Coastal North Atl	Surface	1174																																									
SOMLIT-Roscoff	2009	2019	Coastal North Atl	Surface and 60m	801																																									
ECOSCOPA	2017	2019	Coastal North Atl	Surface	67																																									
PENZE	2011	2020	River Brittany	Surface and sub-surface	148																																									
AULNE	2009	2010	River Brittany	Surface	27																																									
ELORN	2009	2009	River Brittany	Surface	28																																									
BIOZAIRE	2003	2004	Trop Atlantic	Water Column	87																																									
EGEE	2005	2007	Trop Atlantic	Surface	199																																									
PIRATA-FR	2009	2017	Trop Atlantic	Surface, Water Column	513																																									
PLUMAND	2007		Trop Atlantic	Surface	38																																									
OUTPACE	2015		Trop Pacific	Water Column	240																																									
PANDORA	2012		Solomon Sea	Water Column	178																																									
TARA-Pacific	2016	2018	Trop Pac North Atl	Surface and sub-surface	325																																									
TARA-Ocean	2009	2012	Global Ocean	Surface + 400m	123																																									
TARA-Microbiome	2021	2022	Atlantic	Surface, Water Column	216																																									
ACE	2016	2017	Southern Ocean	Surface, Water Column	135																																									
MOBYDICK	2019		Southern Ocean	Water Column	64																																									
CLIM-EPARSES *	2019		Indian	Surface	790																																									
OISO *	1998	2018	South Indian	Surface	24950																																									
DYFAMED	1998	2017	MedSea	Water Column	2118																																									
BOUSSOLE	2014	2019	MedSea	Surface + 10m	172																																									
SOMLIT-PointB	2007	2015	MedSea Coastal	Surface + 50m	2397																																									
ANTARES	2010	2016	MedSea	Water Column	502																																									
MOLA	2010	2013	MedSea Coastal	Water Column	66																																									
SOLEMIO	2016	2018	MedSea Coastal	Water Column	212																																									
MOOSE-GE	2010	2019	MedSea	Water Column	1847																																									
LATEX	2010		MedSea	Water Column	51																																									
CARBORHONE	2011	2012	MedSea	Water Column	706																																									
CASCADE	2011		MedSea	Water Column	218																																									
DEWEX	2013		MedSea	Water Column	367																																									
SOMBA	2014	2014	MedSea	Water Column	203																																									
AMOR-BFLUX	2015		MedSea Coastal	Water Column	6																																									
PEACETIME	2017	2017	MedSea	Water Column	233																																									
PERLE	2018	2021	MedSea	Water Column	805																																									

217
218
219
220
221
222
223
224
225
226
227
228
229
230



231 **Figure 1:** Locations of A_T and C_T data (1993-2022) in the Global Ocean and the Western Mediterranean Sea
232 (white box, insert) in the SNAPO-CO2-v1 dataset. Figure produced with ODV (Schlitzer, 2018).

233

234 3 Method, accuracy, repeatability, inter-comparison and quality control

235

236 3.1 Method and accuracy

237

238 Since 2003, the discrete samples returned back at SNAPO-CO2 Service facilities (LOCEAN, Paris),
239 were analyzed simultaneously for A_T and C_T by potentiometric titration using a closed cell (Edmond, 1970;
240 Goyet et al., 1991). The same technique was used at sea for surface water underway measurements during OISO
241 and CLIM-EPARSEES cruises (indicated by * in Table 1). For two time series, the dataset also includes
242 measurements obtained before 2000 using other techniques: the DYFAMED time-series observations measured
243 between in 1998 and 2000 in the Mediterranean Sea (Copin-Montégut and Bégovic, 2002; Coppola et al., 2020;
244 Lange et al., 2023) and the SURATLANT time-series values acquired from 1993 to 1997 in the North Atlantic
245 subpolar gyre (Reverdin et al., 2018). We also include A_T data in the river Penzé (Brittany) in 2019-2020 (Yann
246 Bozec, SBR/Roscoff, pers. comm.).

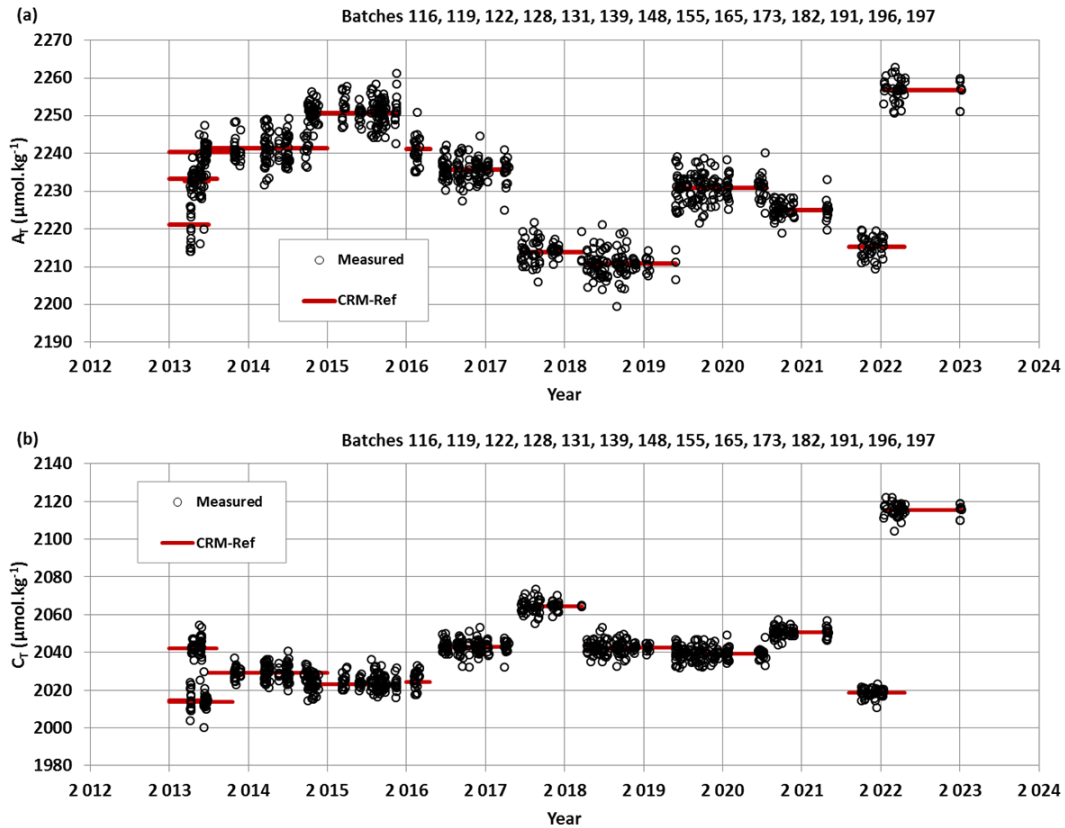
247

248 In the late 1980s the so-called “JGOFS-IOC Advisory Panel on Ocean CO₂” recommended the need for
249 standard analysis protocols and for developing Certified Reference Materials (CRMs) for inorganic carbon
250 measurements (Poisson et al., 1990; UNESCO, 1990, 1991). The CRMs were provided to international
251 laboratories by Pr. A. Dickson (Scripps Institution of Oceanography, San Diego, USA), starting in 1990 for C_T
252 and 1996 for A_T , respectively. These CRMs were thus always available to us and used to calibrate the
253 measurements (CRM Batch numbers used for each cruise are listed in Supplementary file (Table S2). The
254 concentrations of CRMs we used vary between 2193 and 2426 $\mu\text{mol kg}^{-1}$ for A_T and between 1968 and 2115
255 $\mu\text{mol kg}^{-1}$ for C_T corresponding to the range of concentrations observed in open ocean water. The CRMs
256 accuracy, as indicated in the certificate for each Batch, is around $\pm 0.5 \mu\text{mol kg}^{-1}$ for both A_T and C_T
(www.nodc.noaa.gov/ocads/oceans/Dickson_CRM/batches.html).

257

258 Results of analyses performed on 965 CRM bottles (different Batches) in 2013-2023 are presented in
Figure 2. The standard-deviations of the differences of measurements were on average around $\pm 3.5 \mu\text{mol kg}^{-1}$ for

259 both A_T and C_T . For unknown reasons, the differences were occasionally up to 10-15 $\mu\text{mol kg}^{-1}$ (0.8% of the
 260 data, Figure S2). These few CRM measurements were discarded for the data processing. On average, and
 261 excluding some outliers, standard-deviations of the differences for 1090 CRM analyses were $\pm 2.71 \mu\text{mol kg}^{-1}$ for
 262 A_T and $\pm 2.86 \mu\text{mol kg}^{-1}$ for C_T , respectively. We did not detect any specific signal for CRM analyses (e.g., larger
 263 uncertainty depending on the Batch number or temporal drifts during analyses, Figure 2) but for some cruises the
 264 accuracy based on CRMs could be slightly better than 3 $\mu\text{mol kg}^{-1}$ (e.g. Marrec et al., 2014; Touratier et al.,
 265 2016; Ganachaud et al., 2017; Wimart-Rousseau et al., 2020a).

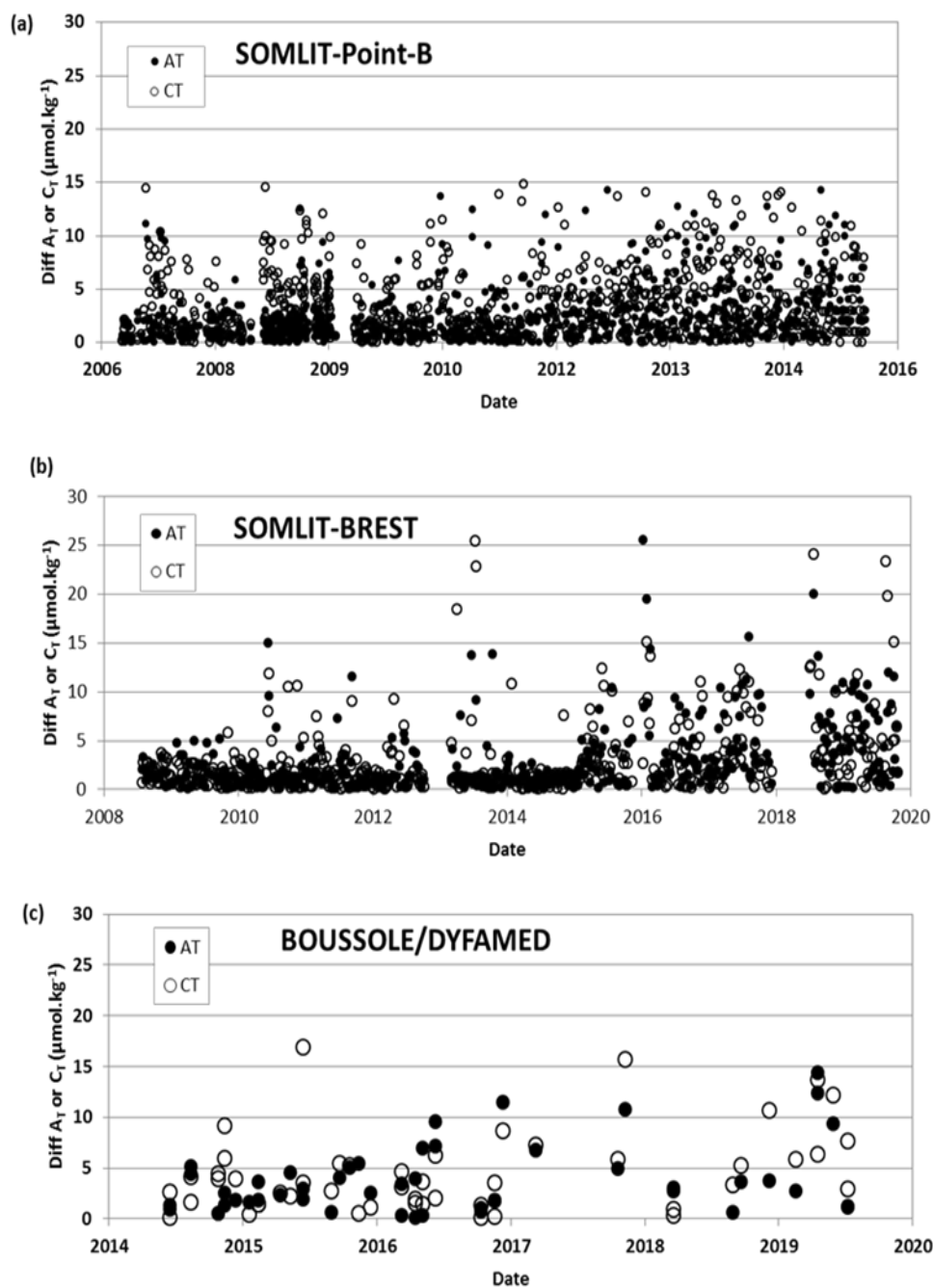


288 **Figure 2:** A_T (a) and C_T (b) analyses for different CRM Batches measured in 2013-2023. For these 965 analyses
 289 the mean and standard-deviations of the differences with the CRM reference were $-0.1 (\pm 3.4) \mu\text{mol kg}^{-1}$ for A_T
 290 and $0.1 (\pm 3.7) \mu\text{mol kg}^{-1}$ for C_T .

293 3.2 Repeatability

294
 295 For some projects, duplicates have been regularly sampled (SOMLIT-Point-B, SOMLIT-BREST,
 296 BOUSSOLE/DYFAMED) or replicate bottles sampled at selected depths at fixed stations during the cruises (e.g.
 297 OUTPACE-2015, SOMBA-2014). Results of A_T and C_T repeatability are synthesized in Table 2 and Figure 3
 298 shows example of regular duplicates from the times-series SOMLIT-Point-B in the coastal Mediterranean Sea,
 299 SOMLIT-Brest in the Bay of Brest, coastal Iroise Sea and BOUSSOLE/DYFAMED in the Ligurian Sea. For the
 300 26 OISO cruises conducted between 1998 and 2018 and the CLIM-EPARSEES cruise in April 2019, the
 301 repeatability was evaluated from duplicate analyses (within 20 minutes time) of continuous sea surface
 302 underway sampling at the same location (when the ship was stopped). Similarly to what was found for the CRM
 303 measurements (Figure S2), differences in duplicates are occasionally higher than 10-15 $\mu\text{mol kg}^{-1}$ (Figure 3) but
 304 most of the duplicates for all projects are within 0 to 3 $\mu\text{mol kg}^{-1}$. Based on the CRM analyses and replicates for

305 different projects, different regions and different periods, we estimated A_T and C_T data to be consistent to better
306 than $4 \mu\text{mol kg}^{-1}$.



347 **Figure 3:** Results of duplicate A_T and C_T analyses from the time-series (a) SOMLIT-Point-B in the coastal
348 Mediterranean Sea (Kapsenberg et al., 2017), (b) SOMLIT-BREST in the Bay of Brest, coastal Iroise Sea (Salt
349 et al., 2016 and unpublished) and (c) BOUSSOLE/DYFAMED in the Ligurian Sea (Merlivat et al., 2018; Golbol
350 et al., 2020). The plots show differences in duplicates for both A_T (filled circles) and C_T (open circles). Standard-
351 deviations of these duplicates are listed in Table 2.

352

353
 354
 355
 356
 357
 358
 359
 360
 361
 362
 363
 364
 365
 366
 367
 368
 369
 370
 371
 372
 373
 374
 375
 376

Table 2: Repeatability of A_T and C_T analyses for cruises with duplicate analysis. The results are expressed as the standard-deviations (Std) of the analysis of replicated samples. Nb = the number of replicates for each Time-series or Cruise (a). For the 26 OISO cruises (1998-2018) and for simplicity we list the mean repeatability obtained for all cruises.

Cruise	Nb	Std A_T $\mu\text{mol kg}^{-1}$	Std C_T $\mu\text{mol kg}^{-1}$	Reference
OUTPACE	12	3.64	3.68	Wagener et al. (2018)
SOMBA	13	2.00	3.30	Keraghel et al. (2020)
SOMLIT-Point-B	786	2.63	3.10	Kapsenberg et al. (2017)
SOMLIT-Brest	446	3.34	3.67	Salt et al. (2016) + unpub
BOUSSOLE	48	3.47	4.02	Merlivat et al. (2018); Golbol et al. (2020)
CLIM-EPARSE	122	2.20	2.30	Lo Monaco et al. (2020, 2021)
OISO 1998-2018	1162	2.06	2.28	Metzl et al. (2006) and (b)

(a) See Figure 3 for the results of regular duplicates for 3 time-series (SOMLIT-Point-B, SOMLIT-BREST, and BOUSSOLE).

(b) Metadata and data available at www.nodc.noaa.gov/ocads/oceans/VOS_Program/OISO.html

3.3 Inter-comparisons

377
 378
 379
 380
 381
 382
 383
 384
 385

Inter-comparisons of measurements performed with different technics help to evaluate the quality of the data and detect potential biases when merging the data in the same region obtained by different laboratories at different periods. This is especially important to interpret long-term trends of A_T and C_T as well as for $p\text{CO}_2$ and pH calculated with A_T/C_T pairs. For ocean acidification studies, this also refers to the “climate goal” for which an accuracy for A_T and C_T better than $\pm 2 \mu\text{mol kg}^{-1}$ is needed (Newton et al., 2015; Tilbrook et al., 2019). For the projects in this data synthesis, inter-laboratory comparisons were performed occasionally and summarized below.

386
 387

3.3.1 CHANNEL project

388
 389
 390
 391
 392
 393
 394
 395
 396

As part of the time-series CHANNEL (2012-2015) in the Western English Channel, Marrec et al. (2014) analyzed surface samples collected bi-monthly in 2011-2013. A_T analyses were performed with a TA-ALK-2 system (Appolo SciTech.) while C_T measurements were acquired with an AIRICA system (Marianda Inc.) Based on CRM analyses (Batch #92) the accuracy was estimated $\pm 3 \mu\text{mol kg}^{-1}$ for A_T and $\pm 1.5 \mu\text{mol kg}^{-1}$ for C_T (Marrec et al., 2014). When comparing with the samples measured at LOCEAN/Paris for the year 2012, Marrec et al. (2014) concluded that between the two methods the concentrations were within $\pm 2 \mu\text{mol kg}^{-1}$ and $\pm 3 \mu\text{mol kg}^{-1}$ for A_T and C_T respectively. This is close to the “climate goal” offering confident results for long-term trend analysis of the carbonate system in this region.

397
 398

3.3.2 SURATLANT project

399
 400
 401

In the frame of the SURATLANT project in the subpolar North Atlantic gyre, some samples collected at the same time (in 2005, 2006, 2010, 2015, and 2016) were also analyzed onshore for A_T and/or C_T by other

laboratories using different technics (e.g. coulometric method) and the results summarized by Reverdin et al. (2018). For C_T , the mean (and STD) differences between LOCEAN values and from 4 other laboratories range between $-0.7 (\pm 4.6)$ and $-6.5 (\pm 3.4) \mu\text{mol kg}^{-1}$ depending on the cruise. For A_T the mean differences with 2 other laboratories range from $-0.6 (\pm 4.1) \mu\text{mol kg}^{-1}$ to $+2.3 (\pm 4.8) \mu\text{mol kg}^{-1}$.

406

407 3.3.3 OVIDE project

408

409 During OVIDE cruises conducted since 2002 in the North Atlantic along a section from Greenland to
410 Portugal (Lherminier et al., 2007; Mercier et al., 2015) samples have been taken (since 2006) to complement, for
411 summer, the SURATLANT time-series in the North Atlantic subpolar gyre (NASPG). The OVIDE samples at
412 the surface and along the water-column at a few stations were measured back at LOCEAN for A_T and C_T (Metzl
413 et al., 2018). This enables us to compare our data with the measurements performed on-board by the IIM group
414 in Vigo/Spain (e.g. Pérez et al., 2010, 2013, 2018; Vazquez-Rodriguez et al., 2012). The OVIDE data have been
415 regularly quality controlled in CARINA and GLODAP data products (Velo et al., 2009; Key et al., 2010; Olsen
416 et al., 2016, 2019, 2020). The results of inter-comparisons are gathered in Table 3. For OVIDE in 2006 we
417 identified (for unknown reason) a large difference between our original A_T values compared to the A_T data
418 qualified in GLODAP and we thus corrected our A_T data by $+7.2 \mu\text{mol kg}^{-1}$. However, no correction was applied
419 for C_T . For other OVIDE cruises, differences for A_T range between $-4.5 (\pm 4.11) \mu\text{mol kg}^{-1}$ and $-0.05 (\pm 3.43)$
420 $\mu\text{mol kg}^{-1}$ depending on the cruise (i.e. A_T measured at LOCEAN was always slightly lower than onboard
421 measurements). For C_T , we compared our measurements onshore with C_T values calculated with A_T and pH
422 measured onboard. Most of the mean C_T differences are slightly positive (i.e. C_T measured at LOCEAN was
423 always higher, except for 2010). Taking into account all errors associated with the sampling, the transport of
424 samples, the instrumentations, the data processing, or the calculations for C_T using A_T /pH pairs (around $8.8 \mu\text{mol}$
425 kg^{-1} , Orr et al, 2018), the comparisons between LOCEAN and IIM data for OVIDE cruises are deemed
426 acceptable and large differences for both A_T and C_T ($> 4 \mu\text{mol kg}^{-1}$) are far from being systematic (Table 3). The
427 data from SURATLANT and OVIDE can then be merged to complete the time-series in the NASPG in summer
428 and to better describe the seasonality of the oceanic carbonate system. For example, in 2010, when the North
429 Atlantic Oscillation (NAO) was strongly negative, the SURATLANT data showed a rapid decrease of C_T
430 concentrations in the NASPG between early June and August (Figure 4), with C_T concentrations in August much
431 lower than other years (Racapé et al., 2014). This leads to a rapid drop in $f\text{CO}_2$ in 2009-2010, such that the
432 NASPG was a strong CO_2 sink (Leseurre et al., 2020). The winter-to-summer seasonal decrease of C_T in 2010 in
433 the north NASPG was on average $-77 \mu\text{mol kg}^{-1}$ (Figure 4) much larger than in the climatology (range -50 to -55
434 $\mu\text{mol kg}^{-1}$, Takahashi et al., 2014; Reverdin et al., 2018). The OVIDE data in late June 2010 and SURATLANT
435 in August 2010 confirmed this signal that was linked to a pronounced primary productivity in that period (Figure
436 4, Henson et al., 2013; Racapé et al., 2014; Mc Kinley et al., 2018). Notice that for this period no $f\text{CO}_2$
437 observations were available in July-September 2010 in SOCAT data product and the A_T/C_T data presented here
438 could be used to calculate $f\text{CO}_2$ to complement the $f\text{CO}_2$ dataset in this region like was done for other periods
439 (Mc Kinley et al., 2011).

440

441
442
443
444
445
446
447
448
449
450
451
452
453
454
455
456
457
458
459
460
461
462
463
464
465
466
467
468
469
470
471
472
473
474
475
476
477
478
479
480
481
482
483
484
485
486
487
488
489
490
491
492
493
494
495
496

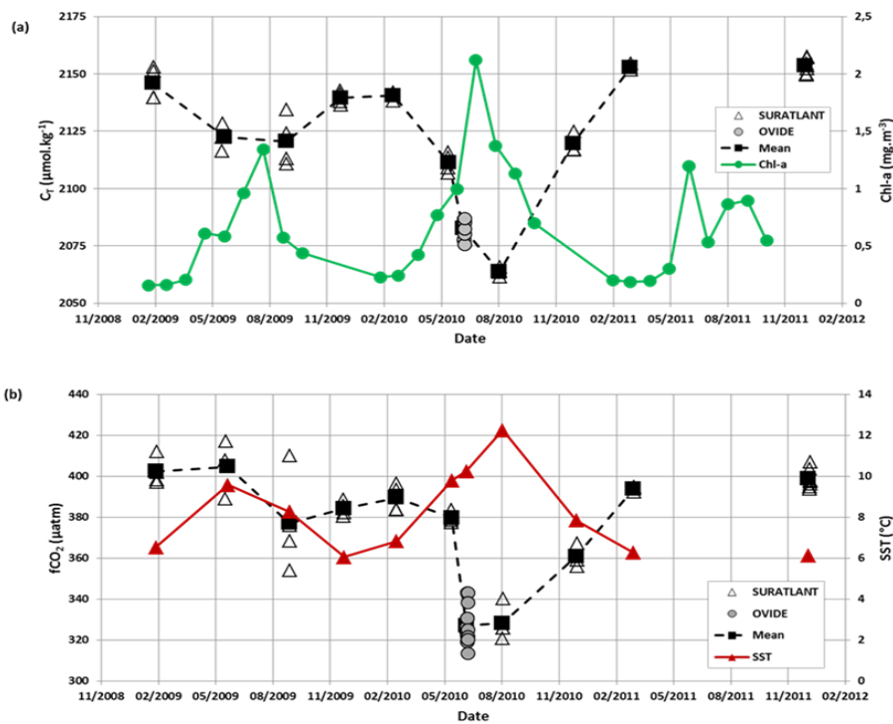


Figure 4: (a) Time-series of C_T concentrations ($\mu\text{mol.kg}^{-1}$) for 2009-2011 in surface waters in the North Atlantic subpolar gyre (zone 59°N - 33°W) based on SURATLANT (open triangles) and OVIDE-2010 (grey circles) data. In 2009, SURATLANT data were available in February, June, September and December, while in 2010 data available in March, June, August and December and in 2011 data only available for March and December. The OVIDE data in late June 2010 completed the temporal cycle and confirmed the strong seasonal signal and low C_T concentrations in summer 2010 not seen in 2009 (or in 2011 as there is no data in summer). The mean observations for each period describe the C_T seasonal cycles in 2009 and 2010 (Black squares, dashed line). The monthly surface chlorophyll-a concentrations (Chl-a, mg.m^{-3}) averaged in the same region based on MODIS are also shown (Green dots and line) highlighting the high productivity during the summer 2010. Chl-a monthly data extracted from MODIS (Giovanni/NASA, last access 3/5/19). (b): Time-series of $f\text{CO}_2$ (μatm) for the same cruises (same symbols) calculated with A_T/C_T and using the K1, K2 constants from Lueker et al (2000). Mean SST ($^\circ\text{C}$) indicated (red triangles). In June 2010 oceanic $f\text{CO}_2$ decreased by $53 \mu\text{atm}$ in 2 weeks.

Table 3: Comparisons of A_T and C_T samples measured back at LOCEAN with measurements onboard by IIM Laboratory (F. Pérez, Vigo, Spain) for OVIDE cruises in the North Atlantic. Nb= Number of samples. ND= No Data. The results listed indicate the mean and standard-deviations of the differences (LOCEAN-IIM). For A_T , IIM values were measured on-board. For C_T , IIM values were calculated from A_T and pH both measured onboard. The IIM data were quality controlled and here taken from the GLODAP data products (Olsen et al, 2016, 2019).

Cruise Year	Nb A_T	A_T (LOCEAN) - A_T (IIM) $\mu\text{mol kg}^{-1}$	Nb C_T	C_T (LOCEAN) - C_T (IIM) $\mu\text{mol kg}^{-1}$
OVIDE-2006	14	-2.0 (\pm 5.9) (*)	14	1.1 (\pm 2.5)
OVIDE-2008	29	-4.5 (\pm 4.1)	29	3.8 (\pm 3.1)
OVIDE-2010	41	-2.0 (\pm 2.3)	41	-2.4 (\pm 3.3)
OVIDE-2012	37	-0.1 (\pm 8.8)	ND	ND
GEOVIDE-2014	57	-0.1 (\pm 3.4)	54	2.4 (\pm 7.9)

(*) for the OVIDE 2006 cruise original difference for A_T was $-9.0 (\pm 5.8) \mu\text{mol kg}^{-1}$ and LOCEAN A_T data were corrected by $+7.2 \mu\text{mol kg}^{-1}$ based on the mean concentrations in deep layers. No corrections were applied for A_T and C_T for other cruises.

497 3.3.4 PENZE river

498

499 The comparisons described above concern the open ocean region with A_T and C_T concentrations in a
500 range of concentrations close to the CRM references (used by the different laboratories). Another example of
501 comparison is presented here for samples obtained along a river and thus for waters with low salinity and A_T
502 concentrations (river Penzé in North Brittany). In 2019-2020, A_T was measured at SBR laboratory (Station
503 Biologique de Roscoff) by a potentiometric method (using a Titrino-847 plus Metrohm) calibrated with CRM
504 (Batch #131) for a final accuracy of $\pm 2.1 \mu\text{mol kg}^{-1}$ (Gac et al., 2020). Although the samples were measured
505 with different techniques the A_T /Salinity relationships are very coherent for both datasets (Figure 5). The
506 regressions for each period are for A_T (in $\mu\text{mol kg}^{-1}$):

507

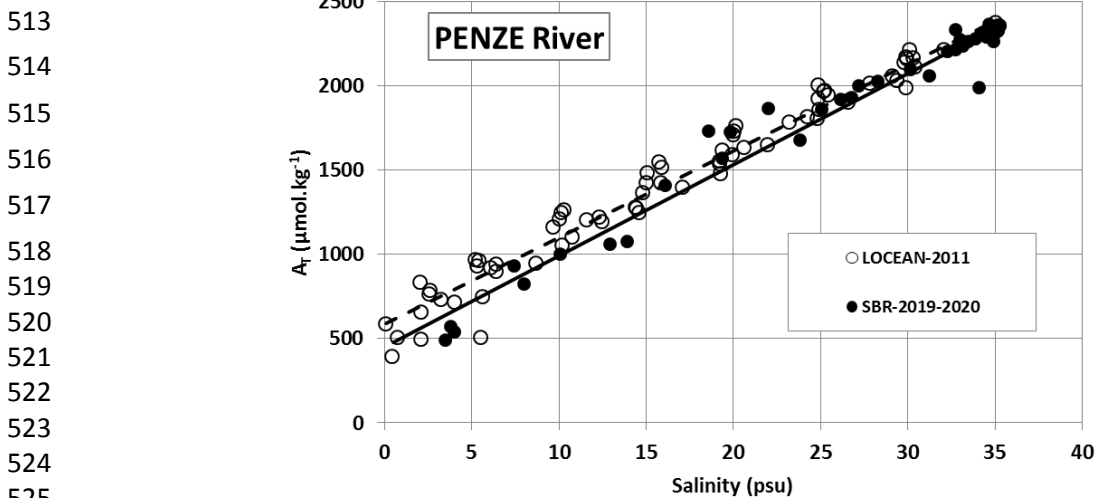
508 In 2011 (78 samples): $A_T = 51.525 (\pm 0.944) S + 583.95 (\pm 19.94) (r^2 = 0.975)$

509 In 2019-2020 (70 samples): $A_T = 54.022 (\pm 1.018) S + 450.23 (\pm 31.53) (r^2 = 0.976)$

510

511 Therefore we added the A_T data measured in 2019-2020 to complete the synthesis for this location (river Penzé).

512



513

514 **Figure 5:** Total alkalinity (A_T) versus salinity for samples measured in 2011 and 2019 in the river Penzé, North
528 Brittany (Gac et al., 2020). A_T samples were measured at LOCEAN in 2011 (open circles, dashed-line) and at
529 SBR laboratory (Roscoff) in 2019 (filled circles, black line).

530

531 3.4 Quality control assigned flags

532

533 Identifying each data with an appropriate flag is very convenient for selecting the data (good,
534 questionable or bad). Here we used 4 flags for each property (flags 2 = good, 3= questionable, 4=bad, and 9= no
535 data) following the WOCE program and used in other data products such as SOCAT (Bakker et al., 2016) or
536 GLODAP (Olsen et al., 2016, 2019, 2020; Lauvset et al., 2021). During the data-processing, we first assigned a
537 flag for each A_T and C_T data based on the standard error in the calculation of A_T and C_T concentrations (non-
538 linear regression, Dickson et al. 2007). By default, if the standard-deviation on the regression is $> 1 \mu\text{mol kg}^{-1}$,
539 we assigned a flag 3 (questionable) although the data could be acceptable and then used for interpretations. Flag
540 3 was also assigned when salinity was doubtful or when differences of duplicates were large (e.g. $\pm 20 \mu\text{mol kg}^{-1}$).
541 1). Flags 4 (bad or certainly bad) were assigned when clear anomalies were detected for unknown reason (e.g. a

542 sample probably not fixed with HgCl_2). A secondary quality control was performed by the PIs of each project
 543 based on data inspection, duplicates, A_T /Salinity relationship, or the mean observations in deep layers where
 544 large variability in A_T and C_T is unlikely to occur from year to year. An example presents all data from the
 545 MOOSE-GE cruises conducted in 2010-2019 in the Mediterranean Sea (Coppola et al., 2020; Testor et al., 2010)
 546 where clear outliers have been identified (Figure S3). For the 10 MOOSE-GE cruises and a total of 1847 A_T and
 547 C_T analyses, 26 were identified flagged as bad (flag 4), 139 for A_T and 141 for C_T listed as questionable (flag 3)
 548 and 1682 for A_T and 1680 for C_T considered as good data (flag 2, i.e. more than 90%). Similar control was
 549 performed for each project.

550 The synthesis of various cruises in the same region and period also offers verification and secondary
 551 control of the data. For example, several cruises were conducted in the Mediterranean Sea in 2014 (MOOSE-GE,
 552 SOMBA, ANTARES and DYFAMED). The mean values of C_T and A_T in the deep layers ($> 1800\text{m}$) for each
 553 cruise confirmed the coherence of the data (Table 4). This enabled to merge the different datasets for
 554 interpretations of the temporal trends and processes driving the CO_2 cycle (Coppola et al., 2019, 2020; Ulses et
 555 al., 2023) or to train and validate a regional neural network to reconstruct the carbonate system (e.g. CANYON-
 556 MED, Fourier et al., 2020, 2022).

557
 558
 559 **Table 4:** Mean observations in the deep layers ($> 1800\text{m}$) of the Western Mediterranean Sea for different cruises
 560 conducted in 2014. Results in deep layers ($> 1800\text{m}$) for the DEWEX cruise in 2013 and the PEACETIME
 561 cruise in 2017 in the same region are also listed. N- A_T and N- C_T are A_T and C_T normalized at salinity = 38. Nb =
 562 number of data (with flag 2). Standard-deviations are in brackets. References for these cruises are listed in
 563 Supplementary Material.

Cruise	Period	Nb	Pot. Temp ($^{\circ}\text{C}$)	Salinity (PSU)	N- A_T ($\mu\text{mol kg}^{-1}$)	N- C_T ($\mu\text{mol kg}^{-1}$)
All cruises	Feb/Dec-2014	76	12.905 (0.007)	38.486 (0.005)	2562.9 (5.3)	2303.7 (4.7)
ANTARES	Feb/Nov-2014	14	12.913 (0.004)	38.488 (0.006)	2564.0 (3.8)	2301.9 (3.5)
DYFAMED	Mar/Dec-2014	9	12.905 (0.0016)	38.487 (0.004)	2560.1 (5.0)	2304.3 (6.8)
MOOSE-GE	Jul-2014	21	12.909 (0.004)	38.487 (0.005)	2565.6 (4.6)	2303.5 (4.1)
SOMBA	Aug/Sep-2014	32	12.899 (0.005)	38.483 (0.005)	2561.5 (5.6)	2304.6 (4.8)
DEWEX	Feb/Apr-2013	44	12.903 (0.010)	38.588 (0.006)	2556.0 (4.3)	2294.0 (5.7)
PEACETIME	May/Jun-2017	7	12.904 (0.002)	38.486 (0.003)	2567.2 (10.6)	2308.1 (8.9)

593 The total number of data for the Global Ocean and the Mediterranean Sea are gathered in Table 5 with
 594 corresponding flags for each property. Overall, the synthesis includes more than 94% of good data for both A_T

595 and C_T . About 5% are questionable and 2% are likely bad. Overall, we believe that all data (with flag 2) in this
 596 synthesis have an accuracy better than $4 \mu\text{mol kg}^{-1}$ for both A_T and C_T , the same as for quality-controlled data in
 597 GLODAP (Olsen et al., 2020; Lauvset et al., 2021). The uncertainty ranges between the “Climate goal” ($2 \mu\text{mol}$
 598 kg^{-1}) and the “Weather Goal” ($10 \mu\text{mol kg}^{-1}$) for ocean acidification studies (Newton et al., 2015; Tilbrook et al.,
 599 2019). This accuracy is also relevant to validate or constraint data-based methods that reconstruct A_T and C_T
 600 fields with an error of around $10\text{-}15 \mu\text{mol kg}^{-1}$ for both properties (Bittig et al., 2018; Broullón et al., 2019, 2020;
 601 Fourrier et al., 2020; Chau et al., 2023).

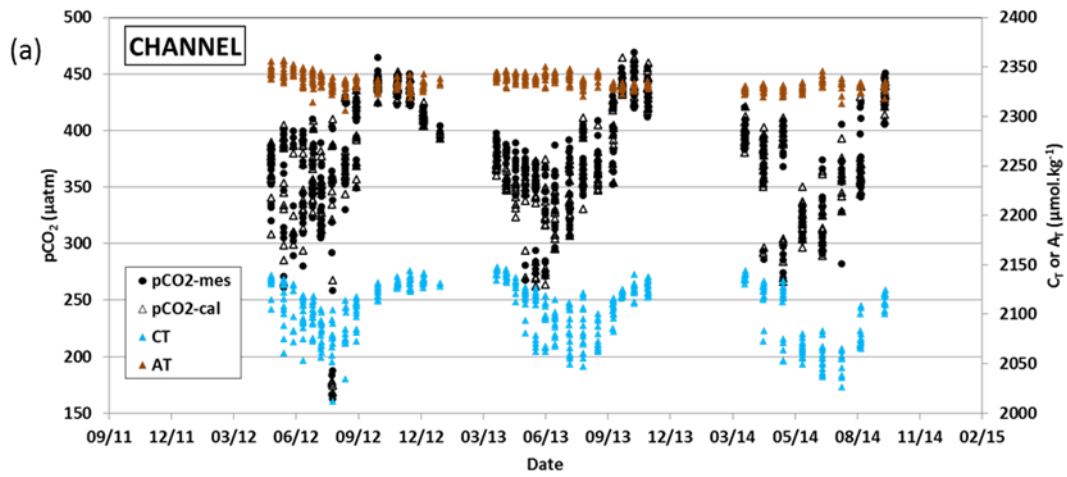
602
 603 **Table 5:** Number of Temperature, Salinity, A_T and C_T data in the synthesis identified for flags 2, 3, 4, 9. The
 604 data are given for the full data-set Global Ocean and for the Mediterranean Sea. Last column is the percentage of
 605 flag 2 (Good).
 606

	Flag 2	Flag 3	Flag 4	Flag 9	% Flag 2
Global Ocean					
Temperature	43538	410	0	478	99.07
Salinity	44033	319	2	71	99.28
A_T	39331	2144	1165	1787	92.24
C_T	39921	2091	1148	1279	92.50
Mediterranean Sea					
Temperature	9843	1	0	65	99.99
Salinity	9879	8	2	20	99.99
A_T	8853	425	411	220	91.37
C_T	8854	451	389	211	91.33

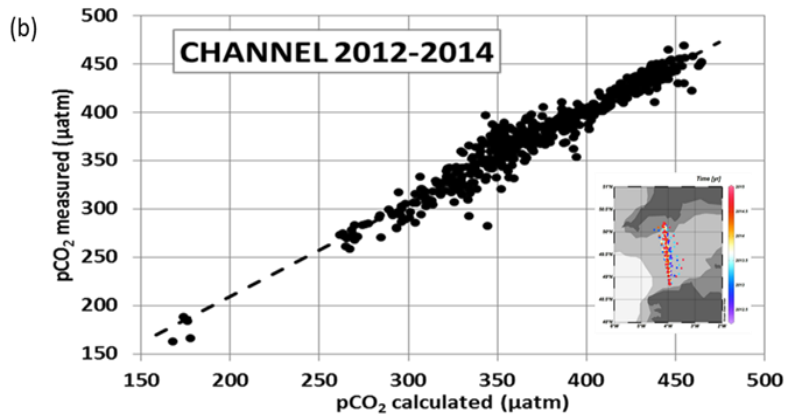
627 3.5 Using A_T and C_T to calculate $f\text{CO}_2$ and pH and compare with $f\text{CO}_2$ and pH measurements

630 For some projects, the A_T and C_T data presented in this synthesis were used to calibrate or validate in
 631 situ $f\text{CO}_2$ sensors (Bozec et al., 2011; Marrec et al., 2014; Merlivat et al., 2018). The A_T and C_T data were also
 632 used to calculate $f\text{CO}_2$ and to derive associated air-sea CO_2 fluxes, especially during periods when no direct $f\text{CO}_2$
 633 measurements were available (e.g. in the North Atlantic, Figure 4, Watson et al., 2009; Mc Kinley et al., 2011).
 634 For example, Marrec et al. (2014) successfully used the calculated $p\text{CO}_2$ (with A_T/C_T pairs) to adjust the drift of
 635 the $p\text{CO}_2$ data recorded with a Contros-HydroC/CO2 FT sensor mounted on a FerryBox for regularly sampling
 636 the Western English Channel (CHANNEL project). Here we show the results for the period 2012-2014 (Figure
 637 6). In this region the total alkalinity is relatively constant over time; the average of A_T for 528 samples at
 638 different seasons and years is $2334.4 (\pm 7.2) \mu\text{mol kg}^{-1}$. On the opposite, the C_T concentrations show distinctive
 639 seasonality, with higher concentrations in winter and lower in summer when biological activity is pronounced
 640 (Marrec et al., 2013, 2014; Kitidis et al., 2019). This controls the seasonal $p\text{CO}_2$ distribution revealed each year
 641 in both measured and calculated $p\text{CO}_2$ (Figure 6). For 528 co-located samples the mean difference between
 642 calculated and measured $p\text{CO}_2$ is $-1.9 (\pm 11.9) \mu\text{atm}$ with no distinct differences depending on the season and
 643 year.
 644

645
646
647
648
649
650
651
652
653
654
655
656
657



658
659
660
661
662
663
664
665
666
667
668
669
670



671
672
673
674
675
676

Figure 6: (a): Time-series of A_T (brown triangles, right Y-axis), C_T (blue triangles, right Y-axis), pCO_2 calculated (open triangles, left Y-axis) and pCO_2 measured (filled circles) in the Western English Channel in 2012-2014 (Marrec et al., 2014). (b): Measured pCO_2 versus calculated pCO_2 for the same samples. The mean difference ($pCO_{2cal}-pCO_{2mes}$) for 528 samples is $-1.9 \mu\text{atm} (\pm 11.9) \mu\text{atm}$. Data from Marrec and Bozec (2016 a,b; 2017). Localization of the samples is shown in the inserted map.

677
678
679
680
681
682
683
684
685
686
687
688
689
690
691
692

In the Ligurian Sea, following the first high frequency in situ fCO_2 measurements in 1995-1997 at the DYFAMED time-series station (Hood and Merlivat, 2001), a new CARIOCA fCO_2 sensor was deployed at that location in 2013 (BOUSSOLE project, Merlivat et al., 2018). The CARIOCA sensor was calibrated with regular A_T/C_T analyses performed at LOCEAN. Based on these data, the mean difference between CARIOCA- fCO_2 measurements and calculated- fCO_2 data was estimated to be around $\pm 4.4 \mu\text{atm}$ for 2013-2015, i.e. the same order than the precision of the CARIOCA sensor ($\pm 5 \mu\text{atm}$, Merlivat et al., 2018). Here we extend the results for the period 2013-2018 (Golbol et al., 2020; data also in SOCAT version v2021, Bakker et al., 2016) and compared the CARIOCA fCO_2 time-series with A_T and C_T data from different cruises (BOUSSOLE, DYFAMED and MOOSE-GE) selected in the layer 0-20m at that location (Figure S4). For 67 co-located samples at different seasons and years, the mean difference between calculated and measured fCO_2 ($fCO_{2cal}-fCO_{2mes}$) was $-3.7 \mu\text{atm} (\pm 10.8) \mu\text{atm}$ where fCO_2 was calculated from A_T/C_T pairs using the constant from Lueker et al (2000). At that location, the alkalinity is relatively constant over 2013-2018 with an average concentration of $2569.8 (\pm 13.2) \mu\text{mol kg}^{-1}$. C_T concentrations show a clear seasonality, decreasing by around $50 \mu\text{mol kg}^{-1}$ from winter to late summer driving the large seasonal cycle of fCO_2 (range $80 \mu\text{atm}$) revealed in both measured and calculated values (here fCO_2 is normalized at 13°C , Figure S4). In addition to calibration purposes, a regional A_T /Salinity relationship was derived from the A_T data measured at that location and successfully used to construct time-

693 series of C_T and pH calculated from the high-frequency CARIOCA fCO_2 data to investigate and interpret the
694 long-term change of fCO_2 and acidification in the Ligurian Sea (Merlivat et al., 2018; Coppola et al., 2020).

695 A CARIOCA sensor was also deployed in 2003 near the SOMLIT-Brest time-series site in the Bay of
696 Brest (Bozec et al., 2011; Salt et al., 2016). As for BOUSSOLE in the Ligurian Sea, samples collected for A_T and
697 C_T were used for validation of the pCO_2 recorded by the CARIOCA sensor and the comparison with calculated
698 pCO_2 showed a good agreement, i.e. $pCO_{2cal} = 0.98 * pCO_{2mes} + 7 \mu atm$ (Bozec et al., 2011). CARIOCA sensors
699 were also deployed on moorings in the Tropical Atlantic (PIRATA project, e.g. Lefèvre et al., 2008, 2016;
700 Parard et al., 2010). With the discrete A_T and C_T data included in this synthesis (EGEE and PIRATA-FR cruises),
701 the fCO_2 data from CARIOCA sensor associated with an adapted A_T /Salinity relationship were used to derive pH
702 (Lefèvre et al., 2016) or C_T time-series to evaluate net community production in the Eastern tropical Atlantic
703 (Parard et al., 2010; Lefèvre and Merlivat 2012).

704 Although this is not a direct instrumental inter-comparison, differences between pCO_2 (or fCO_2)
705 calculated using A_T/C_T pairs with direct pCO_2 measurements give a glimpse of the quality of A_T and C_T data in
706 this synthesis given the uncertainty attached to the pCO_2 or pH calculations (Orr et al., 2015). For example, in
707 the frame of the SURATLANT project in the North Atlantic, calculated fCO_2 data were compared with co-
708 located fCO_2 measurements for different seasons and years (Figure S5). The mean differences ($fCO_{2cal} - fCO_{2mes}$)
709 ranged between $-4.3 \mu atm (\pm 12.9) \mu atm$ (2004-2007, 74 co-located samples) and $-3.0 (\pm 12.1) \mu atm$ (2014-2015,
710 98 co-located samples). The differences are almost the same for different years (and seasons) and are thus
711 attributed to method uncertainties (including sampling time, measurement errors, and data processing). Based on
712 these comparisons and the consistency between data we are confident that the A_T and C_T data presented in this
713 synthesis could be used to calculate fCO_2 (and pH) and interpret temporal changes and drivers of these
714 parameters as well as to estimate air-sea CO_2 fluxes in the North Atlantic (e.g. Corbière et al., 2007; Schuster et
715 al., 2009, 2013; Watson et al., 2009; Metzl et al., 2010; Mc Kinley et al., 2011; Reverdin et al., 2018, Kitidis et
716 al., 2019; Leseurre et al., 2020).

717 The A_T and C_T data in this synthesis have been also successfully used for fCO_2 and air-sea CO_2 fluxes
718 calculations in other regions: the tropical Atlantic (Koffi et al., 2010), the tropical Pacific (Moutin et al., 2018;
719 Wagener et al., 2018), the Solomon sea (Ganachaud et al., 2017) or the Mediterranean sea and coastal zones (De
720 Carlo et al., 2013; Marrec et al., 2015; Kapsenberg et al., 2017; Coppola et al., 2020; Keraghel et al., 2020;
721 Wimart-Rousseau et al., 2020a; Gattuso et al., 2023).

722 In addition, A_T and C_T data in the surface and the water-column are also relevant to calculate pH and
723 evaluate its rate of change for addressing ocean acidification topic in different regions (Kapsenberg et al., 2017;
724 Ganachaud et al., 2017; Wagener et al., 2018; Coppola et al., 2020; Leseurre et al., 2020; Lo Monaco et al.,
725 2021). At the time-series station ECOSCOPA in the Bay of Brest (Fleury et al., 2023; Petton et al., 2023), pH
726 calculated with A_T/C_T data were compared with direct pH measurements (Figure S6). In 2017-2019, pH (at
727 standard temperature 25°C, pH-25C) was always lower than 8 and presented a large seasonal signal of 0.3 (high
728 pH values in spring, low in winter). The mean difference between calculated and measured pH-25C for 46
729 samples was equal to $+0.013 (\pm 0.010)$ which is in the range of the pH uncertainty evaluated by error
730 propagation when calculated from A_T/C_T pairs (A_T and C_T error of $\pm 3 \mu mol kg^{-1}$ leads to pH error of ± 0.0144).
731 Part of these A_T and C_T data used to calculate pH also helped for interpreting the response of marine species to
732 acidification, e.g. pteropodes or coccolithophores (*Emiliana huxleyi*) in the Mediterranean Sea (Howes et al.,
733 2015, 2017; Meier et al., 2014) or in the Southern Ocean (Beaufort et al., 2011). The A_T and C_T data were also

734 supporting environmental analysis in coral reef ecosystems in the tropical Pacific (TARA Expedition, Douville
735 et al., 2022; Lombard et al., 2023; Canesi et al., 2023).

736

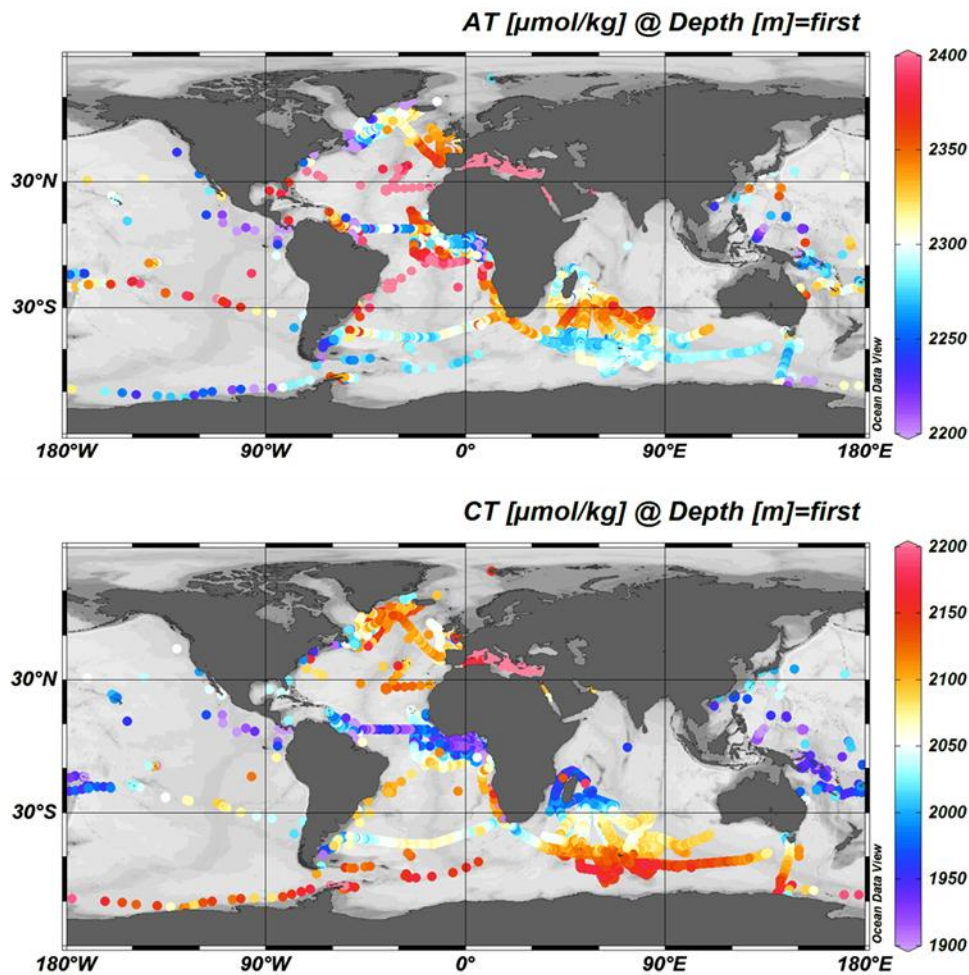
737 4 Global distribution and relationships from A_T and C_T based on the SNAPO-CO2 dataset

738

739 The surface distribution in the global ocean based on the SNAPO-CO2 dataset is presented in Figure 7
740 for A_T and C_T . In the open ocean, high A_T concentrations are identified in the subtropics in all basins (Jiang et al.,
741 2014; Takahashi et al., 2014) with highest concentrations up to $2484 \mu\text{mol kg}^{-1}$ in the central North Atlantic
742 (STRASSE cruise in August 2012, $26^\circ\text{N}/36^\circ\text{W}$). In surface and at depth, the A_T /Salinity and A_T/C_T relationships
743 are clearly identified and structured at regional scale (Figure 8).

744

745



756

757 **Figure 7:** Distribution of A_T (top) and C_T (bottom) concentrations ($\mu\text{mol.kg}^{-1}$) in surface waters (0-10m). Only
758 data with flag 2 are presented in these figures. Figures produced with ODV (Schlitzer, 2018).

759

760

761

762

763

764

765

766

767

768

769

770

771

772

773

774

775

776

777
778
779
780
781
782
783
784
785
786
787
788
789
790
791
792
793
794
795
796
797
798
799
800
801
802
803
804
805
806
807
808
809
810
811
812
813
814
815
816
817
818
819
820
821
822
823
824
825
826
827
828
829
830
831

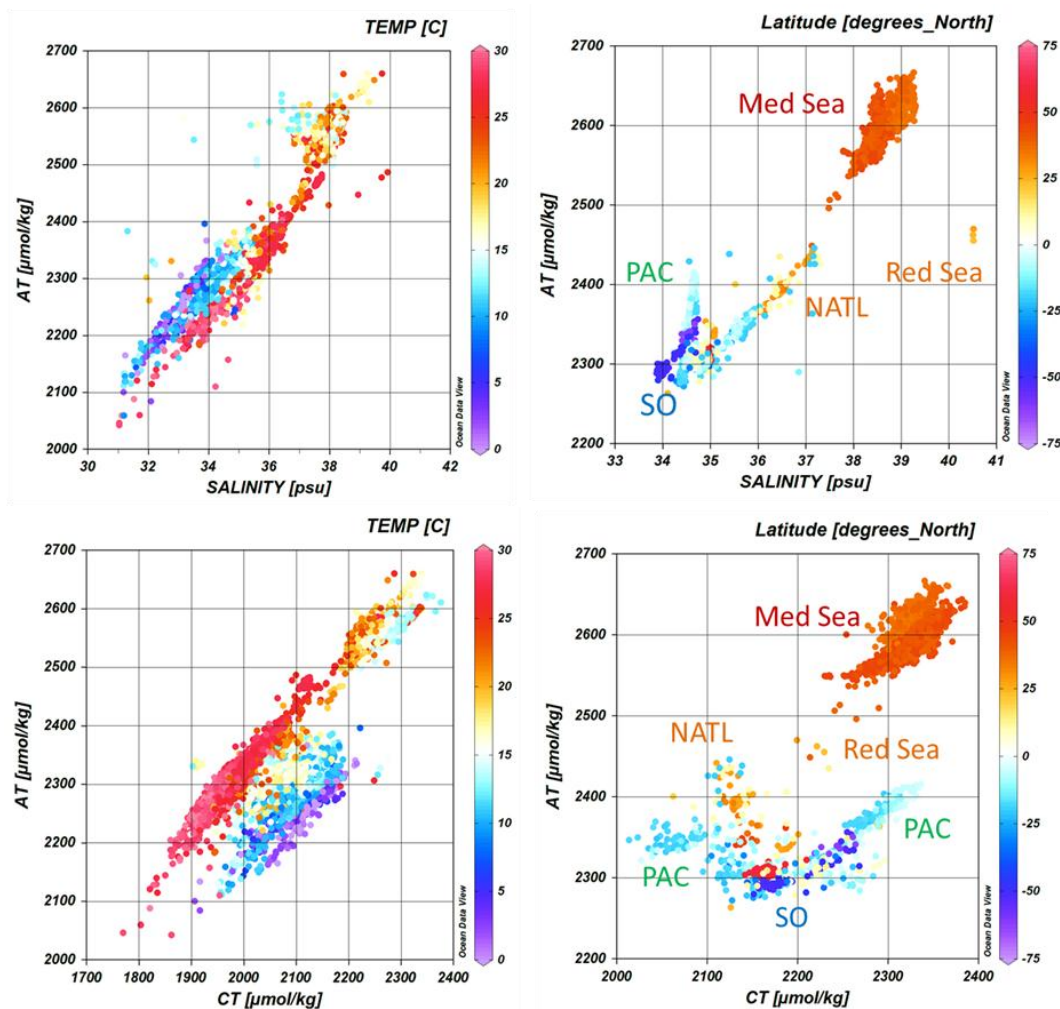


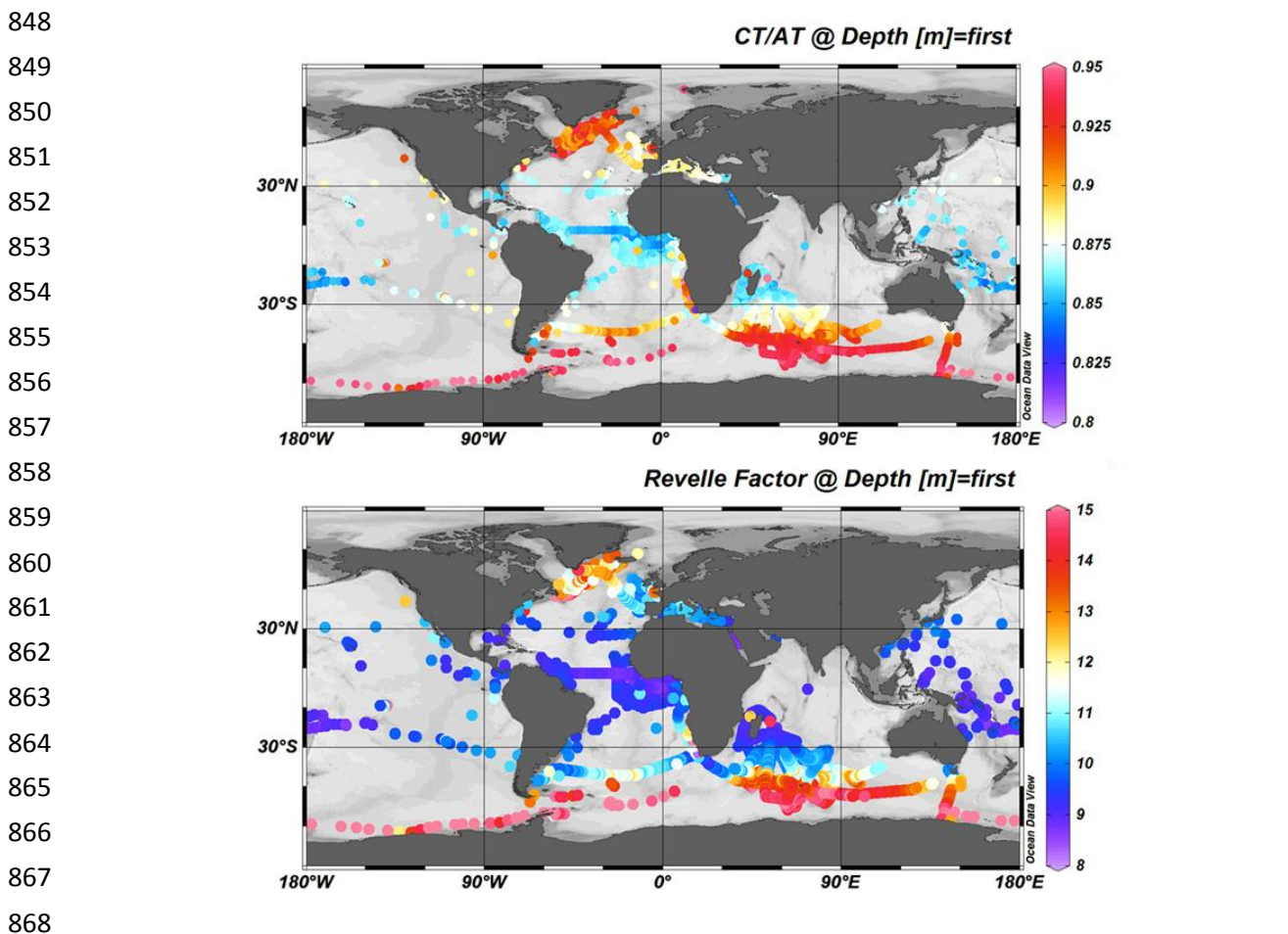
Figure 8: Relationships between A_T and Salinity (upper panel) and A_T versus C_T (lower panel) for samples in surface waters (0-10m and SSS > 31) (left) and in the water column below 100m (right). Only data with flag 2 are presented. The color scales correspond to the temperature (left) or the latitude (right). Some location of data are identified: Mediterranean Sea (Med Sea), Red Sea, Tropical Pacific (PAC), North Atlantic (NATL) and Southern Ocean (SO). Figures produced with ODV (Schlitzer, 2018).

In the Eastern tropical Atlantic (ETA) where the Congo River impacts the salinity field (Vangriesheim et al., 2009), A_T concentrations range between 2100 and 2400 $\mu\text{mol kg}^{-1}$. The regional A_T /Salinity relationship in the ETA based on data from the EGEE cruises in 2005-2007 (Koffi et al., 2010) is robust and validated with more recent measurements from PIRATA-FR cruises in 2010-2019 (Lefevre et al., 2021). The strong A_T /Salinity relationship in the ETA was also recognized using data from the TARA-MICROBIOME cruise in May-July 2022 (Figure S7). Low salinity (< 30) and low A_T (1700-2200 $\mu\text{mol kg}^{-1}$) are also observed in the Western tropical Atlantic near the Amazon River plume. The A_T /Salinity relationships in both river plume regions are very similar (Figure S7).

For C_T , the lowest concentrations were observed in the coastal regions of the Tropical Atlantic, on the eastern side in the Gulf of Guinea (BIOZAIRE cruise in 2003, 6°S/11°E, $C_T=1390 \mu\text{mol kg}^{-1}$, Vangriesheim et al., 2009) and on the Western side in coastal zone off French Guyana (PLUMAND cruise in 2007, 5°N/51°W, $C_T=1512 \mu\text{mol kg}^{-1}$, Lefèvre et al., 2010). Such low C_T concentrations were also observed around 5°N/51°W in the Amazon River plume during the recent EUREC4A-OA cruise in 2020 and the TARA-MICROBIOME cruise in 2021 ($C_T=1451 \mu\text{mol kg}^{-1}$) leading to low oceanic $f\text{CO}_2$ (< 350 μatm) and a CO_2 sink in this region (Olivier et al., 2022).

832 The high C_T concentrations were mainly observed in the Southern Ocean (OISO and ACE cruises)
 833 south of the Polar Front around 50°S linked to the upwelling of C_T -rich deep water (Figure 7, Metzl et al., 2006;
 834 Wu et al., 2019; Chen et al., 2022). This leads to a high C_T/A_T ratio and a high Revelle factor in the Southern
 835 Ocean (Figure 9, Fassbender et al., 2017). The high C_T content and low temperature in the Southern Ocean also
 836 lead to low calcite and aragonite saturation state (Ω) (Takahashi et al., 2014; Jiang et al., 2015). We calculate Ω
 837 from A_T and C_T data at insitu temperature, salinity and pressure. At present the surface ocean is not under-
 838 saturated with regard to aragonite (Figure 10); however, under-saturation levels ($\Omega-Ar < 1$) were found around
 839 500 m in the Southern Ocean (ACE cruise in 2017, MODYDICK cruise in 2018), 1000 m in the Tropical Pacific
 840 (PANDORA 2012 and OUTPACE 2015 cruises) and 2200 m in the North Atlantic (OVIDE 2012 and 2014
 841 cruises, see also Turk et al., 2017) (Figure 10). Samples at 400 m from the TARA-Oceans cruise in 2009-2012
 842 also indicated aragonite under-saturation in the Equatorial Atlantic, Equatorial Pacific, as well as off South
 843 America (73°W-34°S, Chile) associated to equatorial or eastern boundary upwelling systems (Feely et al., 2012;
 844 Lauvset et al., 2020).

845 In surface, $\Omega-Ar > 3$ is found in the latitudinal band 45°S-54°N and $\Omega-Ar < 3$, below the critical
 846 threshold of $\Omega-Ar = 3.25$ that represents a limit for distribution of tropical coral reefs (Hoegh-Guldberg et al.,
 847 2007) is observed at very few locations in the tropics.



869 **Figure 9:** Distribution of the C_T/A_T ratio (top) and the Revelle factor (bottom) in surface waters (0-10m). Only
 870 data with flag 2 were used. Figures produced with ODV (Schlitzer, 2018).

871
 872
 873
 874
 875
 876
 877
 878
 879
 880
 881
 882
 883
 884
 885
 886
 887
 888
 889
 890
 891
 892
 893
 894
 895
 896
 897
 898
 899
 900
 901
 902
 903
 904
 905
 906
 907
 908
 909
 910
 911
 912
 913
 914
 915
 916
 917
 918
 919

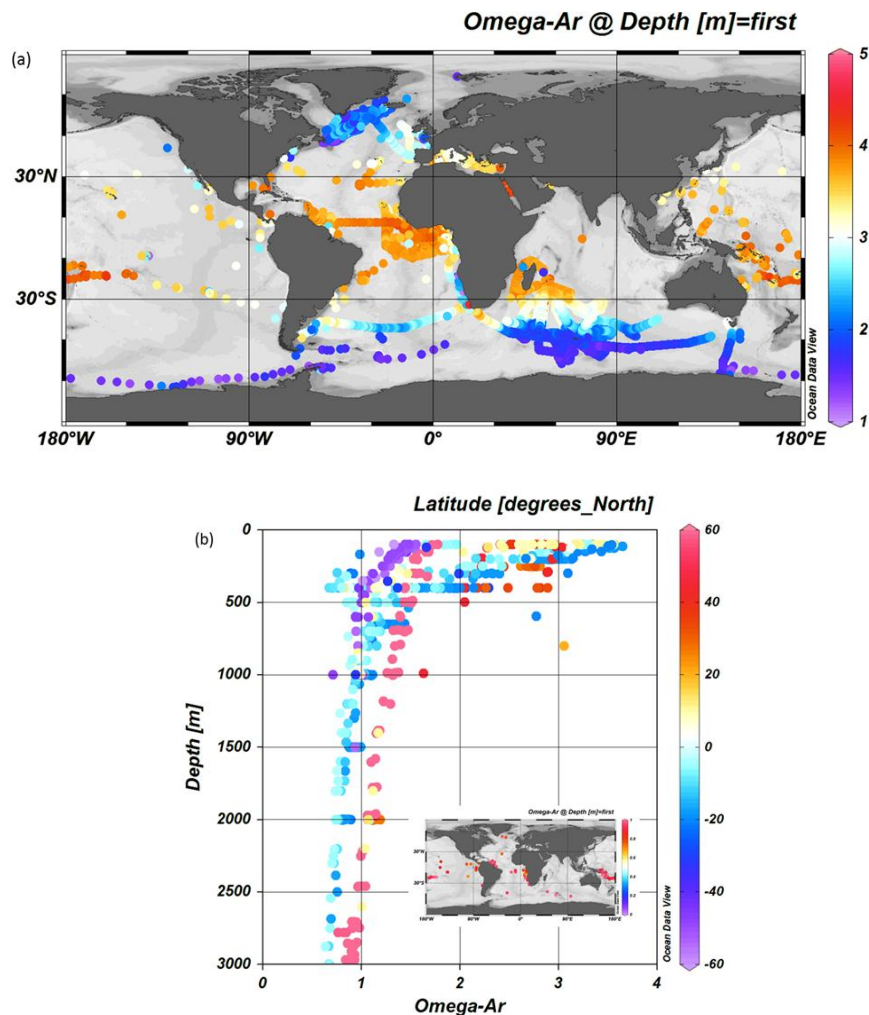


Figure 10: (a): Distribution of the aragonite saturation state (Ω -Ar) in surface waters (0-10m). Only data with flag 2 were used. (b): Depth profiles (100-3000m) of Ω -Ar at few locations in the Tropical Pacific, Atlantic and Southern Oceans. Stations where under-saturation is detected (Ω -Ar<1) at depth are identified in the inserted map. Figures produced with ODV (Schlitzer, 2018).

Compared to the open ocean, A_T concentrations are much higher in the Mediterranean Sea (Copin-Montégut, 1993; Schneider et al., 2007; Álvarez et al., 2023) with values up to $2600 \mu\text{mol kg}^{-1}$ (Figure 8). The A_T and C_T data obtained in 1998-2019 show on average a clear contrast between the northern and southern regions of the Western Mediterranean sea (Figure 11 a, b) with higher concentration in the Ligurian Sea and the Gulf of Lion (Gemayel et al., 2015). However, the basin scale average distribution view smoothed the meso-scale signals recognized in the Mediterranean Sea (e.g. Bosse et al., 2017; Petrenko et al., 2017). In the Gulf of Lion the synthesis of 11 cruises conducted from May 2010 to June 2011 (CARBORHONE, CASCADE, LATEX, MOLA, MOOSE-GE) highlights the contrasting distributions of A_T and C_T in the coastal zones and off shore (Figure 11 c, d). The averaging of all data in 1998-2019 also smoothed the seasonal signal and the inter-annual variability described below.

920
 921
 922
 923
 924
 925
 926
 927
 928
 929
 930
 931
 932
 933
 934
 935
 936
 937
 938
 939
 940
 941
 942
 943
 944
 945
 946
 947

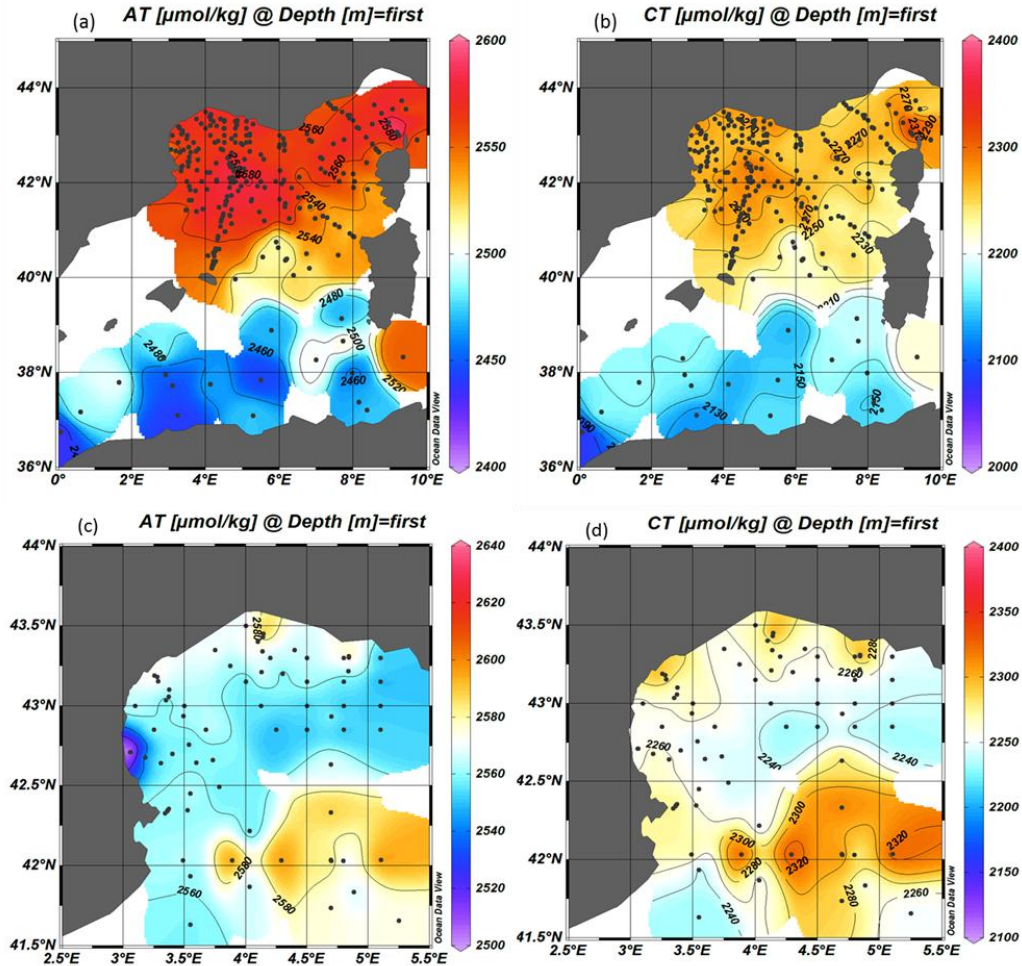


Figure 11: Distribution of A_T (a) and C_T (b) in $\mu\text{mol kg}^{-1}$ in surface waters of the Western Mediterranean Sea (0-10m) from all data for 1998-2019. Detailed distribution of A_T (c) and C_T (d) in $\mu\text{mol kg}^{-1}$ in surface waters of the Gulf of Lion for the period 2010-2011 only (cruises CARBORHONE, CASCADE, LATEX, MOLA, MOOSE-GE). Figures produced with ODV (Schlitzer, 2018).

948 **5 Temporal variations of A_T and C_T : examples from the SNAPO-CO2 dataset**

949

950 Time-series stations such as BATS, ESTOC, HOT in the subtropics and stations in the Irminger Sea or
 951 in the Iceland Sea are the only way to detect the long-term change in the ocean carbonate system in the surface
 952 and the water column (Bates et al., 2014). These important time-series help to understand driving processes (e.g.
 953 Hagens and Middelburg, 2016) and are often used to validate the $p\text{CO}_2$, A_T , C_T , or pH reconstructed fields (e.g.
 954 Rödenbeck et al., 2013; Broullón et al., 2019, 2020; Keppler et al., 2020; Gregor and Gruber, 2021; Chau et al.,
 955 2023; Ma et al., 2023).

956 Here we show examples of the temporal surface variations at locations where data were obtained for
 957 more than 10 years (Figure 12). We thus selected the following contrasting regions: the North Atlantic subpolar
 958 gyre (NASPG around $60^\circ\text{N}/30^\circ\text{W}$, period 1993-2018), the Equatorial Atlantic (at $2^\circ\text{N}-2^\circ\text{S}/12^\circ\text{W}-8^\circ\text{W}$, period
 959 2005-2017), the Indian Ocean subtropical sector ($26-35^\circ\text{S}/50-56^\circ\text{E}$, period 1998-2018), the Indian Ocean high
 960 latitude ($54-60^\circ\text{S}/60-70^\circ\text{E}$, period 1998-2018), the Ligurian Sea (around DYFAMED station, $43.5-42.5^\circ\text{N}/5.5-9^\circ\text{E}$,
 961 period 1998-2019) and times-series stations in the coastal zones off Brittany (period 2008-2019).

962

963
 964
 965
 966
 967
 968
 969
 970
 971
 972
 973
 974
 975
 976
 977
 978
 979
 980
 981
 982
 983
 984
 985
 986
 987
 988
 989
 990
 991
 992
 993
 994
 995
 996
 997
 998
 999
 1000
 1001
 1002
 1003
 1004
 1005
 1006
 1007
 1008
 1009
 1010
 1011

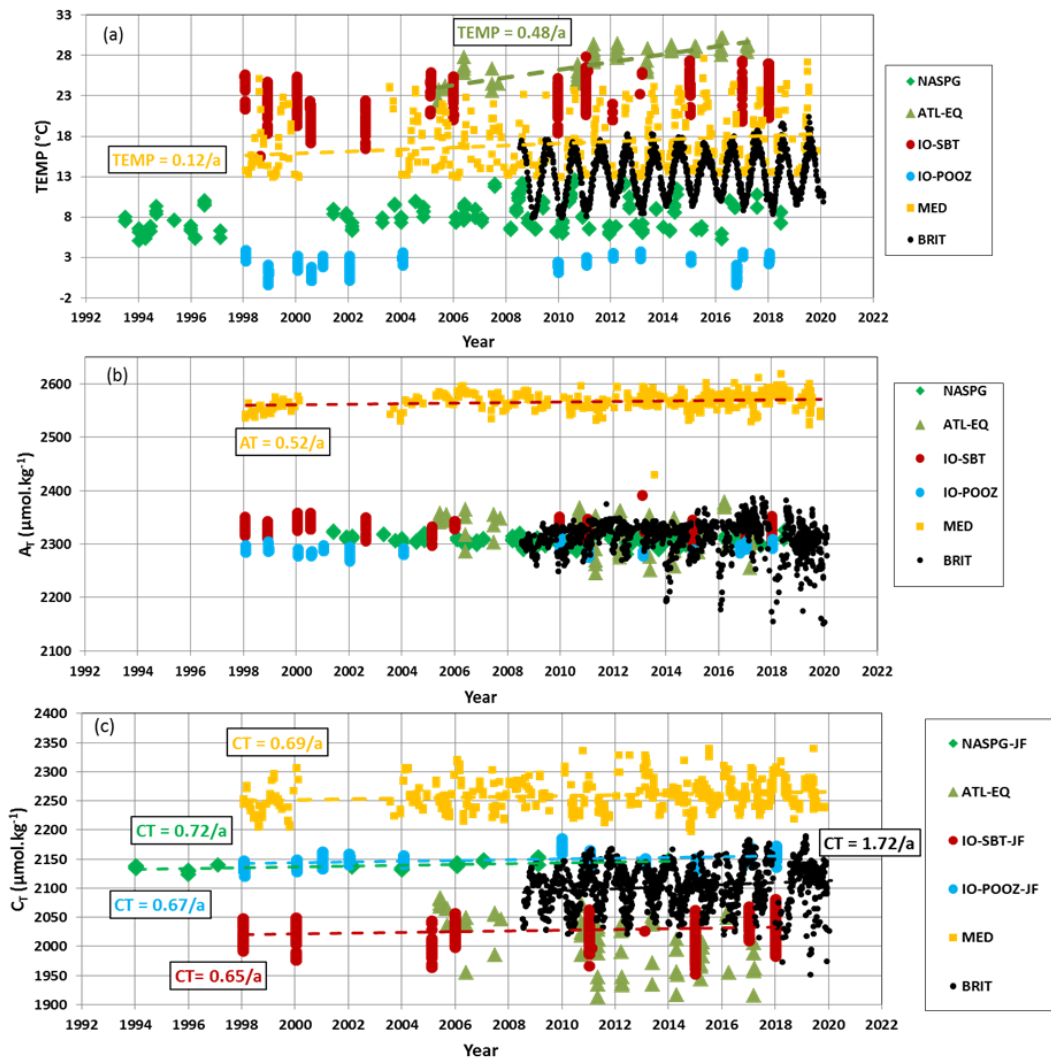


Figure 12: Time-series of (a) sea surface temperature ($^{\circ}\text{C}$), (b) A_T ($\mu\text{mol kg}^{-1}$) and (c) C_T ($\mu\text{mol kg}^{-1}$) in 6 regions: the North Atlantic subpolar gyre (NASPG 1993-2018, green diamond), the Equatorial Atlantic (ATL-EQ, 2005-2017, green triangle), the Indian subtropical sector (IO-SBT, red circle) and high latitude (IO-POOZ, blue circle) (1998-2018), the Ligurian Sea (MED, 1998-2019, orange square) and times-series stations in the coastal zones off Brittany (BRIT, period 2008-2019, black dots). Trends (dashed lines and values) are shown when relevant for the discussion (C_T trends listed in Table 6).

Table 6: Trend of C_T ($\mu\text{mol kg}^{-1} \text{ yr}^{-1}$) and corresponding standard error in 5 selected regions where data were available for more than 10 years (data are shown in Figure 12). The projects/cruises for selection of the data in each domain are indicated.

Region (acronym)	Period	C_T trend ($\mu\text{mol kg}^{-1} \text{ yr}^{-1}$)	Season	Projects/Cruises
North Atlantic (NASPG)	1994-2014	+0.72 (0.17)	Jan-Feb	SURATLANT
Indian Subtropic (IO-SBT)	1998-2018	+0.65 (0.12)	Jan-Feb	OISO
Indian South. (IO-POOZ)	1998-2018	+0.67 (0.04)	Jan-Feb	OISO
Ligurian Sea (MED)	1998-2019	+0.68 (0.18)	All seasons	DYFAMED, BOUSSOLE, MOOSE-GE
Coast Brittany (BRIT)	2008-2019	+1.72 (0.28)	All seasons	Brest, Roscoff, ECOSCOPIA, PENZE

1012 In the 6 regions, there was a progressive warming most clearly detected in the Mediterranean Sea (e.g.
1013 Nykjaer, 2009). From 1998 to 2019 the warming in the Ligurian Sea was $+0.1208^{\circ}\text{C yr}^{-1}$ (± 0.0227) (Figure 12).
1014 In the equatorial Atlantic, the apparent rapid increase of temperature of $+0.48^{\circ}\text{C}\cdot\text{yr}^{-1}$ (± 0.04) in 2005-2017 from
1015 the selected data indicated a change in water masses and circulation. The colder sea surface in 2005 was
1016 associated with the so-called Atlantic Cold Tongue (ACT) which was one of the most intense ATC since 1982
1017 (Caniaux et al., 2011). The ACT also leads to significant changes in oceanic $f\text{CO}_2$ and air-sea CO_2 fluxes (Parard
1018 et al., 2010; Koseki et al., 2023) and explained the high C_T concentrations observed in 2005 in this region
1019 (Figure 12, Koffi et al., 2010).

1020 Total alkalinity presents rather homogenous concentrations in the NASGP and the south Indian Ocean.
1021 Inter-annual variability of A_T is pronounced in the equatorial Atlantic ranging between 2245 and 2378 $\mu\text{mol kg}^{-1}$.
1022 This is mainly related to salinity as normalized A_T values ($N-A_T$, for salinity= 35) do not show such inter-annual
1023 variability (Mean $N-A_T = 2295.7 \pm 4.6 \mu\text{mol kg}^{-1}$, $n= 67$ for 2005-2017, not shown). In the coastal zones off
1024 Brittany, the A_T is also highly variable (Salt et al., 2016; Gac et al., 2021) ranging between 2150 and 2386 μmol
1025 kg^{-1} (Figure 12).

1026 An interesting signal is the progressive increase of A_T in the Mediterranean Sea. The positive A_T trend
1027 of $+0.53$ (± 0.11) $\mu\text{mol kg}^{-1} \text{yr}^{-1}$ ($n=538$) in 1998-2019 in the region offshore was also observed at the coastal
1028 station SOMLIT-Point-B in 2007-2015 but with a faster increase of $+2.08$ (± 0.19) $\mu\text{mol kg}^{-1} \text{yr}^{-1}$ (Kapsenberg et
1029 al., 2017). Close to the DYFAMED site, at station SOMLIT-Point-B, the A_T trend was not linked to salinity
1030 temporal changes as a positive $N-A_T$ trend was also reported, $+0.52$ (± 0.07) $\mu\text{mol kg}^{-1} \text{yr}^{-1}$ (not shown). Based
1031 on data from the PERLE cruises in 2018-2021 a significant increase in A_T was also identified in the Eastern
1032 Mediterranean Sea (Wimart-Rousseau et al., 2021). Along with the increase of C_T and the warming, the A_T
1033 increase would impact on the $f\text{CO}_2$, air-sea CO_2 fluxes and pH temporal changes (Merlivat et al., 2018).
1034 Processes explaining the A_T increase in the Mediterranean Sea are still unexplained and deserve further
1035 investigations (Coppola et al., 2019).

1036 As expected, because of the anthropogenic CO_2 uptake the C_T concentrations increased in most regions
1037 (Figure 12, Table 6). This is identified in the Indian Ocean (in the subtropics and the high latitude), in the
1038 Mediterranean Sea, and in coastal waters off Brittany. However, the signal is more complex in the NASPG. As
1039 previously shown the C_T trend in the NASPG depends on seasons and decades (Metzl et al., 2010; Reverdin et
1040 al., 2018; Fröb et al., 2019; Leseurre et al., 2020). Here we selected only the data in January-February from the
1041 SURATLANT cruises leading a C_T trend of $+0.72$ (± 0.17) $\mu\text{mol kg}^{-1} \text{yr}^{-1}$. Compared to the regions further north
1042 the C_T trend in the NASPG is about half the C_T trends of $+1.44$ (± 0.23) $\mu\text{mol kg}^{-1} \text{yr}^{-1}$ observed in the Iceland
1043 Sea (Olafsson et al., 2009) or $+1.48$ (± 0.22) $\mu\text{mol kg}^{-1} \text{yr}^{-1}$ at station M in the Norwegian Sea (Skjelvan et al.,
1044 2022).

1045 In the coastal zones off Brittany, although there are large seasonal and inter-annual variabilities (Gac et
1046 al., 2021), an annual C_T trend of $+1.72$ (± 0.28) $\mu\text{mol kg}^{-1} \text{yr}^{-1}$ is detected over 10 years (2009 to 2019). The same
1047 is observed in the Mediterranean Sea where the C_T offshore trend of $+0.69$ (± 0.18) $\mu\text{mol kg}^{-1} \text{yr}^{-1}$ is low
1048 compared to what was observed in the coastal zone (SOMLIT-Point-B, $+2.97$ (± 0.20) $\mu\text{mol kg}^{-1} \text{yr}^{-1}$, Kapsenberg
1049 et al., 2017).

1050 In the southern Indian Ocean, C_T concentrations also increased in both subtropical and high latitudes,
1051 two regions where the primary productivity is relatively low (oligotrophic regime in the subtropics and High
1052 Nutrient Low Chlorophyll regime, HNLC, south of the Polar Front). With the data selected for austral summer

1053 (January-February) the C_T trends appeared almost similar in these two regions, around $+0.65 \mu\text{mol kg}^{-1} \text{yr}^{-1}$
1054 (Table 6).

1055 Finally, in the Equatorial Atlantic the selected data around $0^\circ\text{-}10^\circ\text{W}$ highlighted the large variability
1056 linked to the oceanic circulation. Detecting a C_T trend as well as a possible link with anthropogenic carbon
1057 uptake, at least with the data available in 2005-2017, appears to be intricate as it has been previously discussed
1058 for the period 2006-2013 (Lefèvre et al., 2016). However, the signal of the C_T increase is better identified north
1059 or south of the Equator in the Eastern tropical Atlantic sector (Lefèvre et al., 2021).

1060 In the water column A_T and C_T data from dedicated cruises were used to evaluate the anthropogenic CO_2
1061 (C_{ant}) distribution and pH change since pre-industrial era (e.g. PANDORA cruise, Ganachaud et al., 2017;
1062 OUTPACE cruise, Wagener et al., 2018; SOMBA cruise, Keraghel et al., 2020). Time-series at DYFAMED
1063 station also enabled to investigate the temporal variability of C_T , A_T and C_{ant} in the water column (Touratier and
1064 Goyet, 2009; Coppola et al., 2020; Fourier et al., 2022). As an example of the observed temporal variations at
1065 depth we selected the data in the layer 950-1050m in the Ligurian Sea from different cruises (Figure 13). At that
1066 depth both A_T and C_T present some large anomalies especially noticed in 2013 (lower A_T and C_T in February
1067 2013, DEWEX cruise) and in 2018 (higher A_T and C_T in May 2018, MOOSE-GE cruise) the later probably
1068 linked to episodic convective process that occurred in winter 2018 (Fourrier et al., 2022; Coppola et al, 2023).
1069 During the strong convection event in 2013 the positive anomalies of A_T and C_T were mostly identified in the
1070 upper layers (Figure 12c, Ulses et al, 2023).

1071

1072

1073

1074

1075

1076

1077

1078

1079

1080

1081

1082

1083

1084

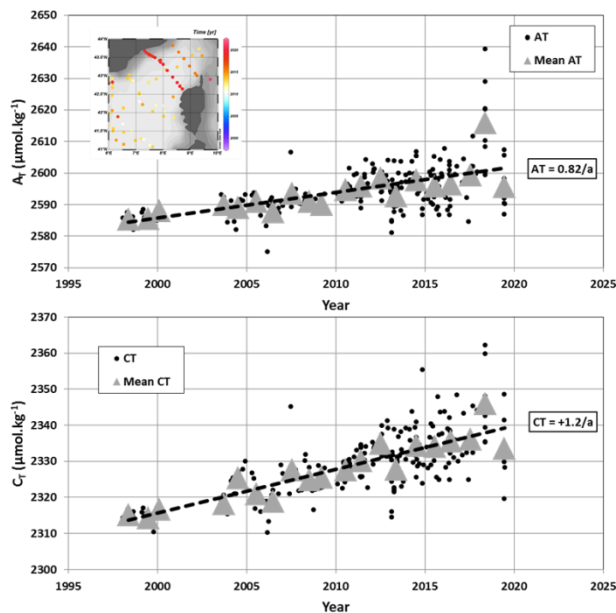
1085

1086

1087

1088

1089



1090

1091

1092

1093

1094

1095

Figure 13: Time-series of A_T ($\mu\text{mol kg}^{-1}$) and C_T ($\mu\text{mol kg}^{-1}$) in the Ligurian Sea (1998-2019) in the layer 950-1050m. Annual mean (grey triangles) was calculated from all data each year (black dots). The trends (dashed line) based on annual mean are $+0.82 (\pm 0.15) \mu\text{mol kg}^{-1} \text{yr}^{-1}$ for A_T and $+1.20 (\pm 0.12) \mu\text{mol kg}^{-1} \text{yr}^{-1}$ for C_T . In this layer data selected are from cruises ANTARES, CASCADE, DEWEX, DYFAMED, MOOSE-GE and PEACETIME (location of stations shown in the inserted map).

1096

1097

1098

1099

In this region the long-term increase of A_T indicates that in addition to the anthropogenic CO_2 signal other processes are at play to explain the rapid C_T trend of $+1.20 (\pm 0.12) \mu\text{mol kg}^{-1} \text{yr}^{-1}$ at depth compared to that observed in surface (Figure 12). The signal at depth is probably linked to the variations of the deep convection and mixing with Levantine intermediate water (LIW, Margirier et al., 2020) with higher A_T and C_T

1100 concentrations. The long-term increase of A_T and C_T at depth (here at 1000m, Figure 13) was also observed
1101 below 2000m (Coppola et al., 2020) a signal that has to be investigated in dedicated analysis using other
1102 properties (O_2 , nutrients, following Fourrier et al. (2022) for the period 2012-2020) and a larger dataset in the
1103 Mediterranean Sea (e.g. GLODAP).

1104

1105 **6 Using A_T and C_T data to validate observations from autonomous instruments**

1106

1107 The dataset presented in this synthesis would also offer interesting observations to validate properties
1108 (A_T and C_T) derived from BGC-Argo floats equipped with pH sensors (e.g. Bushinsky et al., 2019; Mazloff et al.,
1109 2023; Mignot et al., 2023). The water column in situ A_T and C_T data obtained during the Antarctic Circumpolar
1110 Expedition (ACE) in 2016-2017 were collected at location where SOCCOM floats were launched (Walton and
1111 Thomas, 2018). A SOCCOM float (WMO ID 5905069) was launched on January 11th 2017 at 55°S-96°E south
1112 of the Polar Front in the southern Indian Ocean. The pH, temperature and salinity data from the float were then
1113 used to derive A_T and C_T profiles (here using a multiple linear regression (MLR) algorithm, Williams et al.,
1114 2016, 2017). In the top layers the discrete ACE data (Figure 14) present large variability of A_T and C_T
1115 concentrations not captured in the records derived from the float (MLR method somehow smooth the profiles).
1116 However, given the uncertainty in reconstructed A_T from float data ($5.6 \mu\text{mol kg}^{-1}$) the average values in the first
1117 100m were almost identical ($A_{T-ACE} = 2285.1 (\pm 4.4) \mu\text{mol kg}^{-1}$ and $A_{T-float} = 2278.3 (\pm 0.7) \mu\text{mol kg}^{-1}$; $C_{T-ACE} =$
1118 $2139.7 (\pm 9.2) \mu\text{mol kg}^{-1}$ and $C_{T-float} = 2141.1 (\pm 3.2) \mu\text{mol kg}^{-1}$). Moreover below 200m, profiles from the float
1119 are coherent compared to the A_T and C_T measurements (Figure 14). This is encouraging for using float data to
1120 explore the seasonal variability of A_T and C_T in the Southern Ocean (e.g. Williams et al., 2018; Johnson et al.,
1121 2022) and the estimation of anthropogenic CO_2 in the water column in this sector (Figure 14). Here the C_{ant}
1122 concentrations were calculated below 200m (corresponding to the temperature minimum of the winter winter in
1123 the SO and using the TrOCA method, Touratier et al., 2007). The float data suggest that C_{ant} concentrations are
1124 positive down to about 1000m, with maximum values in subsurface. In 2017 the mean C_{ant} concentration at
1125 200m was $49.1 (\pm 9.0) \mu\text{mol kg}^{-1}$. Below that depth, C_{ant} decreased and reduced to $+29.8 (\pm 8.5) \mu\text{mol kg}^{-1}$ in the
1126 layer 300-400m. To complement the C_{ant} inventories based on GLODAP data product (e.g. Gruber et al., 2019)
1127 C_{ant} estimates derived from BGC-Argo floats as evaluated here in the Southern Ocean could be applied in other
1128 locations as was previously tested in the North Pacific (Li et al., 2019).

1129 In surface water as the A_T derived from the float data are deduced using MLR or LIAR methods
1130 (Williams et al., 2017; Carter et al., 2016), the A_T data in the SNAPO-CO2 synthesis could also be used to
1131 identify A_T anomalies not always captured from floats. This is particularly relevant in coccolithophores blooms
1132 areas when low A_T concentrations and high pCO_2 are observed (e.g. Balch et al., 2016 in the Southern Ocean;
1133 Robertson et al., 1994 in the North Atlantic).

1134

1135 **7 Summary and suggestions**

1136

1137 The ocean data synthesized in this product are based on measurements of A_T and C_T performed between
1138 the period 1993 and 2022 with an accuracy of $\pm 4 \mu\text{mol kg}^{-1}$. It offers a large data set of A_T and C_T for the global
1139 ocean and regional biogeochemical studies. It includes more than 44 400 surface and water column observations
1140 in all oceanic basins, in the Mediterranean Sea, in the coastal zones, near coral reefs, and in rivers. For the open
1141 ocean this complements the SOCAT and GLODAP data products (Bakker et al., 2016; Lauvset et al., 2022). For

1142 the coastal sites this also complements the synthesis of coastal time-series only done around North America
 1143 (Fassbender et al., 2018; Jiang et al., 2021; OCADS, 2023).

1144

1145

1146

1147

1148

1149

1150

1151

1152

1153

1154

1155

1156

1157

1158

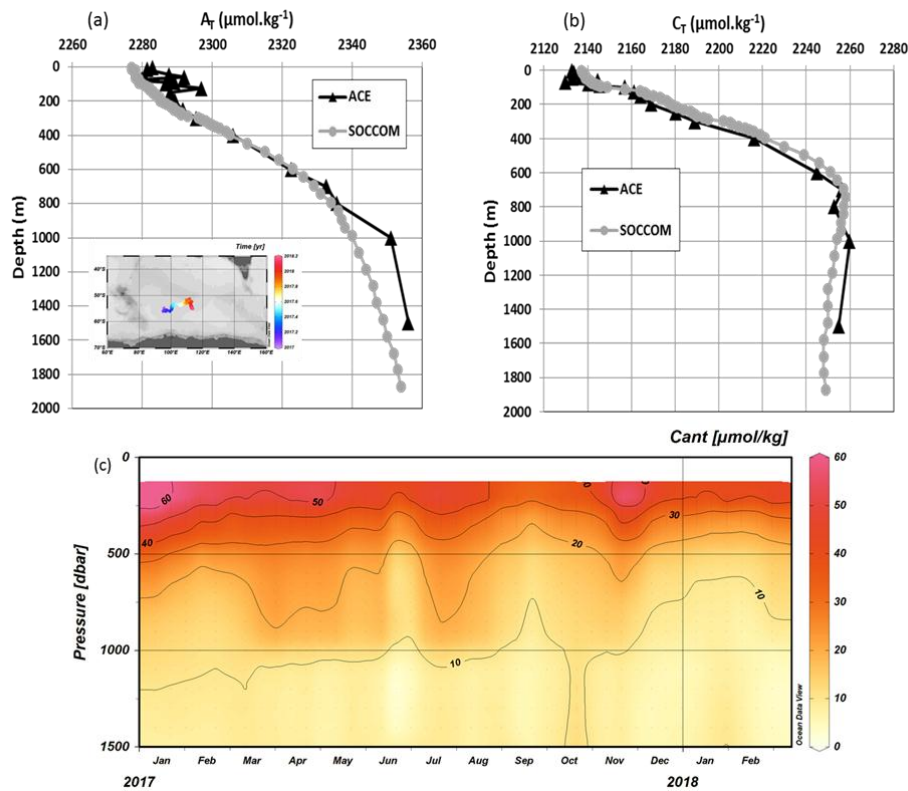
1159

1160

1161

1162

1163



1164 **Figure 14:** Profiles of (a) A_T ($\mu\text{mol kg}^{-1}$) and (b) C_T ($\mu\text{mol kg}^{-1}$) observed at station ACE-20 (55°S-95°E,
 1165 11/1/17, black triangles) compared with the profiles deduced from the SOCCOM float (WMO code 5905069)
 1166 launched at that location (first data on January 12th 2017, grey circles). The location/drift of the float in 2017-
 1167 2018 is shown on the inserted map. (c) Hovmoller section (Pressure/time) of anthropogenic CO₂ concentrations
 1168 (C_{ant} in $\mu\text{mol kg}^{-1}$) estimated from the float data (A_T , C_T , O_2 , T) below 200m (period January 2017-February
 1169 2018). Section produced with ODV (Schlitzer, 2018).
 1170

1171 The SNAPO-CO₂ dataset enables to investigate seasonal variations to decadal trends of A_T and C_T in
 1172 various oceanic provinces. In regions where data are available for more than 2 decades in surface water (North
 1173 Atlantic, Ligurian Sea, Southern Indian Ocean, and coastal regions), all time-series show an increase in C_T .
 1174 Excepted in the Mediterranean Sea, A_T appears relatively constant over time, although the A_T content present
 1175 significant inter-annual variability such as in the NASPG or in the coastal zones including near the Congo and
 1176 Amazon Rivers plumes.

1177 This dataset represents independent data for validation of reconstructed A_T or C_T fields using various
 1178 methods (e.g. Rödenbeck et al., 2013, 2015; Sauzède et al., 2017; Turk et al., 2017; Bittig et al., 2018; Broullón
 1179 et al., 2019, 2020; Land et al., 2019; Keppler et al., 2020; Fourier et al., 2020; Gregor and Gruber, 2021; Sims et
 1180 al., 2023; Chau et al., 2023). It is also useful to validate Earth System Models (ESM) that currently present bias
 1181 to reproduce the seasonal cycle of C_T and A_T due to inadequate representation of biogeochemical cycles,
 1182 including the coupling of biological and physical processes (e.g. Pilcher et al., 2015; Mongwe et al., 2018;
 1183 Lerner et al., 2021). This should be resolved for confident in future projections of the productivity, ocean
 1184 acidification, and the responses of the marine ecosystems (e.g. Kwiatkowski et al., 2020). Recall that OBG or
 1185 ESM models calculate $p\text{CO}_2$ from A_T/C_T pairs and the simulated annual CO₂ flux might be correct when

1186 compared to observations but for wrong reasons (e.g. Goris et al., 2018, Lerner et al., 2021). For example, it has
1187 been shown that biases in A_T in ESM models led to an overestimation of the oceanic fCO_2 trend and thus
1188 uncertainty when predicting the oceanic anthropogenic CO_2 uptake (Lebehot et al., 2019). The simulated
1189 seasonal cycle of fCO_2 is also uncertain in ESM models especially in high latitudes (e.g. Joos et al., 2023). It is
1190 thus important to attempt validating ESM models with A_T and C_T data such as presented in this synthesis.

1191 This dataset would also serve for validating autonomous platforms capable of measuring pH and fCO_2
1192 variables and, along with SOCAT and GLODAP datasets, provides an additional reference dataset for the
1193 development and validation of regional biogeochemical models for simulating air-sea CO_2 fluxes. It is also
1194 essential for training and validating neural networks capable of predicting variables in the carbonate system,
1195 thereby enhancing observations of marine CO_2 at different spatial and temporal scales.

1196 The data presented here are available online on the Seanoë server (Metzl et al., 2023,
1197 <https://doi.org/10.17882/95414>) and is divided in two files: one for the Global Ocean, and one for the
1198 Mediterranean Sea. The sources of the original datasets (doi) with the associated references are listed in the
1199 Supplementary Material (Table S3, S4). We invite the users to comment on any anomaly that would have not
1200 been detected or to suggest potential misqualification of data in the present product (e.g. data probably good
1201 although assigned with flag 3, probably wrong). The SNAPO-CO2 dataset will be regularly updated on Seanoë
1202 data server with new observations controlled and archived.

1203

1204 **8 Data availability**

1205 Data presented in this study are available at Seanoë: <https://www.seanoë.org>, <https://doi.org/10.17882/95414>
1206 (Metzl et al., 2023).

1207

1208 *Author contributions.* NM prepared the data synthesis, the figures and wrote the draft of the manuscript with
1209 contributions from all authors. JF measured the discrete samples since 2014, with the help from CM and CLM,
1210 and prepared the individual reports for each project. NM and JF pre-qualified the discrete A_T/C_T data. CLM and
1211 NM are co-Is of the ongoing OISO project and qualified the underway A_T/C_T data from OISO and CLIM-
1212 EPARSEES cruises. All authors have contributed either to organizing cruises, sample collection and/or data
1213 qualification, and reviewed the manuscript.

1214

1215 *Competing interest.* The authors declare that they have no conflict of interest.

1216

1217 *Acknowledgments.* The A_T and C_T data presented in this study were measured at the SNAPO-CO2 facility
1218 (Service National d'Analyse des Paramètres Océaniques du CO_2) housed by the LOCEAN laboratory and part of
1219 the OSU ECCE Terra at Sorbonne University and INSU/CNRS analytical services. Support by INSU/CNRS, by
1220 OSU ECCE Terra and by LOCEAN, is gratefully acknowledged as well as support by different French "Services
1221 nationaux d'Observations", such as OISO/CARAUS, SOMLIT, PIRATA, SSS and MOOSE. We thank the
1222 research infrastructure ICOS (Integrated Carbon Observation System) France for funding a large part of the
1223 analyses. We thank the French oceanographic fleet ("Flotte océanographique française") for financial and
1224 logistic support for most cruises listed in this synthesis and for the OISO program
1225 (<https://campagnes.flotteoceanographique.fr/series/228/>). We acknowledge the MOOSE program (Mediterranean
1226 Ocean Observing System for the Environment, <https://campagnes.flotteoceanographique.fr/series/235/fr/>)
1227 coordinated by CNRS-INSU and the Research Infrastructure ILICO (CNRS-IFREMER). AWIPEV-CO2 was

1228 supported by the Coastal Observing System for Northern and Arctic Seas (COSYNA), the two Helmholtz large-
1229 scale infrastructure projects ACROSS and MOSES, the French Polar Institute (IPEV) as well as the European
1230 Union's Horizon 2020 research and innovation projects Jericho-Next (No 871153 and 951799), INTAROS (No
1231 727890) and FACE-IT (No 869154). The BOUSSOLE time series project was funded by the Centre National
1232 d'Etudes Spatiales (CNES) and the European Space Agency (ESA ESRIN contract 4000119096/17/I-BG), and
1233 the first three years of the CO₂ time series at that site were funded by the French Agence Nationale de la
1234 Recherche (ANR). The EURECA4-OA cruise was also supported by the EUREC4A-OA JPI Ocean and Climate
1235 program. We thank Tara Ocean Foundation and many institutes and funding agencies for supporting TARA
1236 cruises since 2009. The OISO program was supported by the French institutes INSU (Institut National des
1237 Sciences de l'Univers) and IPEV (Institut Polaire Paul-Emile Victor), OSU Ecce-Terra (at Sorbonne Université),
1238 and the French program SOERE/Great-Gases. The CLIM-EPARSES cruise was supported by TAAF (Terres
1239 Australes et ANtariques Françaises), Fondation du Prince Albert II de Monaco, IRD, OSU Ecce-Terra, CNRS,
1240 MNHN, LOCEAN and LSCE laboratory. Data from the float launched during the ACE cruise were made freely
1241 available by the Southern Ocean Carbon and Climate Observations and Modeling (SOCCOM) Project funded by
1242 the National Science Foundation, Division of Polar Programs (NSF PLR -1425989), supplemented by NASA,
1243 and by the International Argo Program and the NOAA programs that contribute to it. The Argo Program is part
1244 of the Global Ocean Observing System (<http://doi.org/10.17882/42182>, <http://argo.jcompos.org>). We thank
1245 Frédéric Merceur (IFREMER) for preparing the page and data availability on Seanoë. We thank Patrick
1246 Raimbault (retired, former at MIO, Marseille) for managing the MOOSE project until 2019. We thank all
1247 colleagues and students who participated to the cruises and have carefully collected the precious seawater
1248 samples. We warmly acknowledge our colleague Christian Brunet (retired) for his supportive help for the
1249 analysis since the start of the Service facility SNAPO-CO₂. We would like to pay tribute to our late colleague
1250 Frédéric Diaz who contributed to the LATEX cruise in 2010. We thank the associated editor Xingchen Wang to
1251 manage this manuscript, Marta Álvarez and a (more or less) anonymous reviewer for their suggestions that
1252 helped to improve this article.

1253

1254 **References**

1255

1256 Álvarez, M., Catalá, T. S., Civitarese, G., Coppola, L., Hassoun, A. E.R., Ibello, V., Lazzari, P., Lefevre, D.,
1257 Macías, D., Santinelli, C. and Ulses, C.: Chapter 11 - Mediterranean Sea general biogeochemistry, Editor(s):
1258 Katrin Schroeder, Jacopo Chiggiato, *Oceanography of the Mediterranean Sea*, Elsevier, Pages 387-451,
1259 <https://doi.org/10.1016/B978-0-12-823692-5.00004-2>, 2023.

1260

1261 Bakker, D. C. E., Pfeil, B., Smith, K., Hankin, S., Olsen, A., Alin, S. R., Cosca, C., Harasawa, S., Kozyr, A.,
1262 Nojiri, Y., O'Brien, K. M., Schuster, U., Telszewski, M., Tilbrook, B., Wada, C., Akl, J., Barbero, L., Bates, N.
1263 R., Boutin, J., Bozec, Y., Cai, W.-J., Castle, R. D., Chavez, F. P., Chen, L., Chierici, M., Currie, K., De Baar, H.
1264 J. W., Evans, W., Feely, R. A., Fransson, A., Gao, Z., Hales, B., Hardman-Mountford, N. J., Hoppema, M.,
1265 Huang, W.-J., Hunt, C. W., Huss, B., Ichikawa, T., Johannessen, T., Jones, E. M., Jones, S., Jutterstrøm, S.,
1266 Kitidis, V., Körtzinger, A., Landschützer, P., Lauvset, S. K., Lefèvre, N., Manke, A. B., Mathis, J. T., Merlivat,
1267 L., Metzl, N., Murata, A., Newberger, T., Omar, A. M., Ono, T., Park, G.-H., Paterson, K., Pierrot, D., Ríos, A.
1268 F., Sabine, C. L., Saito, S., Salisbury, J., Sarma, V. V. S. S., Schlitzer, R., Sieger, R., Skjelvan, I., Steinhoff, T.,
1269 Sullivan, K. F., Sun, H., Sutton, A. J., Suzuki, T., Sweeney, C., Takahashi, T., Tjiputra, J., Tsurushima, N., Van
1270 Heuven, S. M. A. C., Vandemark, D., Vlahos, P., Wallace, D. W. R., Wanninkhof, R. and Watson, A. J.: An
1271 update to the Surface Ocean CO₂ Atlas (SOCAT version 2). *Earth System Science Data*, 6, 69-90.
1272 doi:10.5194/essd-6-69-2014. 2014

1273

1274 Bakker, D. C. E., Pfeil, B., Landa, C. S., Metzl, N., O'Brien, K. M., Olsen, A., Smith, K., Cosca, C., Harasawa,
1275 S., Jones, S. D., Nakaoka, S.-I., Nojiri, Y., Schuster, U., Steinhoff, T., Sweeney, C., Takahashi, T., Tilbrook, B.,
1276 Wada, C., Wanninkhof, R., Alin, S. R., Balestrini, C. F., Barbero, L., Bates, N. R., Bianchi, A. A., Bonou, F.,
1277 Boutin, J., Bozec, Y., Burger, E. F., Cai, W.-J., Castle, R. D., Chen, L., Chierici, M., Currie, K., Evans, W.,
1278 Featherstone, C., Feely, R. A., Fransson, A., Goyet, C., Greenwood, N., Gregor, L., Hankin, S., Hardman-
1279 Mountford, N. J., Harlay, J., Hauck, J., Hoppema, M., Humphreys, M. P., Hunt, C. W., Huss, B., Ibáñez, J. S.
1280 P., Johannessen, T., Keeling, R., Kitidis, V., Körtzinger, A., Kozyr, A., Krasakopoulou, E., Kuwata, A.,
1281 Landschützer, P., Lauvset, S. K., Lefèvre, N., Lo Monaco, C., Manke, A., Mathis, J. T., Merlivat, L., Millero, F.
1282 J., Monteiro, P. M. S., Munro, D. R., Murata, A., Newberger, T., Omar, A. M., Ono, T., Paterson, K., Pearce, D.,
1283 Pierrot, D., Robbins, L. L., Saito, S., Salisbury, J., Schlitzer, R., Schneider, B., Schweitzer, R., Sieger, R.,
1284 Skjelvan, I., Sullivan, K. F., Sutherland, S. C., Sutton, A. J., Tadokoro, K., Telszewski, M., Tuma, M., Van
1285 Heuven, S. M. A. C., Vandemark, D., Ward, B., Watson, A. J., and Xu, S.: A multi-decade record of high-quality
1286 fCO₂ data in version 3 of the Surface Ocean CO₂ Atlas (SOCAT), *Earth Syst. Sci. Data*, 8, 383-413,
1287 doi:10.5194/essd-8-383-2016. 2016.
1288
1289 Bakker, D.C.E., Alin, S.R., Bates, N.R., Becker, M., Feely, R. A., Gritzalis, T. , Jones, S. D., Kozyr, A., Lauvset,
1290 S. K., Metzl, N., Munro, D.R., Nakaoka, S.-I., Nojiri, Y., O'Brien, K., Olsen, A., Pierrot, D., Rehder, G.,
1291 Steinhoff, T., Sutton, A., Sweeney, C., Tilbrook, B., Wada, C., Wanninkhof, R., and all >100 SOCAT
1292 contributors: An alarming decline in the ocean CO₂ observing capacity. Available at www.socat.info, 2023.
1293
1294 Balch, W.M., Bates, N.R., Lam, P.J., Twining, B.S., Rosengard, S. Z., Bowler, B.C., Drapeau, D.T., Garley, R.,
1295 Lubelczyk, L.C., Mitchell, C. and Rauschenberg S.: Factors regulating the Great Calcite Belt in the Southern
1296 Ocean and its biogeochemical significance. *Global Biogeochem. Cycles*, 30, doi:10.1002/2016GB005414, 2016
1297
1298 Beaufort, L., Probert, I., de Garidel-Thoron, T., Bendif, E.M., Ruiz-Pino, D., Metzl, N., Goyet, C., Buchet, N.,
1299 Coupel, P., Grelaud, M., Rost, B., Rickaby, R.E.M., and de Vargas C.: Sensitivity of coccolithophores to
1300 carbonate chemistry and ocean acidification. *Nature*, doi:10.1038/nature10295. 2011
1301
1302 Bittig, H.C., Steinhoff, T., Claustre, H., Fiedler, B., Williams, N.L., Sauzède, R., Körtzinger, A. and Gattuso, J.-
1303 P.: An Alternative to Static Climatologies: Robust Estimation of Open Ocean CO₂ Variables and Nutrient
1304 Concentrations From T, S, and O₂ Data Using Bayesian Neural Networks. *Front. Mar. Sci.* 5:328. doi:
1305 10.3389/fmars.2018.00328, 2018
1306
1307 Bockmon, E. E., and Dickson, A. G.: An inter-laboratory comparison assessing the quality of seawater carbon
1308 dioxide measurements. *Marine Chemistry*, 171, 36-43, doi:10.1016/j.marchem.2015.02.002, 2015.
1309
1310 Bosse, A., Testor, P., Mayot, N., Prieur, L., D'Ortenzio, F., Mortier, L., Le Goff, H., Gourcuff, C., Coppola, L.,
1311 Lavigne, H. and Raimbault, P.: A submesoscale coherent vortex in the Ligurian Sea: From dynamical barriers to
1312 biological implications. *J. Geophys. Res. Oceans*, 122, doi:10.1002/2016JC012634., 2017.
1313
1314 Bozec, Y., Merlivat, L., Baudoux, A.-C., Beaumont, L., Blain, S., Bucciarelli, E., Danguy, T., Grossteffan, E.,
1315 Guillot, A., Guillou, J., Répécaud, M., and Tréguer, P.: Diurnal to inter-annual dynamics of pCO₂ recorded by a
1316 CARIOCA sensor in a temperate coastal ecosystem (2003–2009). *Marine Chemistry*, 126, 1-4, 13-26,
1317 10.1016/j.marchem.2011.03.003. 2011
1318
1319 Broullón, D., Pérez, F. F., Velo, A., Hoppema, M., Olsen, A., Takahashi, T., Key, R. M., Tanhua, T., González-
1320 Dávila, M., Jeansson, E., Kozyr, A., and van Heuven, S. M. A. C.: A global monthly climatology of total
1321 alkalinity: a neural network approach, *Earth Syst. Sci. Data*, 11, 1109–1127, [https://doi.org/10.5194/essd-11-](https://doi.org/10.5194/essd-11-1109-2019)
1322 1109-2019. 2019
1323
1324 Broullón, D., Pérez, F. F., Velo, A., Hoppema, M., Olsen, A., Takahashi, T., Key, R. M., Tanhua, T., Santana-
1325 Casiano, J. M., and Kozyr, A.: A global monthly climatology of oceanic total dissolved inorganic carbon: a
1326 neural network approach, *Earth Syst. Sci. Data*, 12, 1725–1743, <https://doi.org/10.5194/essd-12-1725-2020>.
1327 2020

1328
1329 Bushinsky, S. M., Landschützer, P., Rödenbeck, C., Gray, A. R., Baker, D., Mazloff, M. R., Resplandy L.,
1330 Johnson K. S., and Sarmiento, J. L.: Reassessing Southern Ocean air-sea CO₂ flux estimates with the addition of
1331 biogeochemical float observations. *Global Biogeochemical Cycles*, 33. doi: 10.1029/2019GB006176, 2019.
1332
1333 Canesi, M., Douville, E., Montagna, P., Taviani, M., Stolarski, J., Bordier, L., Dapoigny, A., Coulibaly, G. E. H.,
1334 Simon, A.-C., Agelou, M., Fin, J., Metzl, N., Iwankow, G., Allemand, D., Planes, S., Moulin, C., Lombard, F.,
1335 Bourdin, G., Troublé, R., Agostini, S., Banaigs, B., Boissin, E., Boss, E., Bowler, C., de Vargas, C., Flores, M.,
1336 Forcioli, D., Furla, P., Gilson, E., Galand, P. E., Pesant, S., Sunagawa, S., Thomas, O., Thurber, R. V., Voolstra,
1337 C. R., Wincker, P., Zoccola, D., and Reynaud, S.: Differences in carbonate chemistry up-regulation of long-lived
1338 reef-building corals. *Sci. Rep.* 13, 11589, Doi: 10.1038/s41598-023-37598-9, 2023.
1339
1340 Caniaux, G., Giordani, H., Redelsperger, J-L., Guichard, F., Key, E. and Wade, M.: Coupling between the
1341 Atlantic cold tongue and the West African monsoon in boreal spring and summer. *J. Geophys. Res.*, 119,
1342 C04003, doi:10.1029/2010JC006570., 2011.
1343
1344 Cariou, T., and Bozec, Y.: COMOR-CARBORHONE 1 cruise, RV L'Europe,
1345 <https://doi.org/10.17600/11060060>, 2011a.
1346
1347 Cariou, T., and Bozec, Y.: COMOR-CARBORHONE 2 cruise, RV Téthys II,
1348 <https://doi.org/10.17600/11450150>, 2011b.
1349
1350 Cariou, T., and Bozec, Y.: CARBORHONE 3 cruise, RV Téthys II, <https://doi.org/10.17600/12450020>, 2012a.
1351
1352 Cariou, T., and Bozec Y.: CARBORHONE 4 cruise, RV Téthys II, <https://doi.org/10.17600/12450140>, 2012b.
1353
1354 Carter, B. R., Williams, N. L., Gray, A. R., and Feely, R. A.: Locally interpolated alkalinity regression for global
1355 alkalinity estimation, *Limnol. Oceanogr. Methods*, 14(4), 268–277, doi:10.1002/lom3.10087, 2016.
1356
1357 Chau, T.-T.-T., Gehlen, M., Metzl, N., and Chevallier, F.: CMEMS-LSCE: A global 0.25-degree, monthly
1358 reconstruction of the surface ocean carbonate system, *Earth Syst. Sci. Data Discuss.* [preprint],
1359 <https://doi.org/10.5194/essd-2023-146>, in review, 2023.
1360
1361 Chen, H., Haumann, F. A., Talley, L. D., Johnson, K. S., and Sarmiento, J. L.: The deep ocean's carbon exhaust.
1362 *Global Biogeochemical Cycles*. doi: <https://doi.org/10.1002/essoar.10507757.1>, 2022
1363
1364 Cheng, L. J., Abraham, J., Zhu, J., Trenberth, K. E., Fasullo, J., Boyer, T., Locarnini, R., Zhang, B., Yu, F. J.,
1365 Wan, L. Y., Chen, X. R., Song, X. Z., Liu, Y. L., and Mann, M. E.: Record-setting ocean warmth continued in
1366 2019, *Adv. Atmos. Sci.*, 37, 137-142. <https://doi.org/10.1007/s00376-020-9283-7>, 2020
1367
1368 Claustre, H., Johnson, K. S., and Takeshita, Y.: Observing the Global Ocean with Biogeochemical-Argo. *Annual*
1369 *Review of Marine Science*, 12: 23-48 | DOI: [10.1146/annurev-marine-010419-010956](https://doi.org/10.1146/annurev-marine-010419-010956), 2020.
1370
1371 Conan, P., Guieux, A., and Vuillemin, R.: MOOSE (MOLA), <https://doi.org/10.18142/234>, 2020.
1372
1373 Copin-Montégut, C.: Alkalinity and carbon budgets in the Mediterranean Sea, *Global Biogeochemical Cycles*,
1374 vol. 7, pp. 915–925, 1993.
1375
1376 Copin-Montégut, C., and Bégovic, M.: Distributions of carbonate properties and oxygen along the water column
1377 (0–2000 m) in the central part of the NW Mediterranean Sea (Dyfamed site): influence of the winter vertical
1378 mixing on air–sea CO₂ and O₂ exchanges. *Deep-Sea Research II* 49, 2049–2066, [https://doi.org/10.1016/S0967-](https://doi.org/10.1016/S0967-0645(02)00027-9)
1379 [0645\(02\)00027-9](https://doi.org/10.1016/S0967-0645(02)00027-9), 2002.
1380
1381 Coppola, L., and Diamond-Riquier, E.: MOOSE (DYFAMED), <https://doi.org/10.18142/131>, 2008.

1382
1383 Coppola, L., Raimbault, P., Mortier, L., and Testor, P.: Monitoring the environment in the northwestern
1384 Mediterranean Sea, *Eos*, 100, <https://doi.org/10.1029/2019EO125951>. Published on 25 July 2019.
1385
1386 Coppola, L., Boutin, J., Gattuso, J.-P., Lefèvre, D., and Metzl, N.: The Carbonate System in the Ligurian Sea. In
1387 *The Mediterranean Sea in the Era of Global Change: Evidence from 30 years of multidisciplinary study of the*
1388 *Ligurian Sea*, C. Migon, P. Nival, A. Sciandra, Eds. (ISTE Science Publishing LTD, London, UK, 2020), vol. 1,
1389 chap. 4, pp. 79-104. ISBN: 9781786304285. <https://doi.org/10.1002/9781119706960.ch4>, 2020.
1390
1391 Coppola, L., Fourier, M., Pasqueron de Fommervault, O., Poteau, A., Riquier, E. D. and Béquery, L.:
1392 Highresolution study of the air-sea CO₂ flux and net community oxygen production in the Ligurian Sea by a
1393 fleet of gliders. *Front. Mar. Sci.* 10:1233845. doi: 10.3389/fmars.2023.1233845, 2023
1394
1395 Corbière, A., Metzl, N., Reverdin, G., Brunet, C., and Takahashi, T.: Interannual and decadal variability of the
1396 oceanic carbon sink in the North Atlantic subpolar gyre. *Tellus B*, Vol. 59, issue 2, 168-179, DOI:
1397 10.1111/j.1600-0889.2006.00232, 2007.
1398
1399 D'Ortenzio, F. and Taillandier, V.: BIO-ARGO-MED-2018 cruise, RV Téthys II,
1400 <https://doi.org/10.17600/18000550>, 2018.
1401
1402 De Carlo, E. H., Mousseau, L., Passafiume, O., Drupp, P. and Gattuso J.-P.: Carbonate chemistry and air-sea
1403 CO₂ flux in a NW Mediterranean bay over a four-year period: 2007-2011. *Aquatic Geochemistry*
1404 doi:10.1007/s10498-013-9217-4, 2013.
1405
1406 Dickson, A. G., Sabine, C. L., and Christian, J. R.: Guide to best practices for ocean CO₂ measurements, North
1407 Pacific Marine Science Organization, Sidney, British Columbia, 191, <https://doi.org/10.25607/OBP-1342>, 2007.
1408
1409 Division Plans de DMI – SHOM : PROTEUS2010_LEG1 cruise, RV Pourquoi pas ?,
1410 <https://doi.org/10.17600/10030040>, 2010.
1411
1412 Division Plans de DMI – SHOM: PROTEVSMED_PERLE_2018 cruise, RV L'Atalante,
1413 <https://campagnes.flotteoceanographique.fr/campaign>, 2018.
1414
1415 Doney, S. C., Fabry, V. J., Feely, R. A., and Kleypas, J. A., Ocean acidification: The other CO₂ problem. *Annual*
1416 *Review of Marine Science*, 1(1), 169–192. 10.1146/annurev.marine.010908.163834, 2009
1417
1418 Doney, S. C., Busch, D. S., Cooley, S. R., and Kroeker, K. J.: The Impacts of Ocean Acidification on Marine
1419 Ecosystems and Reliant Human Communities. *Annual Review of Environment and Resources* 45:1,
1420 <https://doi.org/10.1146/annurev-environ-012320-083019>. 2020
1421
1422 Douville, E., Bourdin, G., Lombard, F., Gorsky, G., Fin, J., Metzl, N., Pesant, S., and Tara Pacific Consortium:
1423 Seawater carbonate chemistry dataset collected during the Tara Pacific Expedition 2016-2018. PANGAEA,
1424 <https://doi.org/10.1594/PANGAEA.944420>, 2022.
1425
1426 Durrieu de Madron, X.: CASCADE cruise, RV L'Atalante, <https://doi.org/10.17600/11010020>, 2011.
1427
1428 Durrieu de Madron, X., and Conan, P.: PERLE2 cruise, RV Pourquoi pas ?, <https://doi.org/10.17600/18000865>,
1429 2018
1430
1431 Edmond, J. M.: High precision determination of titration alkalinity and total carbon dioxide content of sea water
1432 by potentiometric titration, *Deep-Sea Res.*, 17, 737–750, [https://doi.org/10.1016/0011-7471\(70\)90038-0](https://doi.org/10.1016/0011-7471(70)90038-0), 1970.
1433
1434 Eldin, G. : PANDORA cruise, RV L'Atalante, <https://doi.org/10.17600/12010050>, 2012.
1435

1436 Eyring, V., Righi, M., Lauer, A., Evaldsson, M., Wenzel, S., Jones, C., Anav, A., Andrews, O., Cionni, I., Davin,
1437 E. L., Deser, C., Ehbrecht, C., Friedlingstein, P., Gleckler, P., Gottschaldt, K.-D., Hagemann, S., Jukes, M.,
1438 Kindermann, S., Krasting, J., Kunert, D., Levine, R., Loew, A., Mäkelä, J., Martin, G., Mason, E., Phillips, A. S.,
1439 Read, S., Rio, C., Roehrig, R., Senftleben, D., Sterl, A., van Ulft, L. H., Walton, J., Wang, S., and Williams, K.
1440 D.: ESMValTool (v1.0) – a community diagnostic and performance metrics tool for routine evaluation of Earth
1441 system models in CMIP, *Geosci. Model Dev.*, 9, 1747–1802, doi:10.5194/gmd-9-1747-2016, 2016.

1442

1443 Fabry, V. J., Seibel, B. A., Feely, R. A. and Orr, J. C.: Impacts of ocean acidification on marine fauna and
1444 ecosystem processes. *ICES J. Mar. Sci.* 65, 414–432. <https://doi.org/10.1093/icesjms/fsn048>, 2008.

1445

1446 Fassbender, A. J., Sabine, C. L., and Palevsky, H. I.: Nonuniform ocean acidification and attenuation of the
1447 ocean carbon sink, *Geophys. Res. Lett.*, 44, 8404–8413, doi:10.1002/2017GL074389., 2017.

1448

1449 Fassbender, A. J., Alin, S. R., Feely, R. A., Sutton, A. J., Newton, J. A., Krembs, C., Bos, J., Keyzers, M., Devol,
1450 A., Ruef, W., and Pelletier, G.: Seasonal carbonate chemistry variability in marine surface waters of the US
1451 Pacific Northwest, *Earth Syst. Sci. Data*, 10, 1367–1401, <https://doi.org/10.5194/essd-10-1367-2018>, 2018.

1452

1453 Feely, R. A., Sabine, C. L., Byrne, R. H., Millero, F. J., Dickson, A. G., Wanninkhof, R., et al.: Decadal changes
1454 in the aragonite and calcite saturation state of the Pacific Ocean. *Global Biogeochemical Cycles*, 26, GB3001.
1455 <https://doi.org/10.1029/2011GB004157>, 2012.

1456

1457 Feely, R. A., Jiang, L.-Q., Wanninkhof, R., Carter, B. R., Alin, S. R., Bednaršek, N., and Cosca, C. E.:
1458 Acidification of the global surface ocean: What we have learned from observations. *Oceanography*,
1459 <https://doi.org/10.5670/oceanog.2023.222>, 2023

1460

1461 Fleury, E., Petton, S., Benabdelmouna, A., and Pouvreau, S., (coord.): Observatoire national du cycle de vie de
1462 l’huître creuse en France. Rapport annuel ECOSCOPIA 2022. R.INT.BREST RBE/PFOM/PI 2023-1, 2023.

1463

1464 Fourier, M., Coppola, L., Claustre, H., D’Ortenzio, F., Sauzède, R. and Gattuso, J.-P.: A regional neural
1465 network approach to estimate water-column nutrient concentrations and carbonate system variables in the
1466 Mediterranean Sea: CANYON-MED. *Frontiers in Marine Science*, 7:620,
1467 <https://www.frontiersin.org/articles/10.3389/fmars.2020.00620>, 2020.

1468

1469 Fourier, M., Coppola, L., D’Ortenzio, F., Migon, C., and Gattuso, J.-P.: Impact of intermittent convection in the
1470 northwestern Mediterranean Sea on oxygen content, nutrients, and the carbonate system. *Journal of Geophysical*
1471 *Research: Oceans*, 127, e2022JC018615. <https://doi.org/10.1029/2022JC018615>, 2022

1472

1473 Friedlingstein, P., O’Sullivan, M., Jones, M. W., Andrew, R. M., Gregor, L., Hauck, J., Le Quéré, C., Luijckx, I.
1474 T., Olsen, A., Peters, G. P., Peters, W., Pongratz, J., Schwingshackl, C., Sitch, S., Canadell, J. G., Ciais, P.,
1475 Jackson, R. B., Alin, S. R., Alkama, R., Arneeth, A., Arora, V. K., Bates, N. R., Becker, M., Bellouin, N., Bittig,
1476 H. C., Bopp, L., Chevallier, F., Chini, L. P., Cronin, M., Evans, W., Falk, S., Feely, R. A., Gasser, T., Gehlen,
1477 M., Gkritzalis, T., Gloege, L., Grassi, G., Gruber, N., Gürses, Ö., Harris, I., Hefner, M., Houghton, R. A., Hurtt,
1478 G. C., Iida, Y., Ilyina, T., Jain, A. K., Jersild, A., Kadono, K., Kato, E., Kennedy, D., Klein Goldewijk, K.,
1479 Knauer, J., Korsbakken, J. I., Landschützer, P., Lefèvre, N., Lindsay, K., Liu, J., Liu, Z., Marland, G., Mayot, N.,
1480 McGrath, M. J., Metz, N., Monacci, N. M., Munro, D. R., Nakaoka, S.-I., Niwa, Y., O’Brien, K., Ono, T.,
1481 Palmer, P. I., Pan, N., Pierrot, D., Pockock, K., Poulter, B., Resplandy, L., Robertson, E., Rödenbeck, C.,
1482 Rodriguez, C., Rosan, T. M., Schwinger, J., Séférian, R., Shutler, J. D., Skjelvan, I., Steinhoff, T., Sun, Q.,
1483 Sutton, A. J., Sweeney, C., Takao, S., Tanhua, T., Tans, P. P., Tian, X., Tian, H., Tilbrook, B., Tsujino, H.,
1484 Tubiello, F., van der Werf, G. R., Walker, A. P., Wanninkhof, R., Whitehead, C., Willstrand Wranne, A.,
1485 Wright, R., Yuan, W., Yue, C., Yue, X., Zaehle, S., Zeng, J., and Zheng, B.: Global Carbon Budget 2022, *Earth*
1486 *Syst. Sci. Data*, 14, 4811–4900, <https://doi.org/10.5194/essd-14-4811-2022>, 2022.

1487

1488 Fröb, F., Olsen, A., Becker, M., Chafik, L., Johannessen, T., Reverdin, G., and Omar, A.: Wintertime fCO₂
1489 variability in the subpolar North Atlantic since 2004. *Geophysical Research Letters*, 46,
1490 <https://doi.org/10.1029/2018GL080554>, 2019.

1491

1492 Gac, J.-P., Marrec, P., Cariou, T., Guillerm, C., Macé, E., Vernet, M., and Bozec, Y.: Cardinal buoys: An
 1493 opportunity for the study of air-sea CO₂ fluxes in coastal ecosystems. *Front. Mar. Sci.* doi:
 1494 10.3389/fmars.2020.00712. 2020.

1495

1496 Gac, J.-P., Marrec, P., Cariou, T., Grosstefan, E., Macé, E., Rimmelin-Maury, P., Vernet, M., and Bozec, Y.:
 1497 Decadal Dynamics of the CO₂ System and Associated Ocean Acidification in Coastal Ecosystems of the North
 1498 East Atlantic Ocean. *Front. Mar. Sci.* 8:688008. doi:10.3389/fmars.2021.688008, 2021.

1499

1500 Ganachaud, A., Cravatte, S., Sprintall, J., Germineaud, C., Albery, M., Jeandel, C., Eldin, G., Metzl, N., Bonnet,
 1501 S., Benavides, M., Heimburger, L.-E., Lefèvre, J., Michael, S., Resing, J., Quéroúé, F., Sarthou, G., Rodier, M.,
 1502 Berthelot, H., Baurand, F., Grelet, J., Hasegawa, T., Kessler, W., Kilepak, M., Lacan, F., Privat, E., Send, U.,
 1503 Van Beek, P., Souhaut, M. and Sonke, J. E.: The Solomon Sea: its circulation, chemistry, geochemistry and
 1504 biology explored during two oceanographic cruises. *Elem Sci Anth*, 5: 33, DOI:
 1505 <https://doi.org/10.1525/elementa.221>, 2017.

1506

1507 Gattuso, J.-P., Magnan, A., Billé, R., Cheung, W. W. L., Howes, E. L., Joos, F., Allemand, D., Bopp, L., Cooley,
 1508 S., Eakin, M., Hoegh-Guldberg, O., Kelly, R. P., Pörtner, H.-O., Rogers, A. D., Baxter, J. M., Laffoley, D.,
 1509 Osborn, D., Rankovic, A., Rochette, J., Sumaila, U. R., Treyer, S., and Turley, C.: Contrasting futures for ocean
 1510 and society from different anthropogenic CO₂ emissions scenarios. *Science* 349:aac4722.doi:
 1511 10.1126/science.aac4722, 2015.

1512

1513 Gattuso, J.-P., Alliouane, S., and Mousseau, L.: Seawater carbonate chemistry in the Bay of Villefranche, Point
 1514 B (France), January 2007 - September 2020. PANGAEA, <https://doi.org/10.1594/PANGAEA.727120>, 2021.

1515

1516 Gattuso, J.-P., Alliouane, S., and Fischer, P.: High-frequency, year-round time series of the carbonate chemistry
 1517 in a high-Arctic fjord (Svalbard), *Earth Syst. Sci. Data*, 15, 2809–2825, [https://doi.org/10.5194/essd-15-2809-](https://doi.org/10.5194/essd-15-2809-2023)
 1518 [2023](https://doi.org/10.5194/essd-15-2809-2023), 2023.

1519

1520 Gattuso, J.-P., Alliouane, S., and Fischer, P.: High-frequency, year-round time series of the carbonate chemistry
 1521 in a high-Arctic fjord (Svalbard) v2. PANGAEA, <https://doi.org/10.1594/PANGAEA.960131>, 2023.

1522

1523 Gemayel, E., Hassoun, A. E. R., Benallal, M. A., Goyet, C., Rivaro, P., Abboud-Abi Saab, M., Krasakopoulou,
 1524 E., Touratier, F., and Ziveri, P.: Climatological variations of total alkalinity and total inorganic carbon in the
 1525 Mediterranean Sea surface waters. *Earth Syst. Dynam.*, 6, 789-800, doi:10.5194/esd-6-789-2015. 2015.

1526

1527 Golbol, M., Vellucci, V., and Antoine, D.: BOUSSOLE, <https://doi.org/10.18142/1>, 2000.

1528

1529 Golbol M., Boutin J., Merlivat L., Vellucci, V., and Antoine, D.: Dissolved Inorganic Carbon and Total
 1530 Alkalinity sampled at Boussole site in the Mediterranean Sea. SEANOE. <https://doi.org/10.17882/71911>, 2020.

1531

1532 Goris, N., Tjiputra, J. F., Olsen, A., Schwinger, J., Lauvset, S. K. and Jeansson, E.: Constraining projection-
 1533 based estimates of the future North Atlantic carbon uptake, *J. Climate*, 31, 3959–3978,
 1534 <https://doi.org/10.1175/JCLI-D-17-0564.1>, 2018.

1535

1536 Goyet, C., Beauverger, C., Brunet, C., and Poisson, A.: Distribution of carbon dioxide partial pressure in surface
 1537 waters of the Southwest Indian Ocean, *Tellus B: Chemical and Physical Meteorology*, 43:1, 1-11, DOI:
 1538 [10.3402/tellusb.v43i1.15242](https://doi.org/10.3402/tellusb.v43i1.15242), 1991.

1539

1540 Gregor, L. and Gruber, N.: OceanSODA-ETHZ: a global gridded data set of the surface ocean carbonate system
 1541 for seasonal to decadal studies of ocean acidification, *Earth Syst. Sci. Data*, 13, 777–808,
 1542 <https://doi.org/10.5194/essd-13-777-2021>, 2021.

1543

1544 Gruber, N., Clement, D. , Carter, B. R., Feely, R. A., van Heuven, S., Hoppema, M., Ishii, M., Key, R. M.,
1545 Kozyr, A., Lauvset, S. K., Lo Monaco, C. , Mathis, J. T., Murata, A., Olsen, A., Perez, F. F., Sabine, C. L.,
1546 Tanhua, T., and Wanninkhof, R.: The oceanic sink for anthropogenic CO₂ from 1994 to 2007, *Science* vol. 363
1547 (issue 6432), pp. 1193-1199. DOI: 10.1126/science.aau5153, 2019.

1548

1549 Guieu, C., Desboeufs, K., Albani, S., et al.: BIOGEOCHEMICAL dataset collected during the PEACETIME
1550 cruise. SEANOE. <https://doi.org/10.17882/75747>, 2020.

1551

1552 Hagens, M., and Middelburg, J. J.: Attributing seasonal pH variability in surface ocean waters to governing
1553 factors, *Geophys. Res. Lett.*, 43, doi:10.1002/2016GL071719. 2016.

1554

1555 Henson, S. A., Painter, S. C., Holliday, N. P., Stinchcombe, M. C., and Giering, S. L. C.: Unusual subpolar
1556 North Atlantic phytoplankton bloom in 2010: Volcanic fertilization or North Atlantic Oscillation?, *J. Geophys.*
1557 *Res. Oceans*, 118, 4771–4780, doi:10.1002/jgrc.20363, 2013.

1558

1559 Hoegh-Guldberg, O., Mumby, P.J., Hooten, A.J., Steneck, R.S., Greenfield, P., Gomez, E., Harvell, C.D., Sale,
1560 P.F., Edwards, A.J., Caldeira, K., Knowlton, N., Eakin, C.M., Iglesias-Prieto, R., Muthiga, N., Bradbury, R.H.,
1561 Dubi, A., and Hatziolos, M.E.: Coral reefs under rapid climate change and ocean acidification. *Science* 14,
1562 1737–1742. <https://doi.org/10.1126/science.1152509>, 2007.

1563

1564 Hood, E.M., and Merlivat, L.: Annual to interannual variations of fCO₂ in the northwestern Mediterranean
1565 Sea: Results from hourly measurements made by CARIOCA buoys, 1995-1997, *Journal Of Marine Research*,
1566 59, 113-131, doi: 10.1357/002224001321237399. 2001

1567

1568 Howes, E., Stemmann, L., Assailly, C., Irisson, J.-O., Dima, M., Bijma, J., Gattuso, J.-P.: Pteropod time series
1569 from the North Western Mediterranean (1967-2003): impacts of pH and climate variability. *Mar Ecol Prog Ser*
1570 531: 193-206, doi: 10.3354/meps11322. 2015.

1571

1572 Howes, E. L., Eagle, R., Gattuso, J.-P., and Bijma, J.: Comparison of Mediterranean pteropod shell biometrics
1573 and ultrastructure from historical (1910 and 1921) and present day (2012) samples provides baseline for
1574 monitoring effects of global change. *PLoS ONE* 12:e0167891. 2017.

1575

1576 IPCC. Changing Ocean, Marine Ecosystems, and Dependent Communities. in *The Ocean and Cryosphere in a*
1577 *Changing Climate* 447–588 (Cambridge University Press, 2022). doi:10.1017/9781009157964.007. 2022

1578

1579 Jiang, Z.-P., Tyrrell, T., Hydes, D. J., Dai, M., and Hartman, S. E.: Variability of alkalinity and the alkalinity-
1580 salinity relationship in the tropical and subtropical surface ocean, *Global Biogeochem. Cycles*, 28, 729–742,
1581 doi:10.1002/2013GB004678, 2014.

1582

1583 Jiang, L.-Q., Feely, R. A., Carter, B. R., Greeley, D. J., Gledhill, D. K., and Arzayus K. M.: Climatological
1584 distribution of aragonite saturation state in the global oceans, *Global Biogeochem. Cycles*, 29, 1656–1673,
1585 doi:10.1002/2015GB005198, 2015.

1586

1587 Jiang, L.-Q., Carter, B. R., Feely, R. A., Lauvset, S. K. and Olsen, A.: Surface ocean pH and buffer capacity:
1588 past, present and future, *Sci Rep*, 9(1), 1–11, doi:10.1038/s41598-019-55039-4. 2019.

1589

1590 Jiang, L.-Q., Feely, R. A., Wanninkhof, R., Greeley, D., Barbero, L., Alin, S., Carter, B. R., Pierrot, D.,
1591 Featherstone, C., Hooper, J., Melrose, C., Monacchi, N., Sharp, J. D., Shellito, S., Xu, Y.-Y., Kozyr, A., Byrne, R.
1592 H., Cai, W.-J., Cross, J., Johnson, G. C., Hales, B., Langdon, C., Mathis, J., Salisbury, J., and Townsend, D. W.:
1593 Coastal Ocean Data Analysis Product in North America (CODAP-NA) – an internally consistent data product for
1594 discrete inorganic carbon, oxygen, and nutrients on the North American ocean margins. *Earth System Science*
1595 *Data*, 13(6), 2777–2799. <https://doi.org/10.5194/essd-13-2777-2021>, 2021

1596

1597 Jiang, L.-Q., Dunne, J., Carter, B. R., Tjiputra, J. F., Terhaar, J., Sharp, J. D., et al.: Global surface ocean
1598 acidification indicators from 1750 to 2100. *Journal of Advances in Modeling Earth Systems*, 15,
1599 e2022MS003563. <https://doi.org/10.1029/2022MS003563> , 2023a
1600

1601 Jiang, L.Q., Kozyr, A., Relph, J.M. *et al.* The Ocean Carbon and Acidification Data System. *Sci Data* 10, 136.
1602 <https://doi.org/10.1038/s41597-023-02042-0>, 2023b
1603

1604 Johnson, K. S., Mazloff, M. R., Bif, M. B., Takeshita, Y., Jannasch, H. W., Maurer, T. L., et al.: Carbon to
1605 nitrogen uptake ratios observed across the Southern Ocean by the SOCCOM profiling float array. *Journal of*
1606 *Geophysical Research: Oceans*, 127, e2022JC018859. <https://doi.org/10.1029/2022JC018859>, 2022.
1607

1608 Joos, F., Hameau, A., Frölicher, T. L., and Stephenson, D. B.: Anthropogenic attribution of the
1609 increasing seasonal amplitude in surface ocean pCO₂. *Geophysical Research Letters*, 50, e2023GL102857.
1610 <https://doi.org/10.1029/2023GL102857>, 2023.
1611

1612 Joyce, T. and Corry, C., eds: Requirements for WOCE Hydrographic Programme Data Reporting. WHPO
1613 Publication 90-1 Revision 2, WOCE Report 67/91, Woods Hole, Mass., USA, May 1994.
1614

1615 Kapsenberg, L., Alliouane, S., Gazeau, F., Mousseau, L., and Gattuso, J.-P.: Coastal ocean acidification and
1616 increasing total alkalinity in the northwestern Mediterranean Sea, *Ocean Sci.*, 13, 411-426, doi:10.5194/os-13-
1617 411-2017, 2017.
1618

1619 Keppler, L., Landschützer, P., Gruber, N., Lauvset, S. K., and Stemmler, I.: Seasonal carbon dynamics in the
1620 near-global ocean. *Global Biogeochemical Cycles*, 34, e2020GB006571. doi:10.1029/2020GB006571, 2020.
1621

1622 Keppler, L., Landschützer, P., Lauvset, S.K., and Gruber, N.: Recent trends and variability in the oceanic storage
1623 of dissolved inorganic carbon. *Global Biogeochemical Cycles*, 37, e2022GB007677. Doi:
1624 10.1029/2022GB007677, 2023.
1625

1626 Keraghel, M. A., Louanchi, F., Zerrouki, M., Kaci, M. A., Aït-Ameur, N., Labaste, M., Legoff, H., Taillandier,
1627 V., Harid, R., and Mortier, L.: Carbonate system properties and anthropogenic carbon inventory in the Algerian
1628 Basin during SOMBA cruise (2014): Acidification estimate, *Marine Chemistry*,
1629 <https://doi.org/10.1016/j.marchem.2020.103783>. 2020.
1630

1631 Key, R. M., Kozyr, A., Sabine, C. L., Lee, K., Wanninkhof, R., Bullister, J. L., Feely, R. A., Millero, F. J.,
1632 Mordy, C., and Peng, T. H.: A global ocean carbon climatology: Results from Global Data Analysis Project
1633 (GLODAP), *Global Biogeochemical Cycles*, 18, GB4031, <https://doi.org/10.1029/2004GB002247>, 2004.
1634

1635 Key, R. M., Tanhua, T., Olsen, A., Hoppema, M., Jutterström, S., Schirnick, C., van Heuven, S., Kozyr, A., Lin,
1636 X., Velo, A., Wallace, D. W. R., and Mintrop, L.: The CARINA data synthesis project: introduction and
1637 overview, *Earth Syst. Sci. Data*, 2, 105–121, <https://doi.org/10.5194/essd-2-105-2010>, 2010.
1638

1639 Khatiwala, S., Tanhua, T., Mikaloff Fletcher, S., Gerber, M., Doney, S. C., Graven, H. D., Gruber, N.,
1640 McKinley, G. A., Murata, A., Ríos, A. F., and Sabine, C. L.: Global ocean storage of anthropogenic carbon,
1641 *Biogeosciences*, 10, 2169-2191, <https://doi.org/10.5194/bg-10-2169-2013>, 2013.
1642

1643 Kitidis, V., Shutler, J. D., Ashton, I., Warren, M., Brown, I., Findlay, H., Hartman, S. E., Sanders, R.,
1644 Humphreys, M., Kivimäe, C., Greenwood, N., Hull, T., Pearce, D., McGrath, T., Stewart, B. M., Walsham, P.,
1645 McGovern, E., Bozec, Y., Gac, J.-P., van Heuven, S., Hoppema, M., Schuster, U., Johannessen, T., Omar, A.,
1646 Lauvset, S. K., Skjelvan, I., Olsen, A., Steinhoff, T., Körtzinger, A., Becker, M., Lefèvre, N., Diverrès, D.,
1647 Gkritzalis, T., Cattijisse, A., Petersen, W., Voynova, Y., Chapron, B., Grouazel, A., Land, P. E., Sharples, J., and
1648 Nightingale, P. D.: Winter weather controls net influx of atmospheric CO₂ on the north-west European shelf. *Sci*
1649 *Rep* 9, 20153, doi:10.1038/s41598-019-56363-5. 2019.
1650

1651 Koffi U., Lefevre, N., Kouadio, G., and Boutin, J.: Surface CO₂ parameters and air-sea CO₂ fluxes distribution
1652 in the eastern equatorial Atlantic Ocean. *J. Marine Systems*, doi:10.1016/j.jmarsys/2010.04.010. 2010.
1653

1654 Koffi, U., Georges, K., and Boutin, J.: Partial pressure (or fugacity) of carbon dioxide, dissolved inorganic
1655 carbon, alkalinity, temperature, salinity and other variables collected from Surface underway, discrete sample
1656 and profile observations using CTD, Carbon dioxide (CO₂) gas analyzer and other instruments from ANTEA
1657 and L'ATALANTE in the Gulf of Guinea, North Atlantic Ocean and South Atlantic Ocean from 2005-06-09 to
1658 2007-09-30 (NCEI Accession 0108086). [indicate subset used]. NOAA National Centers for Environmental
1659 Information. Dataset. https://doi.org/10.3334/cdiac/otg.egee1_6. Accessed [date]., 2013
1660

1661 Koseki, S., Tjiputra, J., Fransner, F. et al.: Disentangling the impact of Atlantic Niño on sea-air CO₂ flux. *Nat*
1662 *Commun* 14, 3649. <https://doi.org/10.1038/s41467-023-38718-9>, 2023.
1663

1664 Kwiatkowski, L., Torres, O., Bopp, L., Aumont, O., Chamberlain, M., Christian, J. R., Dunne, J. P., Gehlen, M.,
1665 Ilyina, T., John, J. G., Lenton, A., Li, H., Lovenduski, N. S., Orr, J. C., Palmieri, J., Santana-Falcón, Y.,
1666 Schwinger, J., Séférian, R., Stock, C. A., Tagliabue, A., Takano, Y., Tjiputra, J., Toyama, K., Tsujino, H.,
1667 Watanabe, M., Yamamoto, A., Yool, A., and Ziehn, T.: Twenty-first century ocean warming, acidification,
1668 deoxygenation, and upper-ocean nutrient and primary production decline from CMIP6 model projections,
1669 *Biogeosciences*, 17, 3439–3470, <https://doi.org/10.5194/bg-17-3439-2020>, 2020.
1670

1671 Land, P. E., Findlay, H. S., Shutler, J. D., Ashton, I. G., Holding, T., Grouazel, A., Girard-Ardhuin, F., Reul, N.,
1672 Piolle, J. F., Chapron, B., and Quilfen, Y.: Optimum satellite remote sensing of the marine carbonate system
1673 using empirical algorithms in the global ocean, the Greater Caribbean, the Amazon Plume and the Bay of
1674 Bengal. *Remote Sensing of Environment*, 235, p.111469, doi: 10.1016/j.rse.2019.111469, 2019.
1675

1676 Lange, N., Fiedler, B., Álvarez, M., Benoit-Cattin, A., Benway, H., Buttigieg, P. L., Coppola, L., Currie, K.,
1677 Flecha, S., Honda, M., Huertas, I. E., Lauvset, S. K., Muller-Karger, F., Körtzinger, A., O'Brien, K. M.,
1678 Ólafsdóttir, S. R., Pacheco, F. C., Rueda-Roa, D., Skjelvan, I., Wakita, M., White, A., and Tanhua, T.: Synthesis
1679 Product for Ocean Time-Series (SPOTS) – A ship-based biogeochemical pilot, *Earth Syst. Sci. Data Discuss.*
1680 [preprint], <https://doi.org/10.5194/essd-2023-238>, in review, 2023.
1681

1682 Lauvset, S. K., Gruber, N., Landschützer, P., Olsen, A., and Tjiputra, J.: Trends and drivers in global surface
1683 ocean pH over the past 3 decades. *Biogeosciences*, 12, 1285-1298, doi:10.5194/bg-12-1285-2015, 2015
1684

1685 Lauvset, S. K., Carter, B. R., Perez, F. F., Jiang, L.-Q., Feely, R. A., Velo, A., and Olsen, A.: Processes Driving
1686 Global Interior Ocean pH Distribution, *Global Biogeochem. Cycles*, 34, e2019GB006 229,
1687 <https://doi.org/10.1029/2019GB006229>, 2020.
1688

1689 Lauvset, S. K., Lange, N., Tanhua, T., Bittig, H. C., Olsen, A., Kozyr, A., Álvarez, M., Becker, S., Brown, P. J.,
1690 Carter, B. R., Cotrim da Cunha, L., Feely, R. A., van Heuven, S., Hoppema, M., Ishii, M., Jeansson, E.,
1691 Jutterström, S., Jones, S. D., Karlsen, M. K., Lo Monaco, C., Michaelis, P., Murata, A., Pérez, F. F., Pfeil, B.,
1692 Schirnack, C., Steinfeldt, R., Suzuki, T., Tilbrook, B., Velo, A., Wanninkhof, R., Woosley, R. J., and Key, R. M.:
1693 An updated version of the global interior ocean biogeochemical data product, GLODAPv2.2021, *Earth Syst. Sci.*
1694 *Data*, 13, 5565–5589, <https://doi.org/10.5194/essd-13-5565-2021>, 2021.
1695

1696 Lauvset, S. K., Lange, N., Tanhua, T., Bittig, H. C., Olsen, A., Kozyr, A., Alin, S., Álvarez, M., Azetsu-Scott,
1697 K., Barbero, L., Becker, S., Brown, P. J., Carter, B. R., da Cunha, L. C., Feely, R. A., Hoppema, M., Humphreys,
1698 M. P., Ishii, M., Jeansson, E., Jiang, L.-Q., Jones, S. D., Lo Monaco, C., Murata, A., Müller, J. D., Pérez, F. F.,
1699 Pfeil, B., Schirnack, C., Steinfeldt, R., Suzuki, T., Tilbrook, B., Ulfsbo, A., Velo, A., Woosley, R. J., and Key, R.
1700 M.: GLODAPv2.2022: the latest version of the global interior ocean biogeochemical data product, *Earth Syst.*
1701 *Sci. Data*, 14, 5543–5572, <https://doi.org/10.5194/essd-14-5543-2022>, 2022.
1702

1703 Lebehot, A. D., Halloran, P. R., Watson, A. J., McNeill, D., Ford, D. A., Landschützer, P., Lauvset, S. K.,
1704 and Schuster, U.: Reconciling Observation and Model Trends in North Atlantic Surface CO₂, *Global*
1705 *Biogeochem. Cy.*, 33, 1204–1222, <https://doi.org/10.1029/2019GB006186>, 2019.

1706
1707 Lee, K., Wanninkhof, R., Feely, R. A., Millero, F. J., and Peng, T.-H.: Global relationships of total inorganic
1708 carbon with temperature and nitrate in surface seawater, *Global Biogeochem. Cy.*, 14, 979–994,
1709 <https://doi.org/10.1029/1998GB001087>, 2000.
1710
1711 Lee, K., Tong, L.T., Millero, F.J., Sabine, C.L., Dickson, A.G., Goyet, C., Park, G.H., Wanninkhof, R., Feely,
1712 R.A., and Key, R.M.: Global relationships of total alkalinity with salinity and temperature in surface waters of
1713 the world's oceans. *Geophys. Res. Lett.* 33, L19605. doi10.1029/2006GL027207. 2006.
1714
1715 Lefèvre, D.: MOOSE (ANTARES), <https://doi.org/10.18142/233>, 2010.
1716
1717 Lefèvre, N., Guillot, A., Beaumont, L, and Danguy, T.: Variability of fCO₂ in the Eastern Tropical Atlantic
1718 from a moored buoy. *J. of Geophysical Research-Oceans*, Volume: 113 Issue: C1, DOI:
1719 10.1029/2007JC004146. 2008.
1720
1721 Lefèvre N., and Merlivat, L.: Carbon and oxygen net community production in the eastern tropical Atlantic
1722 estimated from a moored buoy. *Global biogeochemical cycles*, 26(1), 1-14.
1723 <https://doi.org/10.1029/2010GB004018>. 2012.
1724
1725 Lefèvre, N., Diverres, D., and Gallois, F.: Origin of CO₂ undersaturation in the western tropical Atlantic: Tellus
1726 Series B Chemical and Physical Meteorology. Volume: 62 Issue: 5 Special Issue: SI Pages: 595-607 DOI:
1727 10.1111/j.1600-0889.2010.00475.x, 2010.
1728
1729 Lefèvre N.: Carbon parameters along a zonal transect. SEANO. <https://doi.org/10.17882/58575>, 2010.
1730
1731 Lefèvre, N., Veleda, D., Araujo, M., Caniaux, G.: Variability and trends of carbon parameters at a time series in
1732 the eastern tropical Atlantic. *Tellus B*, Co-Action Publishing, 68, pp.30305. 10.3402/tellusb.v68.30305. 2016.
1733
1734 Lefèvre, N., Mejia, C., Khvorostyanov, D., Beaumont, L., and Koffi, U.: Ocean Circulation Drives the
1735 Variability of the Carbon System in the Eastern Tropical Atlantic. *Oceans*, 2021, 2, 126–148.
1736 <https://doi.org/10.3390/oceans2010008>, 2021.
1737
1738 Lefèvre, N.: Discrete profile measurements of dissolved inorganic carbon, total alkalinity, temperature and
1739 salinity collected from R/V Antea French PIRATA cruise in Eastern Tropical Atlantic Ocean from 2009-07-10
1740 to 2010-10-01 (NCEI Accession 0171193), 2018a.
1741
1742 Lefèvre, N.: Discrete surface measurements of dissolved inorganic carbon, total alkalinity, temperature and
1743 salinity collected from R/V Le Suroit French PIRATA cruise in Eastern Tropical Atlantic Ocean from 2011-05-
1744 03 to 2011-05-25 (NCEI Accession 0171197), 2018b.
1745
1746 Lefèvre, N.: Discrete profile measurements of dissolved inorganic carbon, total alkalinity, temperature and
1747 salinity collected from R/V Le Suroit French PIRATA cruise in Eastern Tropical Atlantic Ocean from 2012-03-
1748 21 to 2012-04-30 (NCEI Accession 0171195), 2018c.
1749
1750 Lefèvre, N.: Discrete surface measurements of dissolved inorganic carbon, total alkalinity, temperature and
1751 salinity collected from R/V Le Suroit French PIRATA cruise in Eastern Tropical Atlantic Ocean from 2013-05-
1752 11 to 2013-06-18 (NCEI Accession 0171189), 2018d.
1753
1754 Lefèvre, N.: Discrete profile measurements of dissolved inorganic carbon, total alkalinity, temperature and
1755 salinity collected from R/V Le Suroit French PIRATA cruise in Eastern Tropical Atlantic Ocean from 2014-04-
1756 10 to 2014-05-19 (NCEI Accession 0171194), 2018e.
1757
1758 Lefèvre, N.: Discrete surface measurements of dissolved inorganic carbon, total alkalinity, temperature and
1759 salinity collected from R/V Thalassa French PIRATA cruise in Eastern Tropical Atlantic Ocean from 2015-03-
1760 18 to 2015-04-15 (NCEI Accession 0171196), 2018f.
1761

1762 Lefèvre, N.: Discrete surface measurements of dissolved inorganic carbon, total alkalinity, temperature and
1763 salinity collected from R/V Thalassa French PIRATA cruise in Eastern Tropical Atlantic Ocean from 2016-03-
1764 08 to 2016-04-11 (NCEI Accession 0171190), 2018g.
1765
1766 Lefèvre, N.: Discrete surface measurements of dissolved inorganic carbon, total alkalinity, temperature and
1767 salinity collected from R/V Thalassa French PIRATA cruise in Eastern Tropical Atlantic Ocean from 2017-02-
1768 26 to 2017-03-30 (NCEI Accession 0171191), 2018h.
1769
1770 Le Quéré, C., Moriarty, R., Andrew, R. M., Canadell, J. G., Sitch, S., Korsbakken, J. I., Friedlingstein, P., Peters,
1771 G. P., Andres, R. J., Boden, T. A., Houghton, R. A., House, J. I., Keeling, R. F., Tans, P., Arneeth, A., Bakker, D.
1772 C. E., Barbero, L., Bopp, L., Chang, J., Chevallier, F., Chini, L. P., Ciais, P., Fader, M., Feely, R. A., Gkritzalis,
1773 T., Harris, I., Hauck, J., Ilyina, T., Jain, A. K., Kato, E., Kitidis, V., Klein Goldewijk, K., Koven, C.,
1774 Landschützer, P., Lauvset, S. K., Lefèvre, N., Lenton, A., Lima, I. D., Metzl, N., Millero, F., Munro, D. R.,
1775 Murata, A., Nabel, J. E. M. S., Nakaoka, S., Nojiri, Y., O'Brien, K., Olsen, A., Ono, T., Pérez, F. F., Pfeil, B.,
1776 Pierrot, D., Poulter, B., Rehder, G., Rödenbeck, C., Saito, S., Schuster, U., Schwinger, J., Séférian, R., Steinhoff,
1777 T., Stocker, B. D., Sutton, A. J., Takahashi, T., Tilbrook, B., van der Laan-Luijkx, I. T., van der Werf, G. R., van
1778 Heuven, S., Vandemark, D., Viovy, N., Wiltshire, A., Zaehle, S., and Zeng, N.: Global Carbon Budget 2015,
1779 *Earth Syst. Sci. Data*, 7, 349–396, <https://doi.org/10.5194/essd-7-349-2015>, 2015.
1780
1781 Lerner, P., Romanou, A., Kelley, M., Romanski, J., Ruedy, R., and Russell, G.: Drivers of Air-Sea CO₂ Flux
1782 Seasonality and its Long-Term Changes in the NASA-GISS model CMIP6 submission. *Journal of Advances in*
1783 *Modeling Earth Systems*, 13, e2019MS002028. [Doi:10.1029/2019MS002028](https://doi.org/10.1029/2019MS002028), 2021.
1784
1785 Leseurre, C., Lo Monaco, C., Reverdin, G., Metzl, N., Fin, J., Olafsdottir, S., and Racapé, V.: Ocean carbonate
1786 system variability in the North Atlantic Subpolar surface water (1993–2017), *Biogeosciences*, 17, 2553–2577,
1787 <https://doi.org/10.5194/bg-17-2553-2020>, 2020
1788
1789 Leseurre, C., Lo Monaco, C., Reverdin, G., Metzl, N., Fin, J., Mignon, C., and Benito, L.: Summer trends and
1790 drivers of sea surface fCO₂ and pH changes observed in the southern Indian Ocean over the last two decades
1791 (1998–2019), *Biogeosciences*, 19, 2599–2625, <https://doi.org/10.5194/bg-19-2599-2022>, 2022.
1792
1793 Lherminier, P., Mercier, H., Gourcuff, C., Alvarez, M., Bacon, S., and Kermabon, C.: Transports across the 2002
1794 Greenland-Portugal OVIDE section and comparison with 1997. *J. Geophys. Res.*, 112(C7), C07003,
1795 [doi:10.1029/2006JC003716](https://doi.org/10.1029/2006JC003716), 2007
1796
1797 Li, B. F., Watanabe, Y. W., Hosoda, S., Sato, K., and Nakano, Y.: Quasireal-time and high-resolution
1798 spatiotemporal distribution of ocean anthropogenic CO₂. *Geophysical Research Letters*, 46, 4836–4843.
1799 <https://doi.org/10.1029/2018GL081639>, 2019.
1800
1801 Lo Monaco, C., Álvarez, M., Key, R. M., Lin, X., Tanhua, T., Tilbrook, B., Bakker, D. C. E., van Heuven, S.,
1802 Hoppema, M., Metzl, N., Ríos, A. F., Sabine, C. L., and Velo, A.: Assessing the internal consistency of the
1803 CARINA database in the Indian sector of the Southern Ocean, *Earth Syst. Sci. Data*, 2, 51–70,
1804 <https://doi.org/10.5194/essd-2-51-2010>, 2010.
1805
1806 Lo Monaco, C., Metzl, N., Fin, J., and Tribollet, A.: Sea surface measurements of dissolved inorganic carbon
1807 (DIC) and total alkalinity (TALK), temperature and salinity during the R/V Marion-Dufresne cruise CLIM-
1808 EPARSE (EXPCODE 35MV20190405) in the Indian Ocean and Mozambique Channel from 2019-04-04 to
1809 2019-04-30. (NCEI Accession 0212218). [indicate subset used]. NOAA National Centers for Environmental
1810 Information. Dataset. <https://doi.org/10.25921/26rw-w185>. Accessed [date]. 2020.
1811
1812 Lo Monaco, C., Metzl, N., Fin, J., Mignon, C., Cuet, P., Douville, E., Gehlen, M., Trang Chau, T.T., and
1813 Tribollet, A.: Distribution and long-term change of the sea surface carbonate system in the Mozambique Channel
1814 (1963–2019), *Deep-Sea Research Part II*, <https://doi.org/10.1016/j.dsr2.2021.104936>, 2021
1815

1816 Lombard, F., Bourdin, G., Pesant, S., Agostini, S., Baudena, A., Boissin, E., Cassar, N., Clampitt, M., Conan,
1817 P., Da Silva, O., Dimier, C., Douville, E., Elineau, A., Fin, J., Flores, J.-M., Ghiglione, J.-F., Hume, B. C. C.,
1818 Jalabert, L., John, S. G., Kelly, R. L., Koren, I., Lin, Y., Marie, D., McMinds, R., Mériquet, Z., Metzl, N., Paz-
1819 García, D. A., Luiza Pedrotti, M., Poulain, J., Pujo-Pay, M., Ras, J., Reverdin, G., Romac, S., Röttinger, E.,
1820 Vardi, A., Woolstra, C. R., Moulin, C., Iwankow, G., Banaigs, B., Bowler, C., de Vargas, C., Forcioli, D., Furla,
1821 P., Galand, P. E., Gilson, E., Reynaud, S., Sunagawa, S., Thomas, O., Troublé, R., Vega Thurber, R., Wincker,
1822 P., Zoccola, D., Allemand, D., Planes, S., Boss, E., and Gorsky, G.: Open science resources from the Tara
1823 Pacific expedition across the surface ocean and coral reef ecosystems. *Sci Data* 10, 324 (2023).
1824 <https://doi.org/10.1038/s41597-022-01757-w>, 2022.

1825

1826 Lueker, T. J., Dickson, A. G., and Keeling, C. D.: Ocean pCO₂ calculated from dissolved inorganic carbon,
1827 alkalinity, and equations for K-1 and K-2: validation based on laboratory measurements of CO₂ in gas and
1828 seawater at equilibrium. *Marine Chemistry* 70, 105-119. [https://doi.org/10.1016/S0304-4203\(00\)00022-0](https://doi.org/10.1016/S0304-4203(00)00022-0), 2000.

1829

1830 Ma, D., Gregor, L., and Gruber, N: Four decades of trends and drivers of global surface ocean acidification.
1831 *Global Biogeochemical Cycles*, 37, e2023GB007765. [10.1029/2023GB007765](https://doi.org/10.1029/2023GB007765), 2023.

1832

1833 Maier, C., Watremez, P., Taviani, M., Weinbauer, M. G, and Gattuso, J-P.: Calcification rates and the effect of
1834 ocean acidification on Mediterranean cold-water corals. *Proceedings of the Royal Society B-Biological Sciences*,
1835 279(1734), 1716-1723, doi:10.1098/rspb.2011.1763. 2012.

1836

1837 Margirier, F., Testor, P., Heslop, E. et al. : Abrupt warming and salinification of intermediate waters interplays
1838 with decline of deep convection in the Northwestern Mediterranean Sea. *Sci Rep* 10, 20923. [10.1038/s41598-020-77859-5](https://doi.org/10.1038/s41598-020-77859-5), 2020.

1840

1841 Marrec, P., Cariou, T., Collin, E., Durand, A., Latimier, M., Macé, E., Morin, P., Raimund, S., Vernet, M., and
1842 Bozec, Y.: Seasonal and latitudinal variability of the CO₂ system in the western English Channel based on
1843 Voluntary Observing Ship (VOS) measurements. *Marine Chemistry*, 155 (2013): 29–41. 2013.

1844

1845 Marrec, P., Cariou, T., Latimier, M., Macé, E., Morin, P., Vernet, M., and Bozec, Y.: Spatio-temporal dynamics
1846 of biogeochemical processes and air–sea CO₂ fluxes in the Western English Channel based on two years of
1847 FerryBox deployment. *Journal of Marine Systems*, Special Issue: 5th FerryBox Workshop.
1848 [10.1016/j.jmarsys.2014.05.010](https://doi.org/10.1016/j.jmarsys.2014.05.010). 2014.

1849

1850 Marrec, P., Cariou, T., Macé, E., Morin, P., Salt, L. A., Vernet, M., Taylor, B., Paxman, K., and Y. Bozec:
1851 Dynamics of air–sea CO₂ fluxes in the northwestern European shelf based on voluntary observing ship and
1852 satellite observations, *Biogeosciences*, 12, 5371-5391, doi:10.5194/bg-12-5371-2015. 2015

1853

1854 Marrec, P., and Bozec, Y.: Partial pressure (or fugacity) of carbon dioxide, dissolved inorganic carbon, alkalinity
1855 and salinity collected from Surface underway observations using Carbon dioxide (CO₂) gas analyzer and other
1856 instruments from ARMORIQUE in the English Channel from 2012-04-25 to 2013-01-03 (NCEI Accession
1857 0157472). Version 1.1. NOAA National Centers for Environmental Information. Dataset.
1858 doi:10.3334/CDIAC/OTG.COAST_FERRYBOX_ROSCOFF_PLYMOUTH_2012 [access date]. 2016a.

1859

1860 Marrec, P., and Bozec, Y.: Partial pressure (or fugacity) of carbon dioxide, dissolved inorganic carbon, alkalinity
1861 and salinity collected from Surface underway observations using Carbon dioxide (CO₂) gas analyzer and other
1862 instruments from ARMORIQUE in the English Channel from 2013-03-15 to 2013-12-22 (NCEI Accession
1863 0157444). Version 1.1. NOAA National Centers for Environmental Information. Dataset.
1864 doi:10.3334/CDIAC/OTG.COAST_FERRYBOX_ROSCOFF_PLYMOUTH_2013 [access date]. 2016b.

1865

1866 Marrec, P., and Bozec, Y.: Partial pressure (or fugacity) of carbon dioxide, dissolved inorganic carbon, alkalinity
1867 and salinity collected from surface underway observations using Carbon dioxide (CO₂) gas analyzer and other
1868 instruments from ARMORIQUE in the English Channel from 2014-03-18 to 2014-10-09 (NCEI Accession
1869 0163193). Version 1.1. NOAA National Centers for Environmental Information. Dataset.
1870 doi:10.3334/CDIAC/OTG.COAST_FERRYBOX_ROSCOFF_PLYMOUTH_2014 [access date]. 2017.

1871

1872 Mazloff, M. R., Verdy, A., Gille, S. T., Johnson, K. S., Cornuelle, B. D., and Sarmiento, J.: Southern Ocean
1873 acidification revealed by biogeochemical-Argo floats. *Journal of Geophysical Research: Oceans*, 128,
1874 e2022JC019530. <https://doi.org/10.1029/2022JC019530>, 2023.

1875

1876 McCulloch, M., Trotter, J., Montagna, P., Falter, J., Dunbar, R., Freiwald, A., Försterra, G., López Correa, M.,
1877 Maier, C., Rüggeberg, A., and Taviani, M.: Resilience of cold-water scleractinian corals to ocean acidification:
1878 Boron isotopic systematics of pH and saturation state up-regulation. *Geochimica et Cosmochimica Acta*, Volume
1879 87, 21-34. <http://dx.doi.org/10.1016/j.gca.2012.03.027>. 2012

1880

1881 McKinley, G. A., Fay, A. R., Takahashi, T., and Metzl, N.: Convergence of atmospheric and North Atlantic
1882 carbon dioxide trends on multidecadal timescales. *Nature Geoscience*. doi:10.1038/NGEO1193. 2011.

1883

1884 McKinley, G. A., Ritzer, A. L. and Lovenduski, N. S.: Mechanisms of northern North Atlantic biomass
1885 variability, *Biogeosciences*, 15(20), 6049–6066, doi:<https://doi.org/10.5194/bg-15-6049-2018>, 2018.

1886

1887 Meier, K. J. S., Beaufort, L., Heussner, S., and Ziveri, P.: The role of ocean acidification in *Emiliana huxleyi*
1888 coccolith thinning in the Mediterranean Sea, *Biogeosciences*, 11, 2857–2869, [https://doi.org/10.5194/bg-11-](https://doi.org/10.5194/bg-11-2857-2014)
1889 2857-2014, 2014.

1890

1891 Mercier, H., Lherminier, P., Sarafanov, A., Gaillard, F., Daniault, N., Desbruyères, D., Falina, A., Ferron, B.,
1892 Huck, T., and Thierry, V.: Variability of the meridional overturning circulation at the Greenland-Portugal Ovide
1893 section from 1993 to 2010. *Progress in Oceanography*, 132, 250-261, doi:10.1016/j.pocean.2013.11.001. 2015

1894

1895 Merlivat, L., Boutin, J., Antoine, D., Beaumont, L., Golbol, M., and Vellucci, V.: Increase of dissolved inorganic
1896 carbon and decrease in pH in near-surface waters in the Mediterranean Sea during the past two decades,
1897 *Biogeosciences*, 15, 5653-5662, <https://doi.org/10.5194/bg-15-5653-2018>, 2018.

1898

1899 Metzl, N., Brunet, C., Jabaud-Jan, A., Poisson, A., and Schauer, B.: Summer and winter air-sea CO₂ fluxes in
1900 the Southern Ocean *Deep Sea Res I*, 53, 1548-1563, doi:10.1016/j.dsr.2006.07.006. 2006.

1901

1902 Metzl, N., Tilbrook, B., Bakker, D., Le Quéré, C., Doney, S., Feely, R., Hood M., and Dargaville, R.: Global
1903 Changes in Ocean Carbon: Variability and Vulnerability. *Eos, Transactions of the American Geophysical Union*
1904 88 (28): 286-287. doi: 10.1029/2007EO280005, 2007.

1905

1906 Metzl, N., Corbière, A., Reverdin, G., Lenton, A., Takahashi, T., Olsen, A., Johannessen, T., Pierrot, D.,
1907 Wanninkhof, R., Ólafsdóttir, S. R., Ólafsson, J., and Ramonet, M.: Recent acceleration of the sea surface fCO₂
1908 growth rate in the North Atlantic subpolar gyre (1993-2008) revealed by winter observations, *Global*
1909 *Biogeochem. Cycles*, 24, GB4004, doi:10.1029/2009GB003658, 2010.

1910

1911 Metzl, N., and Lo Monaco, C.: OISO - OCÉAN INDIEN SERVICE D'OBSERVATION,
1912 <https://doi.org/10.18142/228>, 1998.

1913

1914 Metzl, N., Pierre, C., and Vangriesheim, A.: Hydrographic and Chemical measurements during the R/V
1915 L'Atalante BIOZAIRE III Cruise in the Atlantic Ocean (14 December, 2003 - 7 January 2004).
1916 <http://cdiac.esd.ornl.gov/ftp/oceans/BIOZAIRE3>. Carbon Dioxide Information Analysis Center, Oak Ridge
1917 National Laboratory, US Department of Energy, Oak Ridge, Tennessee. doi:
1918 10.3334/CDIAC/OTG.BIOZAIRE3, 2016.

1919

1920 Metzl, N., Ferron, B. Lherminier, P. Sarthou, G. Thierry, V.: Discrete profile measurements of dissolved
1921 inorganic carbon (DIC), total alkalinity (TALK), temperature and salinity during the multiple ships Observatoire
1922 de la variabilité interannuelle et décennale en Atlantique Nord (OVIDE) project, OVIDE-2006, OVIDE-2008,
1923 OVIDE-2010, OVIDE-2012, OVIDE-2014 cruises in the North Atlantic Ocean from 2006-05-23 to 2014-06-30

1924 (NCEI Accession 0177219). Version 1.1. NOAA National Centers for Environmental Information. Dataset.
 1925 doi:10.25921/v0qt-ms48 [access date], 2018.
 1926
 1927 Metz, N., Fin, J., Lo Monaco, C., et al.: A synthesis of total alkalinity and dissolved inorganic carbon
 1928 measurements in the global ocean (1993-2022) SNAPO-CO2-V1 dataset. SEANOE.
 1929 <https://doi.org/10.17882/95414>, 2023.

1930 Mignot, A., Claustre, H., Cossarini, G., D'Ortenzio, F., Gutknecht, E., Lamouroux, J., Lazzari, P., Perruche, C.,
 1931 Salon, S., Sauzède, R., Taillandier, V., and Teruzzi, A.: Using machine learning and Biogeochemical-Argo
 1932 (BGC-Argo) floats to assess biogeochemical models and optimize observing system design, *Biogeosciences*, 20,
 1933 1405–1422, <https://doi.org/10.5194/bg-20-1405-2023>, 2023.
 1934
 1935 Millero, F. J., Lee, K. and Roche, M.: Distribution of alkalinity in the surface waters of the major oceans. *Mar.*
 1936 *Chem.* **60**, 111–130. [https://doi.org/10.1016/S0304-4203\(97\)00084-4](https://doi.org/10.1016/S0304-4203(97)00084-4). 1998.
 1937
 1938 Mongwe, N. P., Vichi, M., and Monteiro, P. M. S: The seasonal cycle of *p*CO₂ and CO₂ fluxes in the Southern
 1939 Ocean: Diagnosing anomalies in CMIP5 earth system models. *Biogeosciences*, 15(9), 2851–2872.
 1940 <https://doi.org/10.5194/bg-15-2851-2018>, 2018.
 1941
 1942 Mortier, L., Ait Ameer, N., and Taillandier, V.: SOMBA-GE-2014 cruise, RV Téthys II,
 1943 <https://doi.org/10.17600/14007500>, 2014.
 1944
 1945 Moutin, T., and Bonnet, S. : OUTPACE cruise, RV L'Atalante, <https://doi.org/10.17600/15000900>, 2015.
 1946
 1947 Moutin, T., Wagener, T., Caffin, M., Fumenia, A., Gimenez, A., Baklouti, M., Bouruet-Aubertot, P., Pujo-Pay,
 1948 M., Leblanc, K., Lefevre, D., Helias Nunige, S., Leblond, N., Grosso, O., and de Verneil, A.: Nutrient
 1949 availability and the ultimate control of the biological carbon pump in the western tropical South Pacific Ocean,
 1950 *Biogeosciences*, 15, 2961-2989, <https://doi.org/10.5194/bg-15-2961-2018>, 2018.
 1951
 1952 Newton, J.A., Feely, R. A., Jewett, E. B., Williamson, P. and Mathis, J.: Global Ocean Acidification Observing
 1953 Network: Requirements and Governance Plan. Second Edition, GOA-ON,
 1954 <https://www.iaea.org/sites/default/files/18/06/goa-on-second-edition-2015.pdf>, 2015.
 1955
 1956 Nykjaer, L.: Mediterranean Sea surface warming 1985-2006. *Clim. Res.* 39, 11–17. doi: 10.3354/cr00794, 2009.
 1957
 1958 Obernosterer, I.: MOBYDICK-THEMISTO cruise, RV Marion-Dufresne, <https://doi.org/10.17600/18000403>,
 1959 2018.
 1960
 1961 OCADS: Coastal Carbon Data, [https://www.ncei.noaa.gov/access/ocean-carbon-acidification-data-](https://www.ncei.noaa.gov/access/ocean-carbon-acidification-data-system/oceans/coastal_carbon_data.html)
 1962 [system/oceans/coastal carbon data.html](https://www.ncei.noaa.gov/access/ocean-carbon-acidification-data-system/oceans/coastal_carbon_data.html), 2023
 1963
 1964 Olafsson, J., Olafsdottir, S.R., Benoit-Cattin, A., Danielsen, M., Arnarson, T.S., and Takahashi, T.: Rate of
 1965 Iceland Sea acidification from time series measurements. *Biogeosciences* 6, 2661–2668.
 1966 <https://doi.org/10.5194/bg-6-2661-2009>, 2009.
 1967
 1968 Olivier, L., Boutin, J., Reverdin, G., Lefèvre, N., Landschützer, P., Speich, S., Karstensen, J., Labaste, M.,
 1969 Noisel, C., Ritschel, M., Steinhoff, T., and Wanninkhof, R.: Wintertime process study of the North Brazil
 1970 Current rings reveals the region as a larger sink for CO₂ than expected, *Biogeosciences*, 19, 2969–2988,
 1971 <https://doi.org/10.5194/bg-19-2969-2022>, 2022.
 1972
 1973 Olsen, A., Key, R. M., van Heuven, S., Lauvset, S. K., Velo, A., Lin, X., Schirnick, C., Kozyr, A., Tanhua, T.,
 1974 Hoppema, M., Jutterström, S., Steinfeldt, R., Jeansson, E., Ishii, M., Pérez, F. F., and Suzuki, T.: The Global
 1975 Ocean Data Analysis Project version 2 (GLODAPv2) – an internally consistent data product for the world ocean,
 1976 *Earth Syst. Sci. Data*, 8, 297–323, <https://doi.org/10.5194/essd-8-297-2016>, 2016.

1977

1978 Olsen, A., Lange, N., Key, R. M., Tanhua, T., Álvarez, M., Becker, S., Bittig, H. C., Carter, B. R., Cotrim da

1979 Cunha, L., Feely, R. A., van Heuven, S., Hoppema, M., Ishii, M., Jeansson, E., Jones, S. D., Jutterström, S.,

1980 Karlsen, M. K., Kozyr, A., Lauvset, S. K., Lo Monaco, C., Murata, A., Pérez, F. F., Pfeil, B., Schirnack, C.,

1981 Steinfeldt, R., Suzuki, T., Telszewski, M., Tilbrook, B., Velo, A., and Wanninkhof, R.: GLODAPv2.2019 – an

1982 update of GLODAPv2, *Earth Syst. Sci. Data*, 11, 1437–1461, <https://doi.org/10.5194/essd-11-1437-2019>, 2019.

1983

1984 Olsen, A., Lange, N., Key, R. M., Tanhua, T., Bittig, H. C., Kozyr, A., Álvarez, M., Azetsu-Scott, K., Becker, S.,

1985 Brown, P. J., Carter, B. R., Cotrim da Cunha, L., Feely, R. A., van Heuven, S., Hoppema, M., Ishii, M.,

1986 Jeansson, E., Jutterström, S., Landa, C. S., Lauvset, S. K., Michaelis, P., Murata, A., Pérez, F. F., Pfeil, B.,

1987 Schirnack, C., Steinfeldt, R., Suzuki, T., Tilbrook, B., Velo, A., Wanninkhof, R., and Woosley, R. J.: An updated

1988 version of the global interior ocean biogeochemical data product, GLODAPv2.2020, *Earth Syst. Sci. Data*, 12,

1989 3653–3678, <https://doi.org/10.5194/essd-12-3653-2020>, 2020.

1990

1991 Orr, J. C., Epitalon, J.-M., and Gattuso, J.-P.: Comparison of ten packages that compute ocean carbonate

1992 chemistry, *Biogeosciences*, 12(5), 1483–1510, doi:10.5194/bg-12-1483-2015, 2015.

1993

1994 Orr, J. C., Epitalon, J.-M., Dickson, A. G., and Gattuso, J.-P.: Routine uncertainty propagation for the marine

1995 carbon dioxide system, *Marine Chemistry*, Vol. 207, 84-107, doi:10.1016/j.marchem.2018.10.006., 2018.

1996

1997 Parard, G., Lefèvre, N., and Boutin, J.: Sea water fugacity of CO₂ at the PIRATA mooring at 6°S, 10°W. *Tellus-*

1998 *B*, DOI: 10.1111/j.1600-0889.2010.00503.x. 2010.

1999

2000 Pérez F. F., Vázquez-Rodríguez, M., Mercier, H., Velo, A., Lherminier, P. and Ríos, A. F.: Trends of

2001 anthropogenic CO₂ storage in North Atlantic water masses. *Biogeosciences*, 7, 1789-1807, doi:10.5194/bg-7-

2002 1789-2010, 2010.

2003

2004 Pérez, F. F., Mercier, H., Vazquez-Rodriguez, M., Lherminier, P., Velo, A., Pardo, P., Roson, G., and Rios, A.:

2005 Reconciling air-sea CO₂ fluxes and anthropogenic CO₂ budgets in a changing North Atlantic. *Nature*

2006 *Geosciences*, 6, 146-152, doi:10.1038/ngeo1680, 2013.

2007

2008 Pérez, F., Fontela, M., García-Ibáñez, M. et al. : Meridional overturning circulation conveys fast acidification to

2009 the deep Atlantic Ocean. *Nature* 554, 515–518. Doi: 10.1038/nature25493, 2018.

2010

2011 Pesant, S., Not, F., Picheral, M., Kandels-Lewis, S., Le Bescot, N., Gorsky, G., Iudicone, D., Karsenti, E.,

2012 Speich, S., Troublé, R., Dimier, C., Searson, S., and Tara Oceans Consortium Coordinators: Open science

2013 resources for the discovery and analysis of Tara Oceans data. *Scientific Data* 2:150023. doi:

2014 10.1038/sdata.2015.23, 2015.

2015

2016 Petrenko, A.: LATEX10 cruise, RV *Téthys II*, <https://doi.org/10.17600/10450150>, 2010.

2017

2018 Petrenko, A.A., Doglioli, A.M., Nencioli, F., Kersalé, M., Hu, Z., and d'Ovidio, F.: A review of the LATEX

2019 project: mesoscale to submesoscale processes in a coastal environment. *Ocean Dynam.*, doi: 10.1007/s10236-

2020 017-1040-9, 2017.

2021

2022 Petton, S., Pouvreau, S., and Fleury, E. : ECOSCOPA network : high frequency environmental database.

2023 SEANOE. <https://doi.org/10.17882/86131>, 2023.

2024

2025 Pfeil, B., Olsen, A., Bakker, D. C. E., Hankin, S., Koyuk, H., Kozyr, A., Malczyk, J., Manke, A., Metzl, N.,

2026 Sabine, C. L., Akl, J., Alin, S. R., Bates, N., Bellerby, R. G. J., Borges, A., Boutin, J., Brown, P. J., Cai, W.-J.,

2027 Chavez, F. P., Chen, A., Cosca, C., Fassbender, A. J., Feely, R. A., González-Dávila, M., Goyet, C., Hales,

2028 B., Hardman-Mountford, N., Heinze, C., Hood, M., Hoppema, M., Hunt, C. W., Hydes, D., Ishii, M.,

2029 Johannessen, T., Jones, S. D., Key, R. M., Körtzinger, A., Landschützer, P., Lauvset, S. K., Lefèvre, N.,

2030 Lenton, A., Lourantou, A., Merlivat, L., Midorikawa, T., Mintrop, L., Miyazaki, C., Murata, A., Nakadate, A.,

2031 Nakano, Y., Nakaoka, S., Nojiri, Y., Omar, A. M., Padin, X. A., Park, G.-H., Paterson, K., Perez, F. F., Pierrot,
2032 D., Poisson, A., Ríos, A. F., Santana-Casiano, J. M., Salisbury, J., Sarma, V. V. S. S., Schlitzer, R.,
2033 Schneider, B., Schuster, U., Sieger, R., Skjelvan, I., Steinhoff, T., Suzuki, T., Takahashi, T., Tedesco, K.,
2034 Telszewski, M., Thomas, H., Tilbrook, B., Tjiputra, J., Vandemark, D., Veness, T., Wanninkhof, R., Watson,
2035 A. J., Weiss, R., Wong, C. S., and Yoshikawa-Inoue, H.: A uniform, quality controlled Surface Ocean CO₂
2036 Atlas (SOCAT), *Earth Syst. Sci. Data*, 5, 125-143, doi:10.5194/essd-5-125-2013, 2013.

2037

2038 Picheral, M., Searson, S., Taillandier, V., Bricaud, A., Boss, E., Ras, J., Claustre, H., Ouhssain, M., Morin, P.,
2039 Coppola, L., Gattuso, J.-P., Metzl, N., Thuillier, D., Gorsky, G., Tara Oceans Consortium, Coordinators; Tara
2040 Oceans Expedition, Participants: Vertical profiles of environmental parameters measured on discrete water
2041 samples collected with Niskin bottles during the Tara Oceans expedition 2009-2013.
2042 doi:10.1594/PANGAEA.836319, 2014.

2043

2044 Pilcher, D. J., Brody, S. R., Johnson, L., and Bronselaer, B.: Assessing the abilities of CMIP5 models to
2045 represent the seasonal cycle of surface ocean pCO₂, *J. Geophys. Res. Oceans*, 120, 4625–4637,
2046 doi:10.1002/2015JC010759, 2015.

2047

2048 Poisson, A., Culkin, F., and Ridout, P.: Intercomparison of CO₂ measurements. *Deep Sea Research Part A*.
2049 *Oceanographic Research Papers*, 37, 10, 1647-1650, [https://doi.org/10.1016/0198-0149\(90\)90067-6](https://doi.org/10.1016/0198-0149(90)90067-6), 1990.

2050

2051 Pujó-Pay, M., Durrieu de Madron, X., and Conan, P.: PERLE3 cruise, RV Pourquoi pas ?,
2052 <https://doi.org/10.17600/18001342>, 2020.

2053

2054 Pujó-Pay, M., Durrieu de Madron, X., and Conan, P.: PERLE4 cruise, RV L'Atalante,
2055 <https://doi.org/10.17600/18001980>, 2021.

2056

2057 Rabouille C.: AMOR-BFLUX cruise, RV Téthys II, <https://doi.org/10.17600/15008700>, 2015.

2058

2059 Racapé, V., Metzl, N., Pierre, C., Reverdin, G., Quay, P.D., and Olafsdottir, S. R.: The seasonal cycle of the
2060 d13C_{DIC} in the North Atlantic Subpolar Gyre. *Biogeosciences*, 11, 6, 1683-1692, doi:10.5194/bg-11-1683-2014,
2061 2014.

2062

2063 Revelle, R., and Suess, H. E.: Carbon dioxide exchange between atmosphere and ocean and the question of an
2064 increase of atmospheric CO₂ during the past decades. *Tellus* 9, 18–27. doi:10.1111/j.2153-
2065 3490.1957.tb01849.x., 1957.

2066

2067 Reverdin, G.: STRASSE cruise, RV Thalassa, <https://doi.org/10.17600/12040060>, 2012.

2068

2069 Reverdin, G., Metzl, N., Olafsdottir, S., Racapé, V., Takahashi, T., Benetti, M., Valdimarsson, H., Benoit-Cattin,
2070 A., Danielsen, M., Fin, J., Naamar, A., Pierrot, D., Sullivan, K., Bringas, F., and Goni, G.: SURATLANT: a
2071 1993–2017 surface sampling in the central part of the North Atlantic subpolar gyre, *Earth Syst. Sci. Data*, 10,
2072 1901-1924, <https://doi.org/10.5194/essd-10-1901-2018>, 2018.

2073

2074 Reverdin, G., Metzl, N., Olafsdottir, S., Racapé, V., Takahashi, T., Benetti, M., Valdimarsson, H., Quay, P. D.,
2075 Benoit-Cattin, A., Danielsen, M., Fin, J., Naamar, A., Pierrot, D., Sullivan, K., Bringas, F., and Goni, G.:
2076 SURATLANT: a surface dataset in the central part of the North Atlantic subpolar gyre. *SEANOE*.
2077 <https://doi.org/10.17882/54517>, 2022.

2078

2079 Ridame, C., Dekaezemacker, J., Guieu, C., Bonnet, S., L'Helguen, S., and Malien, F.: Contrasted Saharan dust
2080 events in LNLC environments: impact on nutrient dynamics and primary production, *Biogeosciences*, 11, 4783–
2081 4800, <https://doi.org/10.5194/bg-11-4783-2014>, 2014.

2082

2083 Robertson, J. E., Robinson, C., Turner, D. R., Holligan, P., Watson, A. J., Boyd, P., Fernandez, E., and Finch,
2084 M.: The impact of a coccolithophore bloom on oceanic carbon uptake in the northeast Atlantic during summer
2085 1991, *Deep Sea Res., Part I*, 41(2), 297–314, 1994.

2086

2087 Rödenbeck, C., Keeling, R. F., Bakker, D. C. E., Metzl, N., Olsen, A., Sabine, C., and Heimann, M.: Global
2088 surface-ocean pCO₂ and sea–air CO₂ flux variability from an observation-driven ocean mixed-layer scheme,
2089 *Ocean Sci.*, 9, 193–216, <https://doi.org/10.5194/os-9-193-2013>, 2013.

2090

2091 Rödenbeck, C., Bakker, D. C. E., Gruber, N., Iida, Y., Jacobson, A.R., Jones, S., Landschützer, P., Metzl, N.,
2092 Nakaoka, S., Olsen, A., Park, G.-H., Peylin, P., Rodgers, K. B., Sasse, T. P., Schuster, U., Shutler, J. D., Valsala,
2093 V., Wanninkhof, R., Zeng, J. Data-based estimates of the ocean carbon sink variability – First results of the
2094 Surface Ocean pCO₂ Mapping intercomparison (SOCOM). *Biogeosciences* 12: 7251-7278. doi:10.5194/bg-12-
2095 7251-2015, 2015.

2096

2097 Sabine, C. L., Feely, R. A., Gruber, N., Key, R. M., Lee, K., Bullister, J. L., Wanninkhof, R., Wong, C. S.,
2098 Wallace, D. W. R., Tilbrook, B., Millero, F. J., Peng, T.-H., Kozyr, A., Ono, T., and Rios, A. F.: The Oceanic
2099 Sink for Anthropogenic CO₂, *Science*, 305, 367-371, <https://doi.org/10.1126/science.1097403>, 2004.

2100

2101 Sabine, C. L., Hankin, S., Koyuk, H., Bakker, D. C. E., Pfeil, B., Olsen, A., Metzl, N., Kozyr, A., Fassbender,
2102 A., Manke, A., Malczyk, J., Akl, J., Alin, S. R., Bellerby, R. G. J., Borges, A., Boutin, J., Brown, P. J., Cai, W.-
2103 J., Chavez, F. P., Chen, A., Cosca, C., Feely, R.A., González-Dávila, M., Goyet, C., Hardman-Mountford, N.,
2104 Heinze, C., Hoppema, M., Hunt, C. W., Hydes, D., Ishii, M., Johannessen, T., Key, R. M., Körtzinger, A.,
2105 Landschützer, P., Lauvset, S. K., Lefèvre, N., Lenton, A., Lourantou, A., Merlivat, L., Midorikawa, T.,
2106 Mintrop, L., Miyazaki, C., Murata, A., Nakadate, A., Nakano, Y., Nakaoka, S., Nojiri, Y., Omar, A. M., Padin,
2107 X. A., Park, G.-H., Paterson, K., Perez, F. F., Pierrot, D., Poisson, A., Ríos, A. F., Salisbury, J., Santana-
2108 Casiano, J. M., Sarma, V. V. S. S., Schlitzer, R., Schneider, B., Schuster, U., Sieger, R., Skjelvan, I., Steinhoff,
2109 T., Suzuki, T., Takahashi, T., Tedesco, K., Telszewski, M., Thomas, H., Tilbrook, B., Vandemark, D., Veness,
2110 T., Watson, A. J., Weiss, R., Wong, C. S., and Yoshikawa-Inoue, H.: Surface Ocean CO₂ Atlas (SOCAT)
2111 gridded data products, *Earth Syst. Sci. Data*, 5, 145-153, doi:10.5194/essd-5-145-2013, 2013.

2112

2113 Salt, L. A., Beaumont, L., Blain, S., Bucciarelli, E., Grosstefan, E., Guillot, A., L’Helguen, S., Merlivat, L.,
2114 Répécaud, M., Quémener, L., Rimmelin-Maury, P., Tréguer, P., and Bozec, Y.: The annual and seasonal
2115 variability of the carbonate system in the Bay of Brest (Northwest Atlantic Shelf, 2008–2014). *Marine*
2116 *Chemistry*, doi:10.1016/j.marchem.2016.09.003. 2016.

2117

2118 Sasse, T. P., McNeil, B. I., and Abramowitz, G.: A novel method for diagnosing seasonal to inter-annual surface
2119 ocean carbon dynamics from bottle data using neural networks, *Biogeosciences*, 10, 4319–4340,
2120 <https://doi.org/10.5194/bg-10-4319-2013>, 2013.

2121

2122 Sauzède, R., Claustre, H., Pasqueron de Fommervault, O., Bittig, H., Gattuso, J.-P., Legendre, L. and Johnson,
2123 K. S.: Estimates of water-column nutrients and carbonate system parameters in the global ocean: A novel
2124 approach based on neural networks. *Front. Mar. Sci.* 4:128. doi:10.3389/fmars.2017.00128, 2017.

2125

2126 Seelmann, K., Steinhoff, T., Abmann, S., and Körtzinger, A.: Enhance Ocean Carbon Observations: Successful
2127 Implementation of a Novel Autonomous Total Alkalinity Analyzer on a Ship of Opportunity. *Front. Mar. Sci.*
2128 7:571301. doi: 10.3389/fmars.2020.571301, 2020.

2129

2130 Schlitzer, R.: Ocean Data View, Ocean Data View, <http://odv.awi.de> (last access: 13 March 2019), 2018.

2131

2132 Schneider, A., Wallace, D. W. R., and Körtzinger, A.: Alkalinity of the Mediterranean Sea, *Geophys. Res. Lett.*,
2133 34, L15608, doi:10.1029/2006GL028842, 2007.

2134

2135 Schuster, U., Watson, A.J., Bates, N., Corbière, A., Gonzalez-Davila, M., Metzl, N., Pierrot, D. and Santana-
2136 Casiano, M.: Trends in North Atlantic sea surface pCO₂ from 1990 to 2006. *Deep-Sea Res II*,
2137 doi:10.1016/j.dsr2.2008.12.011, 2009.

2138

2139 Schuster, U., McKinley, G. A., Bates, N., Chevallier, F., Doney, S. C., Fay, A. R., González-Dávila, M., Gruber,
2140 N., Jones, S., Krijnen, J., Landschützer, P., Lefèvre, N., Manizza, M., Mathis, J., Metzl, N., Olsen, A., Rios, A.
2141 F., Rödenbeck, C., Santana-Casiano, J. M., Takahashi, T., Wanninkhof, R., and Watson, A. J.: An assessment of
2142 the Atlantic and Arctic sea-air CO₂ fluxes, 1990–2009, *Biogeosciences*, 10, 607–627,
2143 <https://doi.org/10.5194/bg-10-607-2013>, 2013.

2144

2145 Sims, R. P., Holding, T. M., Land, P. E., Piolle, J.-F., Green, H. L., and Shutler, J. D.: OceanSODA-UNEXE: a
2146 multi-year gridded Amazon and Congo River outflow surface ocean carbonate system dataset, *Earth Syst. Sci.*
2147 *Data*, 15, 2499–2516, <https://doi.org/10.5194/essd-15-2499-2023>, 2023.

2148

2149 Skjelvan, I., Lauvset, S.K., Johannessen, T., et al.: Decadal trends in Ocean Acidification from the Ocean
2150 Weather Station M in the Norwegian Sea, *Journal of Marine Systems*,
2151 <https://doi.org/10.1016/j.jmarsys.2022.103775>, 2022.

2152

2153 Speich, S., and The Embarked Science Team: EUREC4A-OA. Cruise Report. 19 January – 19 February 2020.
2154 Vessel: L'ATALANTE. <https://doi.org/10.13155/80129>, 2021

2155

2156 Takahashi, T., Sutherland, S. C., Sweeney, C., Poisson, A., Metzl, N., Tilbrook, B., Bates, N., Wanninkhof, R.,
2157 Feely, R. A., Sabine, C., Olafsson, J., and Nojiri, Y.: Global Sea-Air CO₂ Flux Based on Climatological Surface
2158 Ocean pCO₂, and Seasonal Biological and Temperature Effect. *Deep-Sea Res. II*, 49, 9-10, 1601-1622,
2159 [https://doi.org/10.1016/S0967-0645\(02\)00003-6](https://doi.org/10.1016/S0967-0645(02)00003-6). 2002

2160

2161 Takahashi, T., Sutherland, S. C., Wanninkhof, R., Sweeney, C., Feely, R. A., Chipman, D. W., Hales, B.,
2162 Friederich, G., Chavez, F., Sabine, C., Watson, A. J., Bakker, D. C., Schuster, U., Metzl, N., Yoshikawa-Inoue,
2163 H., Ishii, M., Midorikawa, T., Nojiri, Y., Körtzinger, A., Steinhoff, T., Hoppema, M., Olafsson, J., Arnarson, T.
2164 S., Tilbrook, B., Johannessen, T., Olsen, A., Bellerby, R., Wong, C., Delille, B., Bates, N., and de Baar, H. J.:
2165 Climatological mean and decadal change in surface ocean pCO₂, and net sea air CO₂ flux over the global
2166 oceans. *Deep-Sea Res. II*, 56 (8-10), 554–577, <http://dx.doi.org/10.1016/j.dsr2.2008.12.009>. 2009.

2167

2168 Takahashi, T., Sutherland, S. C., Chipman, D. W., Goddard, J. G., Ho, C., Newberger, T., Sweeney, C. and
2169 Munro, D. R.: Climatological distributions of pH, pCO₂, total CO₂, alkalinity, and CaCO₃ saturation in the
2170 global surface ocean, and temporal changes at selected locations. *Marine Chemistry*, 164, 95–125,
2171 doi:10.1016/j.marchem.2014.06.004. 2014.

2172

2173 Tanhua, T., Pouliquen, S., Hausman, J., O'Brien, K., Bricher, P., de Bruin, T., Buck, J. J. H., Burger, E. F.,
2174 Carval, T., Casey, K. S., Diggs, S., Giorgetti, A., Glaves, H., Harscoat, V., Kinkade, D., Muelbert, J. H.,
2175 Novellino, A., Pfeil, B., Pulsifer, P. L., Van de Putte, A., Robinson, E., Schaap, D., Smirnov, A., Smith, N.,
2176 Snowden, D., Spears, T., Stall, S., Tacoma, M., Thijsse, P., Tronstad, S., Vandenberghe, T., Wengren, M.,
2177 Wyborn, L. and Zhao, Z.: Ocean FAIR Data Services. *Front. Mar. Sci.* 6:440. doi: 10.3389/fmars.2019.00440,
2178 2019.

2179

2180 Tanhua, T., Lauvset, S.K., Lange, N. et al.: A vision for FAIR ocean data products. *Commun Earth Environ* 2,
2181 136. <https://doi.org/10.1038/s43247-021-00209-4>, 2021

2182

2183 Testor, P., Bosse, A., and Coppola, L.: MOOSE-GE, <https://doi.org/10.18142/235>, 2010.

2184

2185 Testor, P.: DEWEX-MERMEX 2013 LEG1 cruise, RV Le Suroît, <https://doi.org/10.17600/13020010>, 2013.

2186

2187 Tilbrook, B., Jewett, E. B., DeGrandpre, M. D., Hernandez-Ayon, J. M., Feely, R. A., Gledhill, D. K., Hansson,
2188 L., Isensee, K., Kurz, M. L., Newton, J. A., Siedlecki, S. A., Chai, F., Dupont, S., Graco, M., Calvo, E., Greeley,

2189 D., Kapsenberg, L., Lebrec, M., Pelejero, C., Schoo, K. L., and Telszewski, M.: An Enhanced Ocean
2190 Acidification Observing Network: From People to Technology to Data Synthesis and Information Exchange.
2191 *Frontiers in Marine Science*, 6, 337, DOI:10.3389/fmars.2019.00337, 2019.

2192

2193 Touratier, F., Azouzi, L. and Goyet, C.: CFC-11, $\Delta 14C$ and $3H$ tracers as a means to assess anthropogenic CO_2
2194 concentrations in the ocean. *Tellus B*, 59(2), 318–325, doi:10.1111/j.1600-0889.2006.00247.x, 2007.

2195

2196 Touratier, F., and Goyet, C.: Decadal evolution of anthropogenic CO_2 in the north western Mediterranean Sea
2197 from the mid-1990's to the mid-2000's. *Deep Sea Research Part I*.doi:10.1016/j.dsr.2009.05.015, 2009.

2198

2199 Touratier, F., Goyet, C., Houpert, L., Durrieu de Madron, X., Lefèvre, D., Stabholz, M., and Guglielmi, V.: Role
2200 of deep convection on anthropogenic CO_2 sequestration in the Gulf of Lions (northwestern Mediterranean Sea).
2201 *Deep-Sea Research Part I*. doi.org/10.1016/j.dsr.2016.04.003, 2016.

2202

2203 Turk, D., Dowd, M., Lauvset, S. K., Koelling, J., Alonso-Pérez, F. and Pérez, F. F.: Can Empirical Algorithms
2204 Successfully Estimate Aragonite Saturation State in the Subpolar North Atlantic? *Front. Mar. Sci.* 4:385. doi:
2205 10.3389/fmars.2017.00385, 2017.

2206

2207 Ulses, C., Estournel, C., Marsaleix, P., Soetaert, K., Fourrier, M., Coppola, L., Lefèvre, D., Touratier, F., Goyet,
2208 C., Guglielmi, V., Kessouri, F., Testor, P., and Durrieu de Madron, X.: Seasonal dynamics and annual budget of
2209 dissolved inorganic carbon in the northwestern Mediterranean deep convection region, *Biogeosciences Discuss.*
2210 [preprint], <https://doi.org/10.5194/bg-2022-219>, in review, accepted, 2023.

2211

2212 UNESCO: Intercomparison of total alkalinity and total inorganic carbon determinations in seawater. UNESCO
2213 Tech. Pap. Mar. Sci. 59., 1990

2214

2215 UNESCO: Reference materials for oceanic carbon dioxide measurements. UNESCO Tech. Pap. Mar. Sci. 60.,
2216 1991

2217

2218 United Nations. The Sustainable Development Goals 2020, 68pp. <https://unstats.un.org/sdgs/report/2020/>, 2020

2219

2220 Vangriesheim A., Pierre, C., Aminot, A., Metzl, N., Baurand, F., and Caprais, J.-C.: The influence of Congo
2221 river discharges in the surface and deep layers of the Gulf of Guinea. *Deep-Sea Res. II*, doi:
2222 10.1016/j.dsr2.2009.04.002, 2009.

2223

2224 Vazquez-Rodriguez, M., Perez, F., Velo, A., Rios, A., and Mercier, H.: Observed acidification trends in the
2225 North Atlantic water masses. *Biogeosciences*, 9, 5217-5230, doi:10.5194/bg-9-5217-2012, 2012.

2226

2227 Velo, A., Perez, F. F., Brown, P., Tanhua, T., Schuster, U., and Key, R. M.: CARINA alkalinity data in the
2228 Atlantic Ocean, *Earth Syst. Sci. Data*, 1, 45–61, <https://doi.org/10.5194/essd-1-45-2009>, 2009.

2229

2230 von Schuckmann, K., Cheng, L., Palmer, M. D., Hansen, J., Tassone, C., Aich, V., Adusumilli, S., Beltrami, H.,
2231 Boyer, T., Cuesta-Valero, F. J., Desbruyères, D., Domingues, C., García-García, A., Gentine, P., Gilson, J.,
2232 Gorfer, M., Haimberger, L., Ishii, M., Johnson, G. C., Killick, R., King, B. A., Kirchengast, G., Kolodziejczyk,
2233 N., Lyman, J., Marzeion, B., Mayer, M., Monier, M., Monselesan, D. P., Purkey, S., Roemmich, D., Schweiger,
2234 A., Seneviratne, S. I., Shepherd, A., Slater, D. A., Steiner, A. K., Straneo, F., Timmermans, M.-L., and Wijffels,
2235 S. E.: Heat stored in the Earth system: where does the energy go?, *Earth Syst. Sci. Data*, 12, 2013–2041,
2236 <https://doi.org/10.5194/essd-12-2013-2020>, 2020.

2237

2238 von Schuckmann, K., Minière, A., Gues, F., Cuesta-Valero, F. J., Kirchengast, G., Adusumilli, S., Straneo, F.,
2239 Ablain, M., Allan, R. P., Barker, P. M., Beltrami, H., Blazquez, A., Boyer, T., Cheng, L., Church, J.,
2240 Desbruyeres, D., Dolman, H., Domingues, C. M., García-García, A., Giglio, D., Gilson, J. E., Gorfer, M.,
2241 Haimberger, L., Hakuba, M. Z., Hendricks, S., Hosoda, S., Johnson, G. C., Killick, R., King, B., Kolodziejczyk,
2242 N., Korosov, A., Krinner, G., Kuusela, M., Landerer, F. W., Langer, M., Lavergne, T., Lawrence, I., Li, Y.,

2243 Lyman, J., Marti, F., Marzeion, B., Mayer, M., MacDougall, A. H., McDougall, T., Monselesan, D. P., Nitzbon,
2244 J., Otosaka, I., Peng, J., Purkey, S., Roemmich, D., Sato, K., Sato, K., Savita, A., Schweiger, A., Shepherd, A.,
2245 Seneviratne, S. I., Simons, L., Slater, D. A., Slater, T., Steiner, A. K., Suga, T., Szekely, T., Thiery, W.,
2246 Timmermans, M.-L., Vanderkelen, I., Wjiffels, S. E., Wu, T., and Zemp, M.: Heat stored in the Earth system
2247 1960–2020: where does the energy go?, *Earth Syst. Sci. Data*, 15, 1675–1709, [https://doi.org/10.5194/essd-15-](https://doi.org/10.5194/essd-15-1675-2023)
2248 [1675-2023](https://doi.org/10.5194/essd-15-1675-2023), 2023.

2249
2250 Wagener, T., Metzl, N., Caffin, M., Fin, J., Helias Nunige, S., Lefevre, D., Lo Monaco, C., Rougier, G., and
2251 Moutin, T.: Carbonate system distribution, anthropogenic carbon and acidification in the western tropical South
2252 Pacific (OUTPACE 2015 transect), *Biogeosciences*, 15, 5221–5236, <https://doi.org/10.5194/bg-15-5221-2018>,
2253 2018a.

2254
2255 Wagener, T., Metzl, N., Caffin, M., Fin, J., Helias Nunige, S., Lefevre, D., Lo Monaco, C., Rougier, G., and
2256 Moutin, T.: Discrete profile measurements of dissolved inorganic carbon (DIC), total alkalinity (TALK),
2257 temperature, salinity and other parameters during the R/V L'Atalante "Oligotrophy from Ultra-oligoTrophy
2258 PACific Experiment" (OUTPACE) cruise (EXPOCODE 35A320150218) in the South Pacific Ocean from 2015-
2259 02-18 to 2015-04-03 (NCEI Accession 0177706). Version 1.1. NOAA National Centers for Environmental
2260 Information. Dataset. doi:10.25921/wbkb-0q19 [access date], 2018b.

2261
2262 Walton, D. W. H., and Thomas, J.: Cruise Report - Antarctic Circumnavigation Expedition (ACE) 20th
2263 December 2016 - 19th March 2017 (1.0). Zenodo. <https://doi.org/10.5281/zenodo.1443511>, 2018.

2264
2265 Wanninkhof, R., Park, G.-H., Takahashi, T., Sweeney, C., Feely, R., Nojiri, Y., Gruber, N., Doney, S. C.,
2266 McKinley, G. A., Lenton, A., Le Quéré, C., Heinze, C., Schwinger, J., Graven, H., and Khatiwala, S.: Global
2267 ocean carbon uptake: magnitude, variability and trends, *Biogeosciences*, 10, 1983–2000, doi:10.5194/bg-10-
2268 1983-2013, 2013.

2269
2270 Watson, A. J., Schuster, U., Bakker, D. C. E., Bates, N., Corbiere, A., Gonzalez-Davila, M., Freidrich, T.,
2271 Hauck, J., Heinze, C., Johannessen, T., Koertzing, A., Metzl, N., Olafsson, J., Olsen, A., Oschlies, A., Padin,
2272 X., Pfeil, B., Rios, A., Santana-Casiano, M., Steinhoff, T., Telszewski, M., Wallace, D. W. R., and Wanninkhof,
2273 R.: Tracking the variable North Atlantic sink for atmospheric CO₂, *Science*, 326, 1391,
2274 doi:10.1126/science.1177394. 2009.

2275
2276 Watson, A. J., Schuster, U., Shutler, J.D. et al.: Revised estimates of ocean-atmosphere CO₂ flux are consistent
2277 with ocean carbon inventory. *Nat Commun* 11, 4422, <https://doi.org/10.1038/s41467-020-18203-3>, 2020.

2278
2279 Williams, N. L., Juranek, L. W., Johnson, K. S., Feely, R. A., Riser, S. C., Talley, L. D., et al.: Empirical
2280 algorithms to estimate water column pH in the Southern Ocean. *Geophysical Research Letters*, 43, 3415–3422.
2281 <https://doi.org/10.1002/2016GL068539>, 2016.

2282
2283 Williams, N. L., Juranek, L. W., Feely, R. A., Johnson, K. S., Sarmiento, J. L., Talley, L. D., Dickson,
2284 A. G., Gray, A. R., Wanninkhof, R., Russell, J. L., Riser, S. C., and Takeshita, Y.: Calculating surface
2285 ocean pCO₂ from biogeochemical Argo floats equipped with pH: An uncertainty analysis, *Global Biogeochem.*
2286 *Cycles*, 31, 591–604, doi:10.1002/2016GB005541., 2017.

2287
2288 Williams, N. L., Juranek, L. W., Feely, R. A., Russell, J. L., Johnson, K. S., and Hales, B.: Assessment of the
2289 carbonate chemistry seasonal cycles in the Southern Ocean from persistent observational platforms. *Journal of*
2290 *Geophysical Research: Oceans*, 123. <https://doi.org/10.1029/2017JC012917>, 2018.

2291
2292 Wimart-Rousseau, C., Lajaunie-Salla, K., Marrec, P., Wagener, T., Raimbault, P., Lagadec, V., Lafont, M.,
2293 Garcia, N., Diaz, F., Pinazo, C., Yohia, C., Garcia, F., Xueref-Remy, I., Blanc, P.-E., Armengaud, A., and
2294 Lefèvre, D.: Temporal variability of the carbonate system and air-sea CO₂ exchanges in a Mediterranean human-
2295 impacted coastal site. *Estuarine, Coastal and Shelf Science*. <https://doi.org/10.1016/j.ecss.2020.106641>, 2020a.

2296

2297 Wimart-Rousseau, C., Wagener, T., Raimbault, P., Lagadec, V., Lafont, M., Garcia, N., and Lefèvre, D.:
2298 Oceanic carbonate chemistry measurements from discrete samples collected at the SOLEMIO station (Bay of
2299 Marseille - North western Mediterranean Sea) between 2016 and 2019. SEANOE.
2300 <https://doi.org/10.17882/72356>, 2020b.
2301
2302 Wimart-Rousseau, C., Wagener, T., Álvarez, M., Moutin, T., Fourier, M., Coppola, L., Nicolas-Chirurgien, L.,
2303 Raimbault, P., D'Ortenzio, F., Durrieu de Madron, X., Taillandier, V., Dumas, F., Conan, P., Pujo-Pay, M. and
2304 Lefèvre, D.: Seasonal and Interannual Variability of the CO₂ System in the Eastern Mediterranean Sea: A Case
2305 Study in the North Western Levantine Basin. *Front. Mar. Sci.* 8:649246. doi: 10.3389/fmars.2021.649246, 2021
2306
2307 WMO/GCOS, 2018: <https://gcos.wmo.int/en/global-climate-indicators>, 2018
2308
2309 Wu, Y., Hain, M. P., Humphreys, M. P., Hartman, S., and Tyrrell, T.: What drives the latitudinal gradient in
2310 open-ocean surface dissolved inorganic carbon concentration?, *Biogeosciences*, 16, 2661-2681,
2311 <https://doi.org/10.5194/bg-16-2661-2019>, 2019.
2312
2313